Innovative tools for offshore wind and DC grids

Deliverable 3.1 – Work Package 3:
Report on the review and evaluation of DC and AC grid operation and interactions in different time frames.

WP3 leader	KU Leuven
Dissemination level	Public
Website	http://innodc.org/
Grant Agreement number	765585
Due delivery	Month 12: 31 August 2018
Project dates	01/09/2017 – 31/08/2021

List of Contributors

Cardiff University	**Wei Liu**, *Jun Liang*
Elia System Operator	**Nathalia de Morais Dias Campos**
KU Leuven	**Vaishally Bhardwaj**, *Jef Beerten*, *Dirk Van Hertem, Hakan Ergun*
Universitat Politècnica de Catalunya	**Saman Dadjo Tavakoli**, *Eduardo Prieto, Oriol Gomis*
U.Porto	**Emily Maggioli**, *Hélder Leite*

Early stage researchers (ESRs) in **bold**, supervisors in *italic*.

Summary

Power systems have been facing changes due to the introduction of renewable energy, distributed generation and HVDC. There has been a shift from traditional AC grids to hybrid AC and DC systems, introducing new challenges and making it crucial to reconsider power system operation in its various domains. In view of this new scenario, this report attempts to provide an insight into the challenges and state-of-the-art with respect to reliability, stability, protection and control of hybrid AC/DC grids. The relevant time frames and the modelling complexity required for studies in each domain are also discussed.

Contents

Part I
Introduction

The latest years have seen a shift of the modern electrical grids towards distributed generation, renewable energy and HVDC. The goals of cutting back on carbon dioxide emissions set by different countries have pushed forward the use of renewable energy sources which have been integrating into the grid on both distribution and transmission levels. On the other hand, the increased connectivity between TSOs, the distance of the connections and the need to integrate offshore wind power have led to HVDC technology being regarded as a key grid enabler that would facilitate the management of future power systems with high amount of renewable generation in a cost-effective manner.

Traditionally, power systems have been mostly based on AC transmission with few back-to-back HVDC interconnections. Thus, the operational framework and system design were based on the characteristics of the predominant AC system. With the large-scale development of HVDC grids and the increasing use of power electronic-interfaced sources, power systems are witnessing major structural changes. The integration of HVDC systems into the existing grid is leading to faster dynamics and increasing the controllability of the overall system. Thus, it is crucial to reconsider power system operation from the point of view of hybrid AC/DC grids.

Some of the challenges observed today include, but are not limited to:

Reliability As the currently applied N-1 reliability criterion does not capture the actual probability of the occurrence of a contingency, it may lead to either situations of higher costs (conservative security margins) or of higher risks. Moreover, there is an upsurge in the system uncertainties due to increased penetration of the renewable energy sources and intra-day markets. Thus, there is a need to shift to probabilistic reliability criteria for an optimal trade-off between costs of measures and risk. Large-scale development of HVDC grids and their characteristic flexibility are being seen as a key facilitator in realizing reliable and economic AC/DC grid operation and mitigating operational uncertainty. Thus, it has become imperative to incorporate the controllable HVDC elements into the security assessment process. However, there are many challenges that need to be addressed with respect to op-

erational framework of AC/DC grid reliability. The Security Constrained Optimal Power Flow (SCOPF), which is used for the reliability assessment, represents a non-linear, non-convex problem with large computational size with large number of discrete variables as well as variety of corrective control strategies.

Stability The increased number of power electronic devices in the grid has blurred the traditional distinction of which type of simulation software is appropriate for different system studies. More in particular, the high frequency interactions between converters and between converters and the grid are making that models that were previously considered to be valid for typical stability studies might no longer be valid. Furthermore, modelling a large power system in detail using models suitable for a large frequency range might not only be prohibitive in terms of computation time but could also require details about components that might not be available due to proprietary restrictions. Therefore, further research is necessary to determine what types of studies can be performed with each tool for power systems with a high penetration of power electronics and to what extent the models used today are accurate.

AC protection One of the issues with using new technology is the impact on the existing infrastructures. When the AC grid is considered, and more specifically the AC protection, it is not clear whether the parameters of the AC transmission grid require adjusting and how this could be determined. Another point to consider is the interaction between AC-DC networks. Numerous studies have been made on that topic, but this is not fully known to what extent it could impact power system protection of the connected countries (including the communication networks between relays and operators, or between relays). Lastly, it is necessary to consider the simplifications made to the grid models for studying AC-DC grids. One of the issues raised is whether the simplifications used are still accurate enough to capture all the needed details and interactions in the system.

DC protection DC fault fault currents have no zero crossings which makes it difficult for traditional circuit breakers to interrupt the fault currents. Therefore, there is a need to develop more complex (and hence more costly) DC circuit breakers to clear the DC faults. Another challenge of DC protec-

tion is that the DC faults propagate faster than in an AC system due to the low impedance in DC grids. As a consequence, much larger fault currents and lower voltage magnitudes occur during a DC fault compared with AC system faults. Locating the DC faults is also a challenge. Most parts of a DC grid can see the DC faults in a short time. The risk of losing the whole DC grid is high if the protection system is not working well.

Control Power-electronic converters lie at the heart of every HVDC system. Their control systems have to be designed to resist most severe disturbances and maintain overall stability of HVDC system in various working conditions. One of the challenges is how to design the control system of an individual converter while considering the dynamics of other converters, high-voltage cables, and other major components of HVDC systems. The interactions between the control systems of ac-dc or dc-dc converters in different locations of HVDC system play a major role in the overall stability of the system. A methodology has to be found to systematically include the impacts of all major parameters in the controller design procedure. Yet, the controller should remain simple enough to be practically implemented.

This report provides an insight into the state-of-the-art associated with the current challenges in the operation of hybrid AC/DC grids in all the various domains discussed above. Each of these domains deals with AC-DC grid phenomena in specific time frames that require different levels of modelling complexity of the same power system components. The required modelling details for each type of study are discussed throughout the report.

Part II
Reliability and Stability of AC/DC Systems

1 Reliable Operation

Vaishally Bhardwaj (supervised by Dirk Van Hertem and Hakan Ergun)

1.1 State of the art with respect to reliability assessment and grid operation

In its broadest sense, power system reliability is defined to be the ability of the system to supply adequate electric service on a nearly continuous basis with few interruptions over an extended period of time [1]. It comprises of two characteristics: power system security and power system adequacy [2]. While power system security refers to the capability to withstand sudden disturbances/ contingencies such as the loss of one or multiple elements e.g. generators, transmission lines, etc., power system adequacy indicates the ability of the system to supply electrical power to the consumers at all times, including the scheduled as well the unscheduled outages of the system components [3].

Reliable operation of the power system essentially involves taking a sequence of decisions while considering uncertainty. It entails meeting an expected level of reliability, determined or set through a reliability criterion while minimizing the overall socio-economic costs of doing so. A reliability criterion may be of deterministic nature wherein only the consequences of the contingencies is considered [4]. On the other hand, a probabilistic reliability criterion inherently accounts for the severity as well as the probability of occurrence of the contingencies [5].

The current reliability planning and operation in Europe is based mostly on the deterministic N-1 reliability criterion [4]. According to this principle,

the system should be able to withstand at all times a credible contingency i.e., the unexpected failure or outage of a single system component (such as a line, transformer, or generator), such that the system is capable of accommodating the new operational situation without violating operational security limits [6].

There are however, different practical interpretations/ implementations of the N-1 criterion between different TSOs and between different time horizons [4]. There are also situations wherein the criteria of N-0 (when N-1 is too expensive) or N-1-1 (stricter) may be implemented. N-0 implies that there is no load curtailment or violation of operational limits in the N-0 system state for the forecast value of real-time load. In case of N-1-1 security, the system is assessed for a sequence of events consisting of a primary contingency followed by a specific secondary contingency. This also applies to situations where a system contingency may be followed by some loss of load. With respect to the use of probabilistic methods for reliable planning and operation, the North American Electric Reliability Corporation, NERC has started carrying out probabilistic assessments in North America and have gained some experience with respect to transmission systems [4].

Each TSO within the ENTSO-E system is responsible for maintaining reliable operation in their control area over a reasonable future time period in view of real-time conditions [6]. This also implies that in the event of any contingency, the operational situation within a TSO's control area must not trigger uncontrollable cascading outage/s that propagate across the borders. Based on the specific operational situation, the power system can be said to be in one of the following system states, wherein each state calls for a different urgency of actions:

In the "Normal" state, the system is within the operational security limits in the N-0 Situation as well as after the occurrence of any contingency from the contingency list, taking into account the effect of the available remedial measures and thus, the security margin reserves.

The "Alert" state highlights the situation where the system is within the operational security limits, however in case of a contingency occurrence, the available remedial actions/ security margins are not sufficient enough to ensure N-1 security.

The "Emergency" scenario refers to the deteriorated state of the system in which there is a violation of the operational limits and there is no guarantee to the global security of the interconnected grid.

"Blackout State" system state is characterized by the collapse of a part

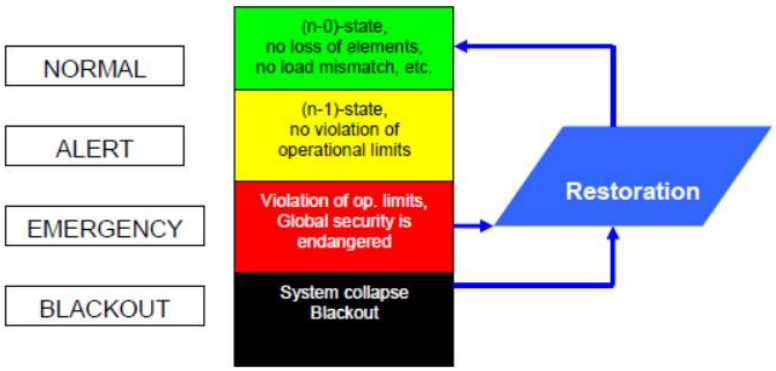

Figure 1: Different system states as per Continental Europe Operational Handbook Policy 5 on Emergency Operations [7].

(partial blackout) or all of the transmission system (total blackout). Measures such as load shedding and controlled system separation may be utilized in order to prevent as much of the system from a widespread blackout.

Both the "Emergency" and the "Blackout" states activate the "Restoration" process with the objective to re-establish the normal system operation and regain operational security.

Two types of approaches can be considered while ensuring reliable grid operation [8]:

1. **Preventive security**: In this case, the preventive control measures ensure N-1 security. Thus, the power system is managed in such a manner that well ahead of the actual operation (typically day-ahead), the system is scheduled so that there are no constraint violations in the power system after the occurrence of a contingency and the resulting automatic control responses in real-time[9].

2. **Preventive-corrective security**: Here, a two-stage decision-making is involved, wherein both preventive and fast-corrective actions (after the contingency) are utilized to remove the violated limits in specific time. As with the preventive security management, the power system is assessed ahead of real-time to investigate whether the real-time operation is within bounds. It allows for the use of fast corrective actions in real-time to correct the cases where the forecasts indicate that N-1 op-

eration is not achieved (but N-0 is) and specific fast corrective actions lead to a new and acceptable state.

In a preventive N-1 secure system, a line contingency has to be allowed without changing the economic dispatch or performing load curtailment. On the other hand, a preventive-corrective approach allows for the violation of the operational limits for a short time interval without damaging the equipment, after which the corrective control kicks in and restores secure system state. Thus, preventive security is more stringent than preventive-corrective security [10]. The latter represents a good trade-off between the cost and the amount of security margins and is getting more relevant in the present context of higher volatility from renewable generation, development of smart grids and the increasing flexibility of demand [11], [12].

Economic operation has always been a major objective of power system management. With the power sector becoming more and more competitive, it is expected to maximize the utilization of the installed assets without sacrificing quality. In this context, Optimal Power Flow (OPF) approach has been used for a long time for addressing the issue of cost-effective power system operation. However, it is equally important to maintain a designated level of security and reserves in the power system. Normally, the objectives of optimality and security are conflicting to each other [13]. Thus, it is necessary to include the system security constraints into the OPF problem in order to obtain solutions that allow operation at least cost while ensuring reliability. With increasing uncertainties in the power system operations, coming from the volatility of renewables and characteristics of liberalized markets, the application of contingency-constrained or Security-Constrained Optimal Power Flow (SCOPF) for reliable solutions in the short-term time frame is becoming extremely pertinent.

A SCOPF is an optimal power flow problem with additional security constraints and involves the minimization of the objective function (e.g. operation cost) by re-dispatching some controllable measures within their limits such that the operational constraints are met in the base case as well as over a set of credible contingencies [12]. It is a non-linear, non-convex, large scale optimization problem with continuous and discrete variables and identifies with the category of Mixed Integer Non-Linear Programming (MINLP).

1.2 Time frames for Reliability Management

Reliability management for a power system encompasses three broad time horizons, long-term system development (planning), mid-term planning (asset management) and short-term system operation (scheduling) [2], each involving a series of activities and the participation of various stakeholders. Thus, the entire time frame covered by the reliability management ranges from year(s)-ahead planning up to real-time operation [14]. The same can be visualized in Figure 2.

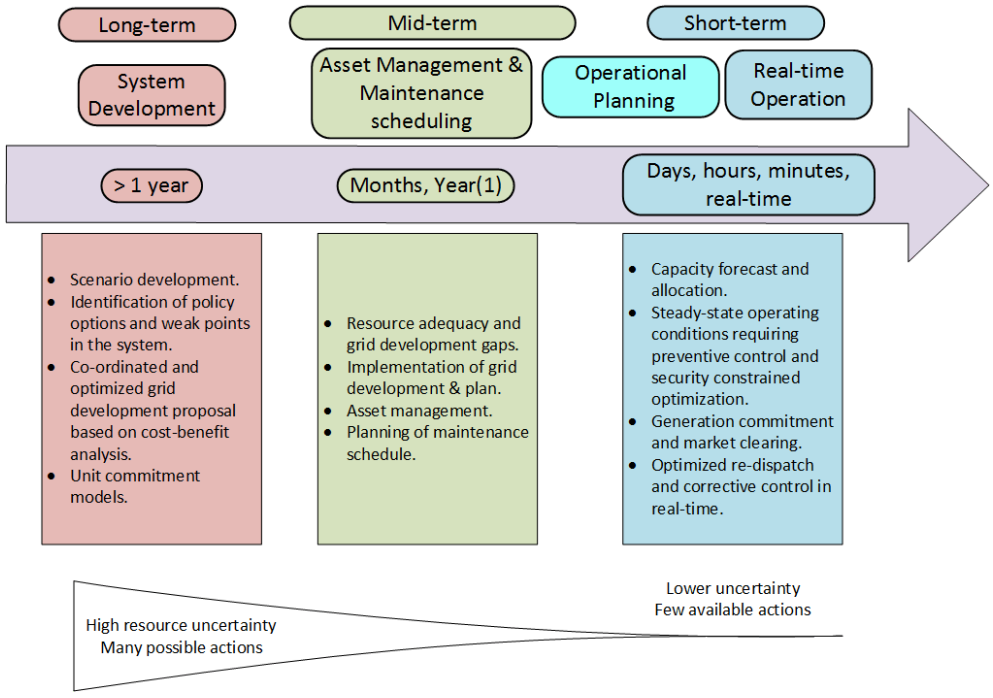

Figure 2: Different time horizons for Reliability Management [14].

While the long-term planning focuses on the development of a coordinated and an optimized expansion plan, the mid-term management directs at identifying resource adequacy and system development gaps, asset management and the planning of maintenance schedules. The short-term system operation comprises of the processes and decisions that enable the system to serve power reliably and economically in the real-time and is divided into operational planning and real-time operations [15].

The operational planning of the system starts from months to days in advance with a view to consider the maintenance plans, prepare generation schedules and analyze available power transfer capacities. Moving towards the actual operations, the TSOs utilize the best forecast of their individual grid situation from 2 days in advance (D-2) in D2CF files to determine the capacity allocation and thus, the available transfer capacity. One day before the actual operation (D-1), energy is traded in the day-ahead market (DAM) while considering the long-term contracts and the available transfer capacities between the different bidding zones. The participants submit bids in the DAM based on this available capacity until gate closure.

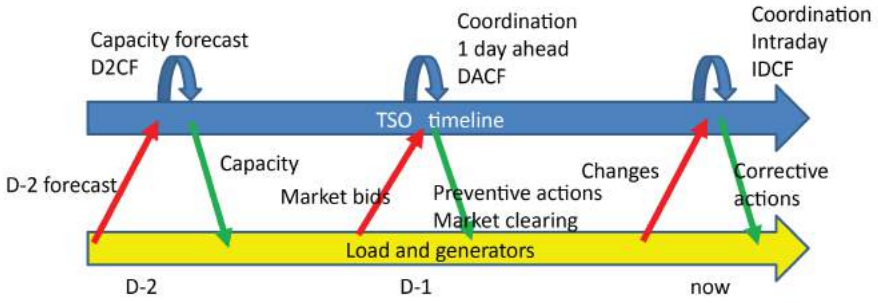

Figure 3: Overview of reliable grid operation [16].

The TSOs then consider the submitted bids and prepare the day-ahead congestion forecasts (DACF) in order to ascertain if the provided schedules can be maintained or if any control measures need to be undertaken. The DACF files reflect the grid conditions with hourly granularity and also consider the generation forecasts of the renewable sources. They are utilized to perform a security-constrained optimization and thereby identify, in cases of any violations, the necessary preventive control measures that need to be taken in order to ensure secure operation. Conversely, the TSO may also decide to undertake the risk of the violations and plan for corrective measures later in case of a contingency. The measures can either be in the form of market actions such as re-dispatch or as TSO control actions such as the changes in the set-points of controllable devices or network topology.

Within the purview of intra-day reliability assessment, the TSO is responsible for monitoring the grid situation and to manage the standard operations. However, when subjected to contingencies, the TSO is required to enforce some corrective measures or even load shedding in severe cases to facilitate

secure grid operation.

1.3 Drivers for re-assessing the security criterion

1.3.1 Shortcomings of N-1 criterion

While the N-1 criterion has been used by the TSOs for enabling reliable planning and operation, there is an emerging need to move towards more comprehensive and probabilistic criteria due to the following reasons:

i There is no common definition of N-1 criterion and thus, it is differently interpreted by different TSOs. There may also be deviations from the criterion in different time horizons [2], [4].

ii As a deterministic reliability criterion, it does not consider the probabilities of the contingencies and they are assumed to be of equal severity and probability [8], [17], [18].

iii The N-1 criterion also does not provide an economic incentive as the costs for corrective actions in case of a contingency are not considered, implying the underlying assumption that the likelihood of usage of corrective actions is low and that they lead to negligible costs in the long-term [12].

iv The criteria may result in inconsistent decision-making as it may lead to higher costs if low-risk cases may be included in studies and higher risks if high failure probability cases are omitted from studies [5], [8].

v It does not account for the stochastic nature of failure of grid elements or the inter-dependencies between different incidents [8].

vi With increasing penetration of the distributed Renewable Energy Sources (RES) and the associated uncertainty, N-1 criterion can only provide limited perspective on grid security [11], [17].

1.3.2 Increased penetration of RES and changing demand patterns

As more and more RES get integrated with the existing grid, they introduce significant amount of uncertainty into the system [12]. There is also the

inclusion of complex control such as through HVDC links and FACTS devices in order to manage the variable behavior of the RES. Other factors such as the introduction of intra-day electricity markets and changing demand patterns have also increased the complexity for the operation as well as the operational planning of the grid.

With the increase in RES and associated uncertainty, it is now expected to consider additional credible contingencies in the contingency list to account for large variations in power injections. This also implies the identification of possible corresponding corrective measures for such injection based contingencies. These assessments would be highly dependent on the time frame of consideration as well as other variables e.g. weather indices, market prices.

As the control areas get more and more interconnected, the possibility for cascaded failures increases and thus, the need for N-k instead of N-1 is being debated for appropriate reliability assessment. The static nature and equal probabilities of the contingencies can also not be considered as they leave out the impact of uncertainty.

Owing to the ongoing changes in the power grids, there is a corresponding escalation in the uncertainties associated with the generation/load forecasts as well as the markets. Thus, the present methodology may not be sufficient/effective for analyzing grid reliability and an urgent need to shift to risk-based or probabilistic reliability assessment criteria for the grid is foreseen. With large-scale development of the HVDC grids and their enhanced control capabilities, it is also imperative to utilize the available flexibility from HVDC grid elements into the existing reliability assessment problem and to consider the contingencies in the HVDC grid. Thus, the futuristic grid operation calls for a comprehensive reliability assessment of the AC/DC hybrid grid in short-term time frames while considering the effect of uncertainty.

1.4 Probabilistic/ Risk-based reliability assessment

There is always some form of uncertainty generally associated with power system operations. This maybe due to the uncertainties in the load, generation as well as network topology. With greater RES generation and smart grid features, these uncertainties have increased manifold. The uncertainty cloud around the system operating point leads to either the consideration of larger security margins at the expense of the market or to operate much closer to the limits so as to escalate the risks. Thus, reliable grid operation

can be essentially considered as a form of risk management [14].

It is also seen that while some contingencies are of high probability and lower severity, there are also others with greater impact on system reliability and yet lower likelihood of occurrence [19]. Thus, the TSO must consider remedial measures for the more probable events in the system and define security margins for handling them. However, for rarer and bigger contingencies with lower probability, it can tolerate some amount of risk in the form of system degradation but eventually decrease the adverse effects on grid reliability. Thus, TSOs have to decide for an optimized operational situation that offers the best quality/continuity of supply such that the costs for the measures are lower than the cost of the risk associated with the contingencies.

It has been established that probabilistic reliability criteria are crucial for ensuring grid reliability in the current situation dominated by the RES and other smart grid characteristics. As these criteria incorporate the likelihood of the occurrence of the contingencies, they provide a better estimation of the actual grid reliability.

One of the ways to formulate the risk is described below [19]. The risk associated with an event i can be given as follows:

$$R_i = P_i \cdot S_i \tag{1}$$

where R_i is the risk associated to the event i, P_i is the likelihood of the event i for a given unit of time (namely an hour) and S_i is the severity associated with the event i, expressed in terms of energy not supplied. The severity is further given as:

$$S_i = G_i \cdot D_i \tag{2}$$

where G_i is the gravity associated to the event i and is equal to violation of the operational criteria expressed in terms of interrupted power (MW). D_i is the restoration time associated to the event i and is the time needed to restore the full load if the event takes place.

Based on above formulation, the mean risk per day may be defined by considering a factor of frequency of exposure as follows:

$$R_i = P_i \cdot S_i \cdot f_i \tag{3}$$

where f_i is the frequency of exposure associated to the event i and is measured as a percentage of the period of analysis where the event will lead to the evaluated severity.

Finally, the cost of the involved risk can be determined as follows:

$$C_i = R_i \cdot c_{ENS} \tag{4}$$

where C_i = cost of the risk, R_i is the risk per day and c_{ENS} is the estimated cost of the energy not supplied.

The above definition for risk and its corresponding costs is based on the measure of energy that would be supplied to the end users if the interruption does not occur. However, there are many other reliability indicators [2] that may be utilized under this general definition of risk and thus, the risk assessment is highly dependent on the choice of the indicators.

It is also pertinent to mention that the above definition does not consider the fact that some loads are more critical than the others and thus, an indicator such as the Value of Lost Load (VOLL) would give a better assessment of the severity associated with the event based on the type and relevance of load.

Employing controllable devices in power system operation can immensely help in handling uncertainty and operating closer to the limits while still maintaining reliability [13]. This can be illustrated with the help of Figure 4(a), wherein the system is initially operating at point A. The gray cloud represents the uncertainty σ_E in the actual position of the system operating point.

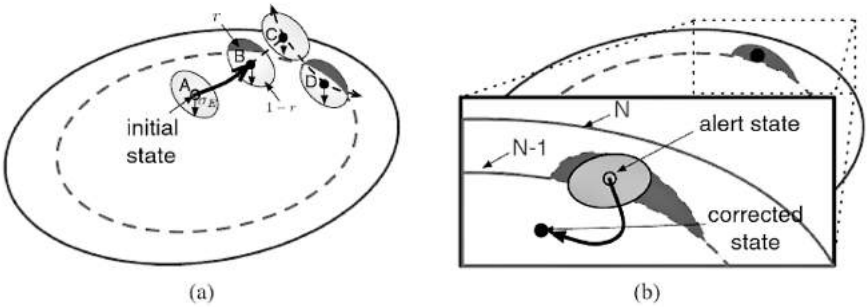

Figure 4: Managing uncertainty with controllable devices [14].

On increasing the power transfer between two zones, the system operating point shifts to point B, which is close to the N-1 security boundary. This operational state corresponds to a power transfer P_T. Owing to the uncertainty in actual position, the probability or risk of being outside the

reliability limits is given by r. On increasing the power transfer even more ($P_T + \Delta P_T$), the system moves to new operating point C outside the reliability limit and thus, with higher risk. If in such a situation, the capabilities of the controllable power system devices e.g. HVDC elements are exploited, the system can be shifted to a new point D wherein the higher power transfer can still be managed with lower risk, equal to that at point B. Thus, the controllable devices aid in better utilization of the existing grid infrastructure while considering reliability. The controllability of the respective devices is also useful in bringing back the system to a normal (N-1 secure) state when the uncertainty cloud might itself lead to a security violation as seen in Figure 4(b).

1.5 HVDC as grid enabler for reliable operation

HVDC systems are characterized by their fast and robust control. With the ongoing development of HVDC grids, it is possible to have fully controllable injections as well as better reliability due to provision of alternative power flow paths. The exchanges between the AC and the DC grids are also completely controllable. Thus, if smart control strategies are implemented, it can lead to optimal usage of the installed assets and decrease the required investments needed in AC/DC grids.

By controlling the set-points for the converters, the power flows in both the AC as well as the DC systems can be influenced. This can be seen with the help of Figure 5, where a shift in the power injection from one HVDC node to another causes corresponding power flows in the AC/DC grid. This can be considered as a re-dispatch of power and can be realized by ensuring that the net sum of the injections for each synchronous zone is equal to zero.

The above flexibility in controlling power injections can aid in increasing power transmission capacities between different zones either directly by changing the DC power flows or indirectly by relieving congestion in another part of the grid [14]. Controllable HVDC links can also be considered for implementing preventive measures during the reliability assessment studies for AC/DC grids. As the operating points of the HVDC converter can be controlled almost instantaneously and the time constants are much faster as compared to the traditional control devices of the AC grid, HVDC elements can be utilized for enforcing corrective control and bringing back the system to a secure operating point. Moreover, exercising the HVDC control measures are less costly for the system operator than performing re-dispatch or

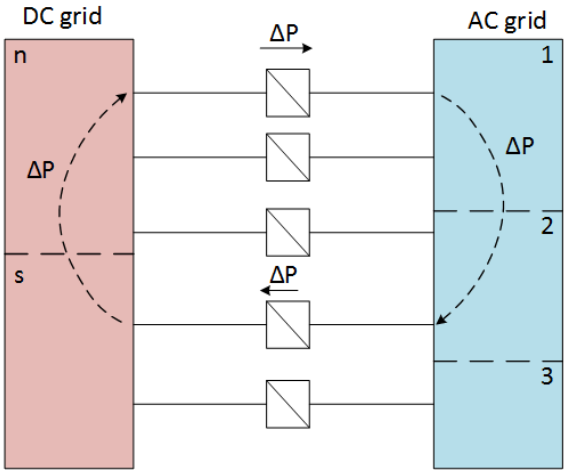

Figure 5: Greater flexibility through HVDC control [14].

load curtailment. With increasing uncertainty in grid operation and the need for fast corrective control, an explicit inclusion of the HVDC systems into the reliability analysis process at all time frames of operation has become essential.

1.6 Challenges in implementing reliable AC/DC grid operation framework

1.6.1 Operational responsibility in AC/DC grids

One of the main challenges for reliability assessment of the AC/DC grid lies in defining how the operational responsibilities are shared amongst the operators [21]. There may be a single system operator for the complete AC/DC grid or different operators for the AC and for the DC grid. Another possibility is that the DC grid may be divided into multiple control areas with different operators. The same might also hold for the AC grid. There may also be the situation wherein the operator for a DC grid control area is also responsible for the AC grid in the same geographical area, such as for a country. Each of the above situations lead to a different set of responsibilities and thus, different frameworks for reliable operation.

In the specific scenario of different DC grid and AC grid operators, the crucial decision would be regarding the responsibility of the AC/DC convert-

ers. This factor would be critical as the usage of the converter controls in optimizing grid situation in a particular grid might lead to non-optimal or adverse situations in the other grid. This aspect is highlighted in Figure 6 where three different possibilities for the AC/DC converter stations are seen: the converter control lies with the AC grid operator, the DC grid operator or is split between both the operators.

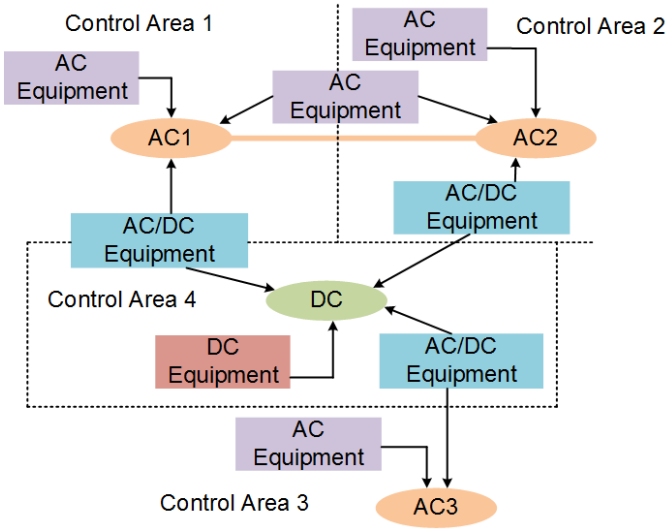

Figure 6: Operational Responsibility [21].

Another example to illustrate the impact of ownership on reliable operation for the AC/DC grid can be seen in Figure 7, where the AC and DC grids are managed by individual operators and connected by five fully controllable converter stations [14]. There exists a large generator on the northern part of the DC grid which has to supply power to a load located south of the AC grid.

There can be many options to transfer this power through the AC/DC grid. One possibility is to transfer the power from north to south using the DC grid and then injecting it into the AC grid close to the load. The other option involves the injection of power directly into the AC grid using northern links and then transferring the power to the load through the AC grid. The third prospect would utilize the power transfer on multiple links between the AC/DC grid. If the objective of the operation is to minimize the losses, then the DC grid operator would prefer the second option more

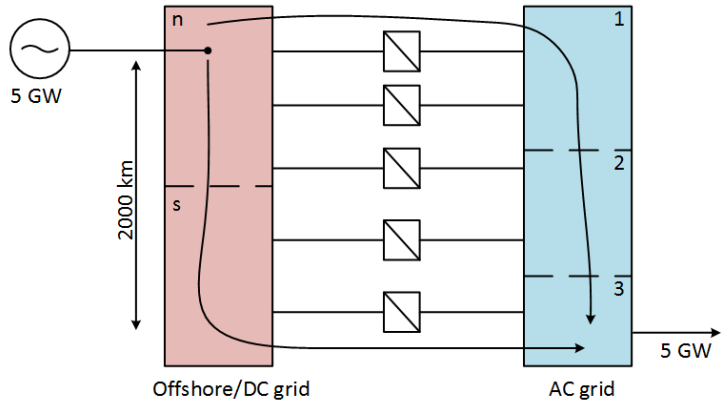

Figure 7: Power transfers in AC/DC grid [14].

than the first. Conversely, the AC grid operator would find the first option more beneficial. In case of power transfer over multiple links, the overall system optimization would be necessary. Thus, the operational strategy and consequent security-based optimization would be highly influenced by the ownership.

1.6.2 Definition of probabilistic reliability criteria for AC/DC Grid

Various probabilistic criteria have been defined in the literature and used for the assessment of grid reliability [2], [4]. They mainly differ in terms of the way in which the probability or risk has been defined for the system as well as the severity or impact of a contingency on the system.

One of the main requirements for the probabilistic reliability criterion is to quantify the amount of risk associated with the system at different stages of short-term operations. With an increase in the number of unpredictable generation sources connected to the grid, it has become necessary that the reliability analysis also considers the large variable injections from such sources as system contingencies [12]. Such events have highly complex interactions with the power system and depend largely on the operating conditions and real-time data. Due to the increasing volatility in grid operation and the interdependencies in a large connected system, the possibilities for the propagation of a single contingency into series of cascading events has also magnified. Thus, there is a need to consider such situations in security assessment instead of the conventional N-1 criterion. Unlike the previously

applied deterministic criteria, the probabilistic criterion for AC/DC grid reliability should factor-in the costs of the post-contingency corrective action control.

Finally, the realization of a probabilistic security assessment for AC/DC hybrid grid operation in multiple time frames would imply the evaluation of the trade-off between the cost of measures (preventive and corrective) and the system risk in each time frame of operation.

1.6.3 Applicability of reliability criterion to AC/DC grid

In order to ascertain the reliability of a hybrid AC/DC grid, it is necessary to consider the impact of contingencies in the AC system on the connected DC system and vice versa [14]. While the outage of an HVDC link could lead to overloads in the AC system, similarly a short circuit in the AC grid may result in the disconnection of a converter station. Normally, a hybrid AC/DC grid would comprise of a number of parallel AC and DC systems and might involve multiple stakeholders. Thus, the applicability of the security criterion needs to be defined. This can be explained by considering the example of N-1 security criterion for a hybrid AC/DC grid. One strategy could be to consider the N-1 security of the whole AC/DC system. Another form of applicability would envisage N-1 security separately for AC grid and DC grid. In case of N-1 reliability for DC grid, the AC system could also be considered as a backup support in the event of a contingency [16]. The similar reliability principle could also hold for the AC grid with support from the connected DC system. Thus, it is seen that the application of the relevant reliability criterion to the hybrid AC/DC grid entails many possibilities. In a scenario of highly interdependent AC/DC systems and multiple participants, an appropriate application of the security criterion is a challenging objective.

1.6.4 Implementation of large scale AC/DC grid security-based optimization

The SCOPF formulation for an AC grid exhibits a challenging problem due to its large problem size [12]. The binary or discrete variables included in the SCOPF problem in order to realize the control actions such as generator start up, transformer load tap changer control, network switching, etc. also pose a problem to achieve a global optimal solution. In case of a preventive-corrective security, there is a corrective action/strategy that needs to be

defined beforehand for each contingency in the grid.

Inclusion of the controllable HVDC systems into the existing AC grid SCOPF problem is seen to be highly relevant for futuristic reliable grid operation. However, such a SCOPF problem would involve larger number of variables and corresponding security constraints. There would also be the need to consider the contingencies in the DC system in the reliability assessment. Due to the controllability of HVDC systems, more possibilities for corrective actions would need to be modeled while determining reliability. For ensuring reliable operations, implementation of the SCOPF problem to multiple time frames of grid operation would be required.

1.7 Mathematical optimal power flow models for AC/DC grids

A typical 3-stage SCOPF formulation is described as follows [12]:

$$\min_{x_0,\ldots,x_c,u_0,\ldots,u_c} f_0(x_0,u_0) \tag{5a}$$

s.t.

$$g_0(x_0,u_0)=0 \tag{5b}$$
$$h_0(x_0,u_0)\leq L_l \tag{5c}$$

$$g_k^s(x_k^s,u_0)=0, \qquad k=1,\ldots,c \tag{5d}$$
$$h_k^s(x_k^s,u_0)\leq L_s, \qquad k=1,\ldots,c \tag{5e}$$
$$g_k(x_k,u_k)=0, \qquad k=1,\ldots,c \tag{5f}$$
$$h_k(x_k,u_k)\leq L_m, \qquad k=1,\ldots,c \tag{5g}$$
$$|u_k-u_0|\leq \Delta u_k, \qquad k=1,\ldots,c \tag{5h}$$

In the above equations f_0 is objective function, k=0 is pre-contingency scenario, k=1,. . . ,c corresponds to c post-contingency scenarios, x_k is state vector, x_k^s is the state vector in short-term time frame, u_k is the vector of control variables, u_k^s is the vector of control variables in short-term time frame, $\Delta u_k = T_k \frac{du_k}{dt}$ is the maximum allowed change in control variables between base case and k^{th} scenario, T_k is time interval for corrective actions and $\frac{du_k}{dt}$ is rate of change of variables, L_s, L_m and L_l denote short-term (emergency), medium-term and long-term (normal) limits, respectively. The limits L_s demarcate

the short-term limits after the occurrence of a contingency and should be met through the preventive actions itself. On the other hand, the medium-term limit L_m is to be satisfied after the execution of predefined corrective actions in the event of a contingency. The long-term limits L_l characterize the normal operation and thus, might require one or more corrective actions by the TSO.

The equations (5b, 5c), (5d, 5e) and (5f, 5g) represent the pre-contingency scenario, the short-term post-contingency scenario and the medium-term post-contingency scenario, respectively. The equality constraints reflected in (5b, 5d, 5f) denote the AC power flow equations, while the inequality constraints in (5c, 5e, 5g) represent the equipment limits as well as the operational limits.

1.7.1 AC Optimal Power Flow Model

The optimal power flow formulations for the AC grid with N number of nodes is given as follows [22]:

$$\theta_r = 0 \tag{6}$$

$$P_i^g - P_i^d = \sum_{(i,j)\epsilon E \cup E^R} P_{ij} \quad \forall \ \ i \,\epsilon\, N \tag{7}$$

$$Q_i^g - Q_i^d = \sum_{(i,j)\epsilon E \cup E^R} Q_{ij} \quad \forall \ \ i \,\epsilon\, N \tag{8}$$

where θ_r represents the voltage angle of the reference bus, P_i^g and Q_i^g are the generator active and reactive powers, P_i^d and Q_i^d depict the load active and reactive powers and E and E^R refer to the set of `from` and `to` edges in the ac network, respectively.

$$P_{ij} = g_{ij}U_i^2 - g_{ij}U_iU_j\cos(\theta_{ij}^{\Delta}) - b_{ij}U_iU_j\sin(\theta_{ij}^{\Delta}) \quad \forall \ \ (i,j)\,\epsilon\ E \cup E^R \tag{9}$$

$$Q_{ij} = -b_{ij}U_i^2 + b_{ij}U_iU_j\cos(\theta_{ij}^{\Delta}) - g_{ij}U_iU_j\sin(\theta_{ij}^{\Delta}) \quad \forall \ \ (i,j)\,\epsilon\ E \cup E^R \tag{10}$$

$$\theta_{ij}^{\Delta} = \theta_i - \theta_j \quad \forall \ \ (i,j)\,\epsilon\, E \tag{11}$$

$$P_{ij}^2 + Q_{ij}^2 = S_{ij,ac}^2 \quad \forall \ \ (i,j)\,\epsilon\, E \tag{12}$$

In above equations, g_{ij} & b_{ij} are the line conductances & susceptances respectively, θ_{ij}^{Δ} is the phase angle difference and the bus voltages are represented by $U_i\angle\theta_i$.

Equations (7) and (8) define the nodal power balance equations of the AC system, whereas equations (9) and (10) describe the voltage drop along the lines. Equation (12) reflects the apparent power of the lines. The above equations represent the equality constraints as given in Equation 5b.

The model constraints represent the generator capabilities, line thermal limits, phase angle limits as well as the bus voltage limits.

i **Generator limits**

$$P_g^{min} \leq P_g \leq P_g^{max} \tag{13}$$

$$Q_g^{min} \leq Q_g \leq Q_g^{max} \tag{14}$$

where P_g^{min}, P_g^{max} are the active power limits and Q_g^{min}, Q_g^{max} are the reactive power limits.

ii **AC Branch limits**

$$S_{ij,ac}^{min} \leq S_{ij,ac} \leq S_{ij,ac}^{max} \tag{15}$$

$$\theta_{ij}^{min} \leq \theta_{ij} \leq \theta_{ij}^{max} \tag{16}$$

where $S_{ij,ac}^{min}$, $S_{ij,ac}^{max}$ are the rated power flow limits and θ_{ij}^{min}, θ_{ij}^{max} are the phase angle difference limits.

iii **AC Node limits**

$$U_{i,ac}^{min} \leq U_{i,ac} \leq U_{i,ac}^{max} \tag{17}$$

where $U_{i,ac}^{min}$, $U_{i,ac}^{max}$ are the bus voltage limits.

1.7.2 Static DC Grid Model

For the purposes of a security-constrained optimization problem, the DC branches are modeled using the steady-state representation in [23] and is shown in Figure 8. The resistance r_d of the single line is divided by the number of poles p_d to quantify for the equivalent resistance.

The power flow equations for DC branches $d \, \epsilon \, D$ between nodes e and f such that $e, f \, \epsilon \, E$ is given as:

$$P_{def}^{dc} + P_{dfe}^{dc} = P_d^{dc,loss} \qquad \forall \quad def \, \epsilon \, \tau^{dc}, \tag{18}$$

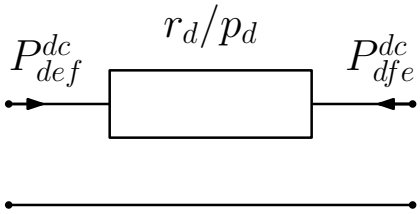

Figure 8: Static DC branch model [23].

where τ^{dc} stands for the DC topology. A non negligible branch resistance $r^s_d \geq 0$ leads to the branch losses given by $P^d_d c, loss \geq 0$. The DC power flow is bound by the ratings of the DC branches at both ends and is given as:

$$-P^{dc,rated}_d \leq P^{dc}_{def}, \leq P^{dc,rated}_d \quad \forall \quad def \, \epsilon \, \tau^{dc} \cup \tau^{dc,rev}, \tag{19}$$

where $\tau^{dc,rev}$ stands for the reverse order of DC nodes.

i **Branch Flow Model:** The power flow on the DC branches is expressed explicitly through the branch current as follows:

$$P^{dc,loss}_d = (\frac{r_d}{p_d}).(I^{dc}_{def})^2 \quad \forall \quad def \, \epsilon \, \tau^{dc}, \tag{20}$$

$$P^{dc}_{def} = U^{dc}_e . I^{dc}_{def} \quad \forall \quad def \, \epsilon \, \tau^{dc}, \tag{21}$$

$$-I^{dc,rated}_d \geq I^{dc}_{def} \geq I^{dc,rated}_d \quad \forall \quad def \, \epsilon \, \tau^{dc} \tag{22}$$

In above equations, P^{dc}_{def} is the power flow on dc line from dc node e to f and P^{dc}_{dfe} is the power flow in the opposite direction. The corresponding current variables are I^{dc}_{def} and I^{dc}_{dfe}, such that $I^{dc}_{def} + I^{dc}_{dfe} = 0$. The voltage magnitude of dc node e is given by U^{dc}_e.

ii **Bus Injection Model:** The BIM representation of the dc line is given by:

$$P^{dc}_{def} = p_d \cdot g^s_d \cdot U^{dc}_e \cdot (U^{dc}_e - U^{dc}_f) \quad \forall \quad def \, \epsilon \, \tau^{dc} \cup \tau^{dc,rev}, \tag{23}$$

where U^{dc}_f is the voltage of node f and $g^s_d = \frac{1}{r^s_d}$, the series conductance of the dc branch d.

1.7.3 Static AC/DC Converter Station Model

A typical model for the AC/DC converter station is considered as per [23] and shown in Figure 9. It comprises of the converter transformer (with tap and series impedance), a filter as a shunt susceptance, a phase reactor as series impedance and the AC/DC converter. While the power electronic converter is an active component, the others are passive in nature. The converter may be of LCC, VSC or MMC configuration. The AC side of the converter station has a complex voltage given by U_i=$U_i^{mag}\angle\theta_i$ and the dc side has a real voltage given by U_e^{dc}. There are also two internal voltages for the converter station demarcated by U_c^f=$U_c^{f,mag}\angle\theta_c^f$ at the filter and U_c^{cv}=$U_c^{cv,mag}\angle\theta_c^{cv}$ at the power electronic converter, respectively. The converter topology is given by τ^{cv}.

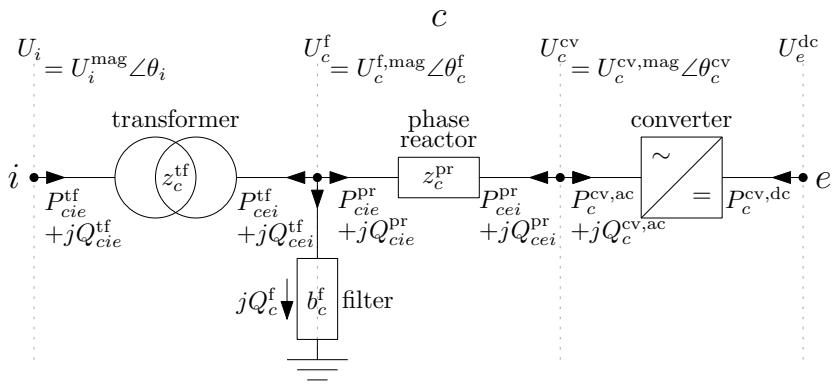

Figure 9: Converter station model [23].

The equations for the individual components are given as follows:

i **Transformer:** The transformer is represented by equivalent admittance of $y_c^{tf} = g_c^{tf} + jb_c^{tf}$. The voltage magnitude transformation factor (tap t_c) has also been taken into consideration as tap setting of converter transformer influences the voltage control performance of the HVDC station. The power flow through transformer can be represented as:

$$P^{tf}_{cie} = g^{tf}_c(\frac{U^{mag}_i}{t_c})^2 - g^{tf}_c\frac{U^{mag}_i}{t_c}U^{f,mag}_c\cos(\theta_i - \theta^f_c) \quad (24)$$
$$-b^{tf}_c\frac{U^{mag}_i}{t_c}U^{f,mag}_c\sin(\theta_i - \theta^f_c) \quad \forall \quad cie \,\epsilon\, \tau^{cv}$$

$$Q^{tf}_{cie} = -b^{tf}_c(\frac{U^{mag}_i}{t_c})^2 + b^{tf}_c\frac{U^{mag}_i}{t_c}U^{f,mag}_c\cos(\theta_i - \theta^f_c) \quad (25)$$
$$-g^{tf}_c\frac{U^{mag}_i}{t_c}U^{f,mag}_c\sin(\theta_i - \theta^f_c) \quad \forall \quad cie \,\epsilon\, \tau^{cv}$$

$$P^{tf}_{cei} = g^{tf}_c(U^{f,mag}_c)^2 - g^{tf}_c U^{f,mag}_c\frac{U^{mag}_i}{t_c}\cos(\theta^f_c - \theta_i) \quad (26)$$
$$-b^{tf}_c U^{f,mag}_c\frac{U^{mag}_i}{t_c}\sin(\theta^f_c - \theta_i) \quad \forall \quad cie \,\epsilon\, \tau^{cv}$$

$$Q^{tf}_{cei} = -b^{tf}_c(U^{mag}_c)^2 + b^{tf}_c U^{f,mag}_c\frac{U^{mag}_i}{t_c}\cos(\theta^f_c - \theta_i) \quad (27)$$
$$-g^{tf}_c U^{f,mag}_c\frac{U^{mag}_i}{t_c}\sin(\theta^f_c - \theta_i) \quad \forall \quad cie \,\epsilon\, \tau^{cv}$$

If the transformer is absent, or if $z^t_c f \approx 0$, the equations for lossless component are used:

$$P^{tf}_{cie} + P^{tf}_{cei} = 0 \quad \forall \quad cie \,\epsilon\, \tau^{cv} \quad (28)$$
$$Q^{tf}_{cie} + Q^{tf}_{cei} = 0 \quad \forall \quad cie \,\epsilon\, \tau^{cv} \quad (29)$$
$$U^{mag}_i = U^{f,mag}_c \quad \forall \quad cie \,\epsilon\, \tau^{cv} \quad (30)$$
$$\theta^f_c = \theta i \quad \forall \quad cie \,\epsilon\, \tau^{cv} \quad (31)$$

ii **Filter:** The reactive power of shunt capacitance having susceptance b^f_c is given by:

$$Q^f_c = -b^f_c(U^{f,mag}_c)^2 \quad \forall \quad cie \,\epsilon\, \tau^{cv} \quad (32)$$

The nodal balance equations between the filter capacitance, phase reactor and transformer are as given below:

$$P^{pr}_{cie} + P^{tf}_{cei} = 0 \quad \forall \quad cie \,\epsilon\, \tau^{cv} \quad (33)$$
$$Q^{pr}_{cie} + Q^{tf}_{cei} + Q^f_c = 0 \quad \forall \quad cie \,\epsilon\, \tau^{cv} \quad (34)$$

iii **Phase Reactor:** The phase reactor impedance (z_c^{pr}) and admittance (y_c^{pr}) are given by the following:

$$z_c^{pr} = r_c^{pr} + jx_c^{pr} \tag{35}$$

$$y_c^{pr} = \frac{1}{z_c^{pr}} = g_c^{pr} + jb_c^{pr} \tag{36}$$

As the phase reactor can be considered as a transformer with tap ratio equal to 1, hence the equations (24) - (27) can be used for phase reactor with loss and lossless configurations, respectively.

iv **AC/DC Converter:** The power flow capabilities for the AC/DC converter are envisaged through the limits given as:

$$P_c^{cv,ac,min} \leq P_c^{cv,ac} \leq P_c^{cv,ac,max} \quad \forall \quad cie \, \epsilon \, \tau^{cv} \tag{37}$$

$$Q_c^{cv,ac,min} \leq Q_c^{cv,ac} \leq Q_c^{cv,ac,max} \quad \forall \quad cie \, \epsilon \, \tau^{cv} \tag{38}$$

$$(P_c^{cv,ac})^2 + (Q_c^{cv,ac})^2 \leq (S_c^{cv,ac,rated})^2 \quad \forall \quad cie \, \epsilon \, \tau^{cv} \tag{39}$$

The active power injected by converter into dc grid is modeled as $P_c^{cv,dc}$(defined at dc bus of converter). This power must also be within the limits specified for the dc side:

$$P_c^{cv,dc,min} \leq P_c^{cv,dc} \leq P_c^{cv,dc,max} \quad \forall \quad cie \, \epsilon \, \tau^{cv} \tag{40}$$

Also,

$$P_c^{cv,ac} + Q_c^{cv,dc} = P_c^{cv,loss} \quad \forall \quad cie \, \epsilon \, \tau^{cv} \tag{41}$$

For the converter losses,a parameterized model is considered as follows:

$$P_c^{cv,loss} = a_c^{cv} + b_c cv \cdot I_c^{cv,mag} + c_c cv \cdot (I_c^{cv,mag})^2 \quad \forall \quad cie \, \epsilon \, \tau^{cv} \tag{42}$$

where $a_c^{cv} \geq 0$W, $b_c^{cv} \geq 0$ (W/A), $c_c^{cv} \geq 0$ (Ω) and $I_c^{cv,mag}$ is the current magnitude on ac side of converter. This current can be defined using active and reactive power injection as well as ac side voltage of converter as per the following equations:

$$(P_c^{cv,ac})^2 + (Q_c^{cv,ac})^2 = (U_c^{cv,mag})^2 (I_c^{cv,mag})^2 \quad \forall \quad cie \, \epsilon \, \tau^{cv} \tag{43}$$

The ac side current of the converter is bound by the rated current limits as:

$$I_c^{cv,mag} \leq I_c^{cv,rated} \quad \forall \quad cie \, \epsilon \, \tau^{cv} \tag{44}$$

$$U_c^{cv,min} \leq U_c^{cv,mag} \leq U_c^{cv,max} \quad \forall \quad cie \, \epsilon \, \tau^{cv} \tag{45}$$

where $U_c^{cv,mag}$ is voltage magnitude at ac bus of converter. Similar to the ac side, the dc converter current is also bound by limits.

$$P_c^{cv,dc} = U_e^{dc} \cdot I_c^{cv,dc,mag} \quad \forall \quad cie \, \epsilon \, \tau^{cv} \tag{46}$$

$$I_c^{cv,dc,min} \leq I_c^{cv,dc,mag} \leq I_c^{cv,dc,max} \quad \forall \quad cie \, \epsilon \, \tau^{cv} \tag{47}$$

For the LCC configuration of the converter, the active and reactive power are linked through the given relation:

$$P_c^{cv,ac} = \cos\varphi_c \cdot S_c^{cv,ac,rated} \quad \forall \quad cie \, \epsilon \, \tau^{cv} \tag{48}$$

$$Q_c^{cv,ac} = \sin\varphi_c \cdot S_c^{cv,ac,rated} \quad \forall \quad cie \, \epsilon \, \tau^{cv} \tag{49}$$

where φ_c in above equations is the thyristor firing angle and is given by $0 \leq \varphi_c^{min} \leq \varphi_c \leq \varphi_c^{max} \leq \pi$.

1.7.4 Nodal Balance Equations

Finally, the nodal equations for the AC/DC grid are given as follows:

$$\sum P_i^g + \sum P_i^{c,ac} + \sum P_{ij}^{ac} + \sum gU_i^2 - \sum P_i^d = 0 \quad \forall \quad i \, \epsilon \, N_{ac} \tag{50}$$

$$\sum Q_i^g + \sum Q_i^{c,ac} + \sum Q_{ij}^{ac} + \sum bU_i^2 - \sum Q_i^d = 0 \quad \forall \quad i \, \epsilon \, N_{ac} \tag{51}$$

$$\sum P_i^g + \sum P_i^{c,dc} + \sum P_{ij}^{ac} + \sum gU_i^2 - \sum P_i^d = 0 \quad \forall \quad i \, \epsilon \, N_{dc} \tag{52}$$

The above formulations for the AC/DC grid aim at minimizing the objective function of the generation costs and is given as follows:

$$minimize : \sum_{i \epsilon N} c_2 i(\Re(S_i^g))^2 + c_1 i(\Re(S_i^g)) + c_{0i} \tag{53}$$

where c_0, c_1 and c_2 represent the generation cost coefficients.

The above security-constrained optimization is characterized as a non-convex, non-linear optimization problem of huge computational size and large number of both continuous and discrete variables. With non-convex optimization, one has to choose between either solving problems with lesser computational time but locally optimal results or else globally optimal solution but with larger computational times [24]. Thus, the current practice in

the electricity industry is to use the so-called DC OPF approximation for this problem. However, such an approximation completely ignores the important aspects of power flow, such as the reactive power and voltage magnitudes and may lead to inexact results. Thus, various convex relaxations of the actual non-linear problem have been established in the literature in order to achieve globally optimal solutions within lesser time. Prominent among these are the semi-definite programming (SDP), the quadratic convex (QC) and the second order cone (SOC) relaxations [22].

In order to implement a framework for reliable operation of AC/DC grids in short-term time frames and under the impact of uncertainty, firstly the inclusion of security constraints into the AC/DC grid optimal power flow model is envisaged. With a view to reduce computational burden and to obtain globally optimal solution for the large-scale mixed integer non-linear problem, different relaxations may be applied and the results thereof analyzed. The next main objective would be to identify a risk-based reliability criterion that ensures optimal trade-off between the cost of measures and cost of associated risks. Finally, the application of the risk-based reliability criterion to multiple time frames of short-term grid operation would be realized through the implementation of the multi-stage SCOPF as discussed in Equation (5). Such a flexible framework would represent the decision making process of transmission system operators and allow them to find better operational procedures than those being applied today.

2 Power System Stability

Nathalia Campos (supervised by Jef Beerten)

Power systems are continuously being subjected to disturbances, some of which are small such as continuous changes in the demand and others which can be severe as is the case of a fault or loss of a generation unit. The grid must be capable, however, to operate in these continuously changing conditions so as to guarantee continuity in the energy supply. When a disturbance occurs, it shifts the system from its initial operating point and it must adjust to the new operating conditions. In this context, power system stability can be regarded as the ability of the system to return to a state of equilibrium after being subjected to disturbances [3].

Figure 10 provides an overview of a traditional classification of power system stability. AC system stability is divided broadly into rotor-angle, frequency and voltage stability according to the physical nature of the stability problem and the main system variables in which it can be observed. These categories are further subdivided according to the size and time span of the disturbance. A short description of each class of stability problem is provided below:

Rotor-angle stability: In a synchronous system, several generators are rotating with the same frequency and the mechanical speed of their rotors are synchronized to this frequency. Rotor-angle stability is then defined as the ability of the synchronous generators to remain synchronized after the grid is subject to a disturbance [25]. If the disturbance is considered small, the stability problem is named small-signal stability since it can be studied by linearizing the equations that describe the system around an operating point. On the other hand, if the disturbance is severe, the system can no longer be considered linear. In this case, the machines suffer large rotor angle excursions and must return to an equilibrium point. This is known as transient stability;

Voltage stability: In addition to the rotor angles, disturbances might also affect the voltage on the grid nodes. Voltage stability is then defined as the

ability of power systems to maintain acceptable voltage levels at its buses when a disturbance occurs;

Frequency stability: Similarly, frequency stability is the ability of the power system to maintain a stable frequency when the system is under a disturbance that creates an imbalance between generation and load.

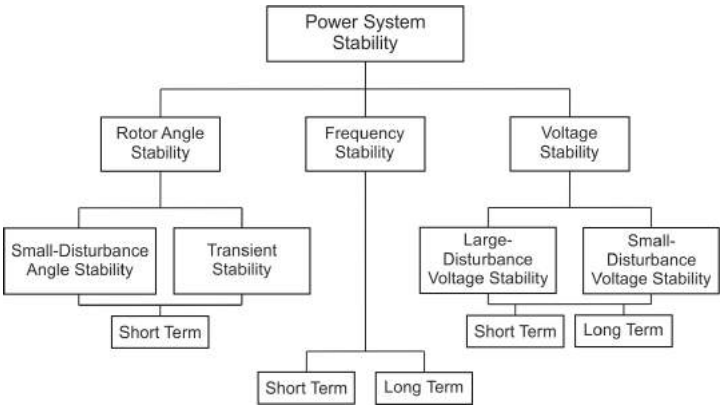

Figure 10: Classification of stability in power systems [25].

Up to this point all the stability problems discussed refer exclusively to AC systems. However, the introduction of DC systems brought with it new stability concerns that have not been fully understood yet. Some of them have been already identified such as DC voltage collapse, DC oscillations and DC energy equilibrium, and others are yet to be determined [26]. It is clear that, in the future, there will be a need to extend the classification of stability to also include emerging issues, both in AC and DC power systems. A preliminary extension is illustrated in Figure 11.

2.1 Timescales of power system phenomena

Traditionally, power system transients have been classified into electromagnetic and electromechanical phenomena. Electromagnetic transients are associated with the energy exchange between inductances and capacitances of the system while electromechanical transients are due to exchanges between the mechanical energy stored in the rotating masses of machines and the electrical energy in the network [27]. Figure 12 illustrates the different power system phenomena and their corresponding timescale and classification.

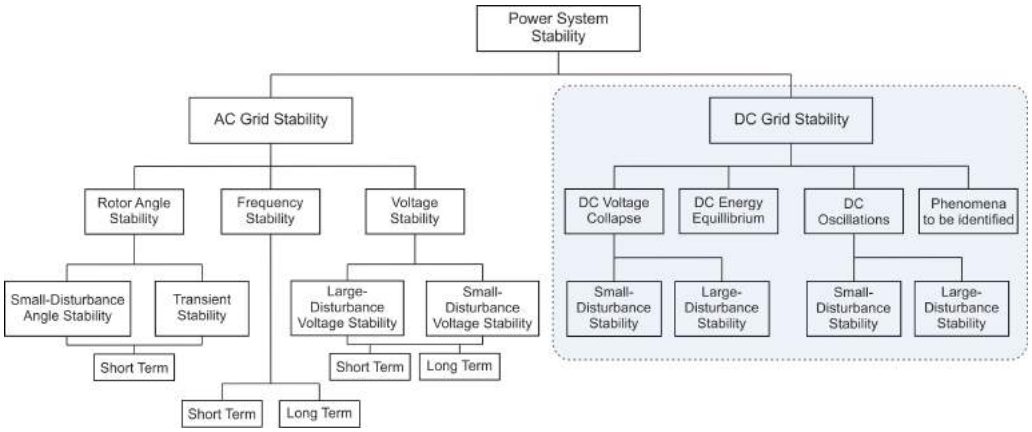

Figure 11: Extended classification of stability in AC and DC power systems (after [26]).

Even though there is a gray zone in the classification of disturbances, it can be said broadly that electromagnetic transients are associated with frequencies above the nominal frequency. They are usually studied using a class of programs known as Electromagnetic Transient Programs (EMTP) where components are modeled in detail and small time steps are used in the simulation. Because of the detail level, these models tend to be valid within a larger frequency range. On the other hand, electromechanical transients are commonly associated with sub synchronous frequencies and are studied using electromechanical stability programs, also known for historical reasons as transient stability programs. The models used in these programs make use of simplifying assumptions and due to that, they are valid only on a restricted frequency range. The advantage of this type of tools is that a larger time step can be used, making it suitable for the study of large power systems and for operational studies that must be computed in a short time.

2.2 Challenges of dynamic stability assessment

In traditional grids, the dynamic behaviour of the system is dictated mainly by the behaviour of its synchronous machines. However, in later years, power systems have seen an increase in the amount of power-electronic interfaced devices due to the growing use of renewable energy sources, high voltage direct current (HVDC) transmission and flexible alternating current trans-

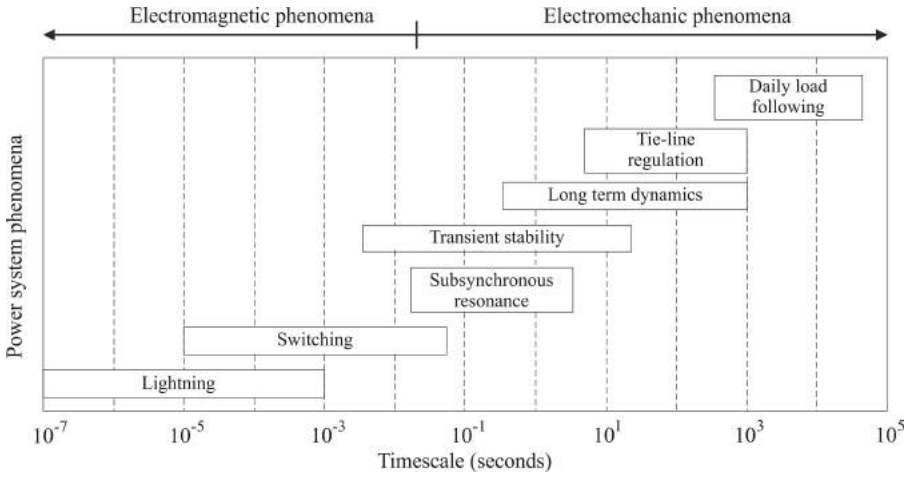

Figure 12: Timescale for power system phenomena [27].

mission system (FACTS) devices. These devices increase the overall grid controllability, but also create new challenges when it comes to understanding how the power system behaves, how to model the problems and how it should be operated.

As the number of power electronic devices present in the power system increases, there is a risk that they will not only interact with the grid but also between each other [28], [29]. These interactions can be undesirable, especially when they could eventually lead the power system to an unstable state.

Power electronic converters have several control loops, some of which present slow dynamics, such as the active and reactive power controls; and others that are faster and can have a large bandwidth, as is typically the case for the inner current controls and the phase locked loop (PLL). Due to the large bandwidth of such controllers, the converter could interact with the grid at its resonant frequencies, possibly leading to harmonic instability [29]. This problem has already been observed in practical installations, as was the case in the BorWin1 HVDC system that connects an offshore wind farm to the onshore AC grid [30]. In addition to that, having a high penetration of power electronic interfaced sources is known to decrease the total system inertia and the power system strength. These, in turn, can create dynamic issues such as frequency and voltage instabilities and affect power quality [31].

The increased number of power electronic devices in the grid has blurred the traditional distinction of which type of simulation software is appropriate for different system studies. More in particular, the high frequency interactions between converters and between converters and the grid are making that models that were previously considered to be valid for typical stability studies might no longer be valid [32], [31]. On the other hand, modelling a large power system in detail using models suitable for a large frequency range might not only be prohibitive in terms of computation time but could also require details about components that might not be available due to proprietary restrictions. Therefore, further research is necessary to determine what types of studies can be performed with each tool and to what extent the models used today are accurate.

2.3 Power system simulation for transient stability studies

In order to be able to simulate large-scale power systems composed of several components it is necessary to ensure that the computational time required to simulate the full system is maintained within reasonable limits. There are several approaches to reducing the simulation time. These range from increasing computational capacity and using more efficient numerical computation techniques to making simplifications in the power system and using approximations to represent components.

The basic principle behind time-domain simulations of power systems consists in representing components, control systems and the network topology by a set of algebraic and differential equations. Simulation programs use numerical integration techniques to solve the differential equations that characterize the power system components and provide the solution for the system variables.

The speed of numerical integration techniques depends, among other factors, on the step size used. For a fixed simulation time, the smaller the simulation time step, the more calculations will be required to simulate the response of the power system. The maximum simulation time step Δt_{max} that can be used while still being able to obtain accurate results is dependent on the frequency content of the signals involved. According to the Nyquist criterion,

$$\Delta t_{max} = \frac{1}{2 f_{max}}, \tag{54}$$

where f_{max} is the maximum frequency component of the signal. In addition to that, a safe margin must also be considered in order to account for the fact that the studied signals might not always be bandlimited and the highest frequency might not be well known before the simulation [33]. One of the modelling techniques that allow the use of a larger time step is the approximation of system variables such as voltages, currents and fluxes by quasi-stationary phasor representations.

This representation supposes that the network signals are subject to only small frequency variations centered at the nominal frequency. This assumption is considered valid when the studies are restricted to slow dynamic phenomena. In this case, the use of phasors allows the 50 or 60 Hz signal to implicitly be filtered out of the response, leaving only the slow electromechanical oscillations in the signal. Since these oscillations have a low frequency in traditional power systems, the maximum frequency observed in the signal is reduced, which ultimately allows for an increase in the simulation time step size, resulting in a gain in simulation speed. In the next sections the details regarding phasor-based approach are discussed and the modelling of some of the power system components are presented to illustrate the concept and its assumptions.

2.3.1 Phasor-based modelling

Phasor-based modelling, also known as root mean square (RMS) modelling, consists of a modelling technique in which phasors are used in the formulation of models for some of the power system components. In general, a phasor can be defined as a complex number that represents the magnitude and angle of a sinusoid [34]. Phasors are defined for sinusoids at a single frequency and can be used to represent steady-state signals in power systems. This is because ideally in steady-state, power system variables such as voltages, currents and fluxes present a sinusoidal behaviour with a single frequency component corresponding to the system nominal frequency ω_0. The use of phasors is not limited, however, to steady-state studies. They can be used to approximate signals that only deviate slightly from a sinusoid at nominal frequency. This is the case when a perturbation occurs in the power system and other frequency components appear in the signals. If the oscillations

created are slow compared to the system frequency, a low-frequency pulsation is superposed to the sinusoid at nominal frequency and the low frequency oscillations are perceived as variations in its "envelope". For this reason, the resulting time-domain signal can be regarded as a modulated signal with carrier frequency ω_0 as illustrated in Figure 13.

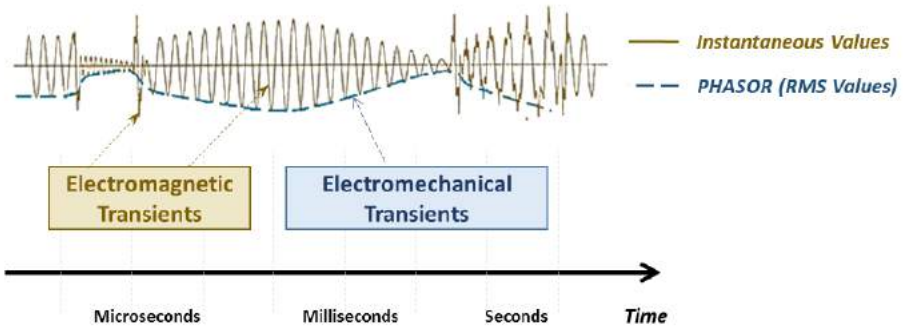

Figure 13: Comparison between instantaneous and phasor variables [35].

These phasors were originally named time-varying phasors since the amplitude and phase vary in time to represent the pulsation observed in the sinusoid. Mathematically, a modulated time-domain signal $e(t)$ of the form

$$e(t) = E(t)cos(\omega_0 t + \delta(t)) \tag{55}$$

can be represented as a phasor $\hat{e}(t)$ by the expression [36]:

$$\hat{e}(t) = E(t)e^{j\delta(t)}. \tag{56}$$

It is also possible to perform the inverse operation and obtain the original signal from its phasor representation by

$$e(t) = \Re[\hat{e}(t)e^{j\omega_0 t}]. \tag{57}$$

2.3.2 The quasi-stationary assumption

The use of phasors can simplify the modelling of basic circuit elements. The application and modelling considering the quasi-stationary assumption will be demonstrated below for the illustrative case of a capacitance and inductance respectively.

The differential equation describing the relationship between voltage and current for a capacitor is given by

$$i_C(t) = C\frac{dv_C(t)}{dt}. \tag{58}$$

Equation (57) can be used in (58) leading to

$$\Re\{\hat{i}_C(t)e^{j\omega_0 t}\} = C\frac{d}{dt}\Re\{\hat{v}_C(t)e^{j\omega_0 t}\}. \tag{59}$$

Considering that $\Re$ is a linear operator, the resulting equation is

$$\hat{i}_C(t) = C\frac{d}{dt}\hat{v}_C(t) + j\omega_0 C\hat{v}_C(t). \tag{60}$$

For steady state phasors, $d\hat{v}_C(t)/dt = 0$ since the magnitude and phase of the phasors are constant. If these quantities are instead time-varying, this is no longer valid but the approximation $d\hat{v}_C(t)/dt \approx 0$ can be made if it is assumed that these quantities typically vary with a slow frequency for the studies under consideration.

In that case, the phasors are called quasi-stationary and the capacitor equation can be simplified to the algebraic form used in steady-state analysis:

$$\hat{i}_C(t) = j\omega_0 C\hat{v}_C(t). \tag{61}$$

The same analysis can be applied to the inductor equation, resulting in

$$\hat{v}_L(t) = j\omega_0 L\hat{i}_L(t). \tag{62}$$

Equations (61) and (62) are well-known expressions used for capacitors and inductors in the phasor domain. The main advantage being that the relationship between voltage and current becomes algebraic and no longer represented by differential equations. The phasor equations for basic circuit elements are implicitly used later when deriving models for the network, including transmission lines and loads.

2.4 Modelling of power system components for stability studies

When using the quasi-stationary assumption, the network is modelled using phasors instead of differential equations as is usual in electromagnetic transient simulations. Due to that simplification, only frequencies close to the

system frequency are captured. For the synchronous machines, the differential equations representing stator flux dynamics are neglected and the stator terminal voltage is represented by phasors. Only slow dynamics are included, corresponding to the rotor, mechanical equations, turbines, power frequency controllers, etc. The general structure of the simulation framework using phasor-based modelling is illustrated in Figure 14.

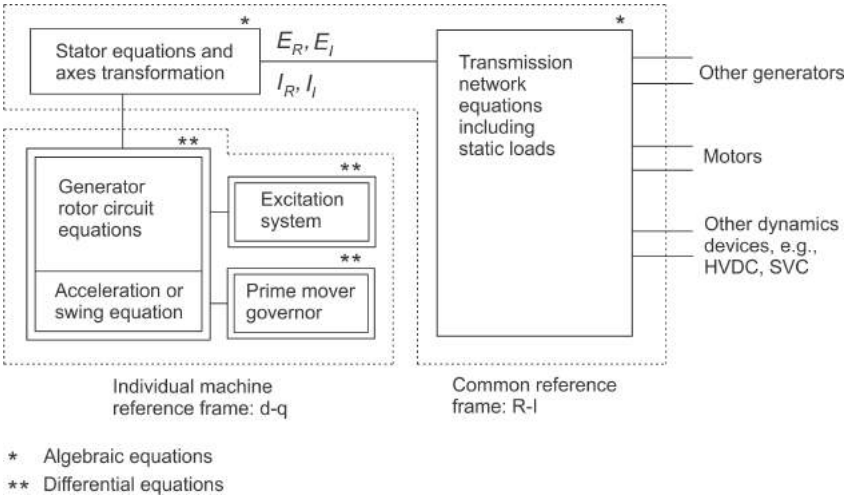

Figure 14: Structure of a transient stability simulation [25].

Mathematically, the overall system is described by a set of differential and algebraic equations of the form

$$\dot{\boldsymbol{x}} = \boldsymbol{f}(\boldsymbol{x}, \boldsymbol{V}), \tag{63}$$

$$\boldsymbol{I}(\boldsymbol{x}, \boldsymbol{V}) = \boldsymbol{Y_N V}, \tag{64}$$

where $\boldsymbol{x}$ is the state vector of the system, $\boldsymbol{V}$ is the vector of the node voltages and $\boldsymbol{I}$ is the vector of currents injected in the nodes and $\boldsymbol{Y_N}$ is the admittance matrix representing the network and loads.

The remainder of this section illustrates the application of the phasor-based modelling to respectively a synchronous machine, a transmission line, the entire AC network and a converter.

2.4.1 Synchronous generators

In the case of a synchronous machine, the choice of the mathematical order of the model (representing the number of state variables used to describe its dynamic behaviour) to be used is dependent on the type of stability study being developed and how close the generators are to the disturbance. As an illustration, the classical second order model, also known as "voltage behind transient reactance" model can be used to represent remote machines or equivalent parts of the system that are not detailed [37]. In cases where a more detailed model is needed, the fourth order two axis model provides a compromise between simplicity and accuracy and it is one of the most commonly used models in stability analysis [38]. A summary of typical synchronous generator modelling using phasor-based assumptions is provided below.

Mechanical equations The speed of a synchronous machine depends on the balance between the mechanical torque applied and the opposing electromagnetic torque. The differential equations representing the machine's mechanical behaviour are given by

$$\frac{d\delta}{dt} = \omega_r - \omega_0, \tag{65}$$

$$\frac{d\omega}{dt} = \frac{\omega_0}{2H}[\bar{T}_m - \bar{T}_e - K_D\Delta\bar{\omega}_r], \tag{66}$$

where $\bar{T}_m$ and $\bar{T}_e$ are the mechanical and electromagnetic torques, respectively, δ is the rotor angle, K_D is the damping factor.

Equation (66) is commonly referred to as the *swing equation* since it represents the swings in the rotor angle when a disturbance occurs. These equations are typically present in all generator models, regardless of their overall model order.

Stator electrical equations Starting from the dynamic description of the stator electrical equations in the dq-frame, the evolution of the flux linkages over time are given by [37]

$$e_d = \frac{d}{dt}\psi_d - \psi_q\omega_r - R_a i_d, \tag{67}$$

$$e_q = \frac{d}{dt}\psi_q + \psi_d \omega_r - R_a i_q, \tag{68}$$

where ψ_d and ψ_q are the flux linkages, i_d and i_q are the stator currents, R_a is the armature resistance and ω_r is the rotor speed.

In transient stability simulations a number of assumptions are made: (i) in order to be consistent with the simplifications applied to the surrounding AC network, the terms $d\psi_d/dt$ and $d\psi_q/dt$ representing the stator transients are neglected, by which the stator electrical equations become algebraic; (ii) the effects of speed variation on the stator voltage are neglected by assuming that ω_r remains constant. Applying these simplifications to (67)–(68), the following set of equations is obtained:

$$e_d = -\psi_q - R_a i_d, \tag{69}$$

$$e_q = \psi_d - R_a i_q. \tag{70}$$

Magnetic equations Magnetic equations relate the stator fluxes and currents to the field voltage. There are several models available and the order of the model depends on the number of state variables considered. As an example, Figure 15 illustrates the equivalent circuits for d- and q-axis for the two axis model commonly used in stability analysis.

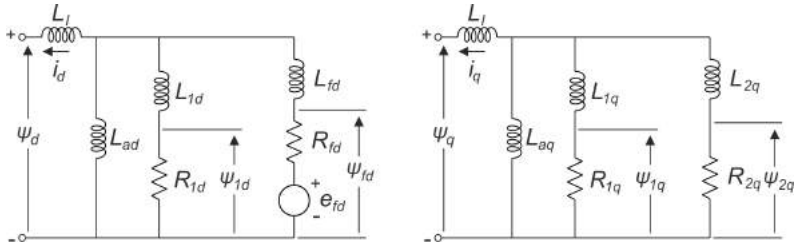

Figure 15: Equivalent machine circuit for d- and q-axis [25].

2.4.2 Transmission lines

As far as transmission lines are concerned, it is common practice to represent them by the lumped equivalent-π model, with all parameters evaluated at the nominal frequency (50 or 60 Hz). This model is obtained by considering that for short lines, the transmission line's series impedance can be lumped and represented by Z. This is equally done for the shunt admittance, which is

lumped with half of the overall value placed at both ends of the transmission line model, resulting in the admittances $Y/2$. This is illustrated in Figure 16.

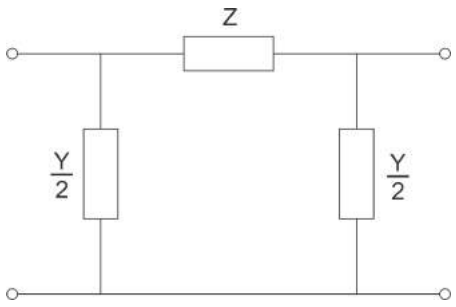

Figure 16: Lumped π circuit model for a transmission line [39].

By evaluating the parameters at nominal frequency, this model thus implicitly assumes that the relevant frequency content of the signals are mainly located around nominal frequency and do not deviate considerably from it. Detailed calculation of the parameters Z and Y can be found in [39].

2.4.3 Network

The quasi-stationary assumption allows simplifications to the representation of the AC network, including transmission lines, transformers and static loads. By using the assumption that signals present only slow dynamic responses and that the dynamics of interest do not deviate significantly from the nominal frequency (or put differently, only represent slow variations from this carrier frequency signal), the network can be represented by a constant admittance or impedance matrix calculated at the nominal frequency. That means that the network is represented by algebraic equations instead of differential equations, which simplifies significantly the study of large systems. The resulting node admittance matrix for transmission lines is represented by the equation below [25].

$$\begin{bmatrix} \hat{I}_1 \\ \hat{I}_2 \\ \dots \\ \hat{I}_n \end{bmatrix} = \begin{bmatrix} Y_{11} & Y_{12} & \cdots & Y_{1n} \\ Y_{21} & Y_{22} & \cdots & Y_{2n} \\ \vdots & \vdots & \ddots & \vdots \\ Y_{n1} & Y_{n2} & \cdots & Y_{nn} \end{bmatrix} \begin{bmatrix} \hat{V}_1 \\ \hat{V}_2 \\ \dots \\ \hat{V}_n \end{bmatrix}, \tag{71}$$

where
n is the number of nodes,
$\hat{I}_i$ is the current phasor flowing into the node,
$\hat{V}_i$ is the node voltage phasor,
Y_{ij} is the mutual admittance between nodes i and j,
Y_{ii} is the self admittance of node i.

2.4.4 Converters

In a phasor-based simulation, the Voltage Source Converter (VSC) can be modelled in a rudimentary form by a controlled voltage source on the AC side and a controlled current source on the DC side, with active power being conserved between the sides [40]. A circuit diagram for this simplified VSC model is illustrated on Figure 17.

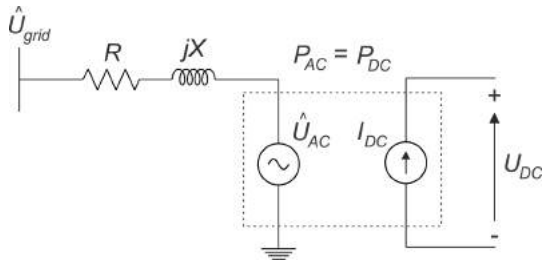

Figure 17: Simplified phasor-based model for a VSC [40].

AC side The controlled voltage source $\hat{U}_{AC}$ is given by the expression

$$\hat{U}_{AC} = (P_{m,Re} + jP_{m,Im})\frac{\sqrt{3}}{2\sqrt{2}}U_{DC}, \tag{72}$$

where $P_{m,Re}$ and $P_{m,Im}$ are the real and imaginary components of the modulation index and U_{DC} is the DC voltage. Here the modulation index $\hat{P}_m = P_{m,Re} + jP_{m,Im}$ is represented as a phasor using a global reference frame which can be set as a reference machine, voltage source or external network.

The equation that represents the AC-side dynamics is given by

$$\hat{U}_{AC} = \hat{U}_{grid} + (R + jX)\hat{I}_{AC}. \tag{73}$$

Coupling between AC and DC sides One of the ways to represent the coupling between the AC and DC sides is through the power balance equations. This can be expressed mathematically as

$$P_{AC} = \Re(\hat{U}_{AC}\hat{I}^*_{AC}) = U_{DC}I_{DC} = P_{DC}. \tag{74}$$

DC side The DC side of the converter model is composed of the controlled current source and a capacitance. For a two- or three-level VSC, the capacitance is equivalent to that of the installed capacitor bank on the output of the DC side while for the MMC the capacitance is the equivalent capacitance of the submodules and it can be written as a function of the number N of submodules and the submodule capacitance C_{SM} as

$$C_{eq} = \frac{6C_{SM}}{N}. \tag{75}$$

Due to the capacitances, the voltage U_{DC} on the DC bus can be considered stable. Therefore, from the power balance equations, the converter acts as a current source given by the expression [41]

$$I_{DC} = \frac{U^d_{AC}I^d_{AC} + U^q_{AC}I^q_{AC}}{U_{DC}}. \tag{76}$$

Control system Given the focus on slow electromechanical dynamics, it is common to only take into account the control loops that have an influence on the corresponding dynamics. As a result, low-level controls are typically not included in the modelling and only the high-level controls are implemented [40]. Further simplifications can be obtained by neglecting the dynamics of the inner current controller. The reason for this choice is that the time steps used in RMS simulation programs are large enough such that the dynamics of the faster controllers have usually died out [41]. The current controller is then represented by solving Equation (73) for the current $\hat{I}_{AC}$ [42].

Summary

The increase in the number of power electronic-interfaced devices in the grid has improved the overall grid controllability but, in turn, gave rise to dynamic issues that could eventually take the system to instability. This has

blurred the traditional distinction of which type of simulation software is appropriate for different system studies. In view of that, this section provided an overview of power system stability and some of the challenges that arise when studying AC/DC grids with the traditional software tools available. The principles behind the traditional phasor-based modelling were reviewed and it is highlighted that this approach is only valid for studying low frequency oscillations. Lastly, a summary was provided of the most commonly used phasor-based models for the main AC/DC power system components: synchronous generators, transmission lines, network and converters. Further research is still necessary to determine what types of studies can be performed with each simulation tool and to what extent the traditional phasor-based models used today are accurate for studying AC and DC systems.

References

[1] International Electrotechnical Commission: IEV 617-01-01, Available at: http://www.electropedia.org/iev/iev.nsf/display?openform&ievref=617-01-01

[2] GARPUR Consortium, "D1.1 State of the art on reliability assessment in power systems", 7th framework programme, EU Commission grant agreement 608540, 2014, Available at: http://www.garpur-project.eu/deliverables

[3] Kundur et al., "Definition and classification of power system stability IEEE/CIGRE joint task force on stability terms and definitions, IEEE Transactions on Power Systems, Vol. 19, No. 2, pp. 1387-1401, May 2004.

[4] GARPUR Consortium, "D1.2 Current practices, drivers and barriers for new reliability standards", 7th framework programme, EU Commission grant agreement 608540, 2014, Available at: http://www.garpur-project.eu/deliverables

[5] McCalley et al., "Probabilistic security assessment for power system operations", Task Force on Probabilistic Aspects of Reliability Criteria of the IEEE PES Reliability, Risk, and Probability Applications Subcommittee, IEEE Power Engineering Society General Meeting 2004.

[6] ENTSO-E: Network Code on Operational Security 24 September 2013. Available at: https://www.entsoe.eu/publications/system-operations-reports/#continental-europe-operation-handbook

[7] ENTSO-E: Continental Europe Operation Handbook – Policy 5 Emergency Operations V3.1. Available at: https://www.entsoe.eu/Documents/Publications/SOC/Continental_Europe/oh/170926_Policy_5_ver3_1_43_RGCE_Plenary_approved.pdf

[8] Capitanescua, F., "Critical review of recent advances and further developments needed in AC optimal power flow", Elsevier Electric Power Systems Research, 136 (2016) 57–68.

[9] Capitanescu, F., Glavic, M., Ernst, D. and Wehenkel, L., “Applications of Security-constrained optimal power flows”, Modern Electric Power Systems Symposium (MEPS06), Wroclaw (Poland), September 2006.

[10] Van den Bergh, K., Couckuyt, D., Delarue, E. and D’haeseleer, W., “Redispatching in an interconnected electricity system with high renewables penetration”, TME Working Paper - Energy and Environment, Electrical Power Systems Research, January 2015.

[11] Stott, B., Alsac, O., "White Paper Optimal Power Flow-Basic requirements for real-life problems and their solutions", Arizona (USA), July 2012.

[12] Capitanescua et al., “State-of-the-art, challenges, and future trends in security constrained optimal power flow”, Elsevier Electric Power Systems Research, May 2011.

[13] Stott, B., Alsac, O., Monticelli, A.J., "Security Analysis and Optimization", Proceedings of the IEEE, Vol.75, No. 12, December 1987.

[14] Van Hertem, D., Gomis-Bellmunt, O., Liang, J.,"HVDC Grids For Offshore and Supergrid of the Future", Wiley IEEE Press, February 2016.

[15] Vanfretti, L., Van Hertem, D., Gjerde, J.O., "Smart Transmission Grids Vision for Europe: Towards a Realistic Research Agenda", D. Mah et al. (eds.), Smart Grid Applications and Developments, Green Energy and Technology, Springer-Verlag London 2014

[16] Van Hertem, D., "Reliable power system operations with hybrid AC/DC grids", ICEE Seoul, 2018.

[17] Kirschen, D.S. and Jayaweera, D., “Comparison of risk-based and deterministic security assessments”, The Institution of Engineering and Technology (IET) Generation, Transmission & Distribution, Vol. 1, No. 4, July 2007.

[18] Heylen, E., Labeeuw, W., Deconinck, G. and Van Hertem, D., “Framework for Evaluating and Comparing Performance of Power System Reliability Criteria”, IEEE Transactions on Power Systems, Vol. 31, No. 6, November 2016.

[19] UCTE OH – Policy 3: Operational Security - Final Version (approved by SC on 19 March 2009). Available at: https://www.entsoe.eu/fileadmin/user_upload/_library/publications/entsoe/Operation_Handbook/Policy_3_Appendix_final.pdf

[20] ENTSO-E Guideline for Cost Benefit Analysis of Grid Development Projects, February 2015, Available at: https://docstore.entsoe.eu/Documents/SDC%20documents/TYNDP/ENTSO-E%20cost%20benefit%20analysis%20approved%20by%20the%20European%20Commission%20on%204%20February%202015.pdf

[21] Renner, R.H., Van Hertem, D., "Ancillary services in electric power systems with HVDC grids", The Institution of Engineering and Technology (IET) Generation, Transmission & Distribution, Vol.9, Iss. 11, pp. 1179-1185, August 2015.

[22] Coffrin, C., Hijazi, H.L., Van Hentenryck, P., "The QC Relaxation: A Theoretical and Computational Study on Optimal Power Flow", IEEE Transactions on Power Systems, Vol.31, No. 4, July 2016.

[23] Ergun, H., Dave, J., Van Hertem, D., Geth, F., "Optimal Power Flow for AC/DC Grids: Formulation, Convex Relaxation, Linear Approximation and Implementation", IEEE Transactions on Power Systems, under review.

[24] Geth, F., D'Hulst, R., Van Hertem, D., "Convex power flow models for scalable electricity market modelling", 24th International Conference & Exhibition on Electricity Distribution (CIRED), The Institution of Engineering and Technology (IET), Open Access Proc. J., Vol.2017, Iss. 1, pp. 989-993, June 2017.

[25] P. Kundur, *Power system stability and control.* New York: McGraw-Hill Inc., 1994.

[26] R. H. Renner, "Interactions of HVDC grids and AC power systems - operation and control," Ph.D. dissertation, KU Leuven, Leuven, 2016.

[27] N. Watson and J. Arrillaga, *Power Systems Electromagnetic Transients Simulation.* Institution of Engineering and Technology, 2007.

[28] B. Ferreira, "Understanding the challenges of converter networks and systems: Better opportunities in the future," *IEEE Power Electronics Magazine*, vol. 3, no. 2, pp. 46–49, June 2016.

[29] A. B. Salas, "Control interactions in power systems with multiple VSC HVDC converters," Ph.D. dissertation, KU Leuven, Leuven, 2018.

[30] C. Buchhagen, C. Rauscher, A. Menze, and J. Jung, "Borwin1 - first experiences with harmonic interactions in converter dominated grids," in *International ETG Congress 2015; Die Energiewende - Blueprints for the new energy age*, Nov 2015, pp. 1–7.

[31] *High Penetration of Power Electronic Interfaced Power Sources (HPoPEIPS)*, European Network of Transmission System Operators for Electricity, Brussels, Belgium, 2017.

[32] J. Beerten, O. Gomis-Bellmunt, X. Guillaud, J. Rimez, A. van der Meer, and D. V. Hertem, "Modeling and control of hvdc grids: A key challenge for the future power system," in *2014 Power Systems Computation Conference*, Aug 2014, 21 pages.

[33] S. Henschel, "Analysis of electromagnetic and electromechanical power system transients with dynamic phasors," Ph.D. dissertation, University of British Columbia, Vancouver, 1999.

[34] C. K. Alexander and M. N. O. Sadiku, *Fundamentals of Electric Circuits*, 5th ed. McGraw-Hill, 2013.

[35] S. Abourida, J. Bélanger, and V. Jalili-Marandi, "Real-time power system simulation: EMT vs. phasor," Montreal, Canada, Tech. Rep., 2016.

[36] V. Venkatasubramanian, "Tools for dynamic analysis of the general large power system using time-varying phasors," *International Journal of Electrical Power & Energy Systems*, vol. 16, no. 6, pp. 365 – 376, 1994.

[37] IEEE Std 1110-1991, "IEEE guide for synchronous generator modeling practices in stability analyses," pp. 1–79, 1991.

[38] F. Milano, *Advances in Power System Modelling, Control and Stability Analysis*. Institution of Engineering and Technology, 2016. [Online].

Available: https://app.knovel.com/hotlink/toc/id:kpAPSMCSAH/advances-in-power-system/advances-in-power-system

[39] M. E. El-Hawary, *Electrical Power Systems: Design and Analysis*. IEEE, 1995, ch. The Transmission Subsystem.

[40] W. G. B4.57, "Guide for the development of models for HVDC converters in a HVDC grid," CIGRE, Tech. Rep., 2014.

[41] R. Irnawan, F. F. da Silva, C. L. Bak, and T. C. Bregnhoj, "Evaluation of half-bridge modular multilevel converter model for vsc-hvdc transient stability studies," in *13th IET International Conference on AC and DC Power Transmission (ACDC 2017)*, Feb 2017, 6 pages.

[42] R. Hendriks, G. Paap, R. Völzke, and W. Kling, "Model of a VSC transmission scheme for wind farm connection for incorporation in power system stability studies," in *Proceedings of Power Systems Computational Conference*, 2008, pp. 14–18.

Part III
Protection

3 Power System Protection

This section starts by covering essential regulation which the TSOs follow, focusing on the voltage and frequency values which should be respected. The second section covers generic requirements for both AC and DC power system protection.

3.1 Transmission System Operator (TSO) Regulation

The aim for this section is to present the main entities responsible for the European Energy network guidelines and regulation, focusing on the operational values acceptable for the Transmission Network Operation and Protection.

As part of the EU's Third Legislative package for energy, the regulation EC No.714/2009 was created, setting out rules for governing access to the network for electricity cross-border exchanges, to ensure the proper function of the EU's internal electricity market [2]. In this context the European Network of Transmission System Operators for Electricity (ENTSO-E) and the Agency for the Cooperation of Energy Regulators (ACER) were created to develop the European Network Codes and Guidelines (rules of operation) which are then adopted by the European Commission (see Figure 18 below) and later on implemented by the member TSOs. These rules seek to ensure there security of supply, competitiveness and affordable energy for Europe's electricity transmission systems.

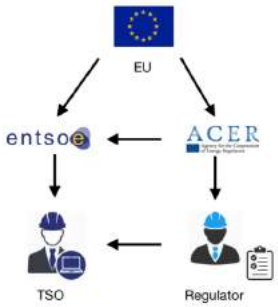

Figure 18: Regulatory relationship between European Energy entities.

The Figure 19 captures some of the main regulations and guidelines for the European Energy Transmission Operators, with a example of specific regulation from Portugal.

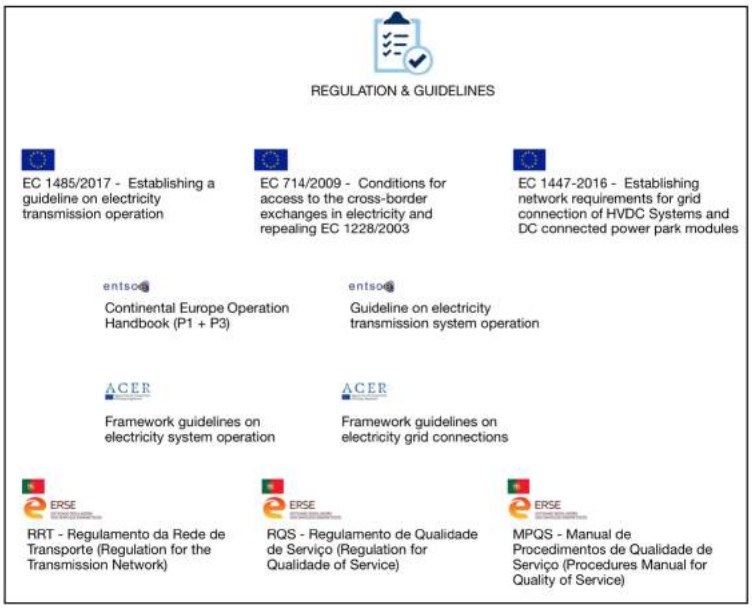

Figure 19: Main Energy and Energy Transmission Regulation in Europe.

The *"Guidelines on Electricity Transmission System Operation"* [3, 2] define operational targets for Transmission system operation. This section will be focused on the generic values for the basic parameters of networks (volt-

age limits and frequency quality). This means that some TSOs may adopt different values if they fulfill the exceptions criteria listed in the Guidelines (when applicable).

Voltage Requirements

- Table 1 and 2 define the normal voltage levels for steady-state at the connection points of the transmission systems and as operational security limits, as defined in Article 27 [2];
- The p.u. allows each TSO to define the values based on their voltage base;
- The requirements covered exclude contingency scenarios.

Synchronous area	Voltage range
Continental Europe	0,90 pu-1,118 pu
Nordic	0,90 pu-1,05 pu
Great Britain	0,90 pu-1,10 pu
Ireland and Northern Ireland	0,90 pu-1,118 pu
Baltic	0,90 pu-1,118 pu

Table 1: Voltage range at the connection point between 110 kV and 300 kV.

Synchronous area	Voltage range
Continental Europe	0,90 pu-1,118 pu
Nordic	0,90 pu-1,05 pu
Great Britain	0,90 pu-1,10 pu
Ireland and Northern Ireland	0,90 pu-1,118 pu
Baltic	0,90 pu-1,118 pu

Table 2: Voltage range at the connection point between 300 kV and 400 kV.

Frequency Quality

- Article 127 defines the frequency quality values [2];
- The nominal frequency for all synchronous areas shall be 50Hz;
- Table 3 defines the frequency quality parameters based on Article 127;

	CE	GB	IE/NI	Nordic
standard frequency range	± 50 mHz	± 200 mHz	± 200 mHz	± 100 mHz
maximum instantaneous frequency deviation	800 mHz	800 mHz	1 000 mHz	1 000 mHz
maximum steady-state frequency deviation	200 mHz	500 mHz	500 mHz	500 mHz
time to recover frequency	not used	1 minute	1 minute	not used
frequency recovery range	not used	± 500 mHz	± 500 mHz	not used
time to restore frequency	15 minutes	15 minutes	15 minutes	15 minutes
frequency restoration range	not used	± 200 mHz	± 200 mHz	± 100 mHz
alert state trigger time	5 minutes	10 minutes	10 minutes	5 minutes

Frequency quality target parameters referred to in Article 127:

Table 3: Frequency quality parameters for synchronous areas.

3.2 Power system protection requirements

3.2.1 Generic Requirements

When selecting a protection component or strategy for the grid, it must fulfill the following generic protection requirements [5]:

- **Reliability:** It is closely linked to dependability and security. Dependability relates to the correct action of the protection against faults which require intervention. Security implies that protections will not act when not required to.
- **Speed:** The protection must act fast to avoid damages to equipment or components, which is achieved by limiting the fault current within the maximum interruptible current and limiting the impact of the disturbance on the network.

- **Sensitivity:** Every fault must be detected.
- **Selectivity:** Only the faulty area and/or components of the system must be isolated. This can be achieved by defining selectivity zones.
- **Robustness:** The protection system must be able to operate even in degraded situations. Redundancy of protections is often used for achieving this requirement.
- **Stability:** After clearing the fault, the system must return to a stable operation within an acceptable time frame.

The main goals of a protection unit are to locate and isolate the fault in the shortest time possible, to minimize the impact of the fault on the equipment they are protecting, but also to allow re-energizing if the fault has been cleared.

3.2.2 DC Protection Requirements

DC system protection is an important part for a DC grid. The basic requirements for DC protection are the same as for the AC system. However, due to the different characteristics between AC and DC systems, DC system protection shows more challenges than that in AC systems.

- **DC protection components:** DC fault currents have no zero-crossings. Traditional circuit breaker cannot interrupt the fault current. The devices that will be used to clear DC faults should be developed for DC protection systems. DCCBs are more complex and costly than conventional ACCBs.
- **Speed:** DC systems have lower impedance than AC systems. And the propagation of DC faults is faster in a DC grid than that in a AC grid. The protection system should clear the DC fault in several milliseconds (5-10ms).
- **Fault locating:** Due to the fast propagation speed of DC faults, most parts of a DC grid can see the faults. The methods to discriminate a DC fault and locate a DC fault is important for a DC protection system. The time that can be used to locate a DC fault in DC networks is more critical than that in AC networks.

4 Protection of AC Transmission Systems

Emily Maggioli (supervised by Hélder Leite)

This section aims to initially provide a high level overview of AC system components, relay protection schemes and typical fault clearing progress. Then focusing on transmission network relay testing and existing models and software. And finally summarizing some of the findings on the interaction between AC-DC networks, focusing on HVDC / VSC impact on AC transmission protections. The importance of performing this investigation is relevant given the changes network paradigm with increased distributed production, investment in offshore wind-farms, but also because of discussions about interconnected country grids through HVDC technologies, which is happening in Europe and around the globe [1] (e.g. EUA GCCIA and UAE).

4.1 Challenges for AC Transmission Protections and Systems

Below are listed some of the questions identified regarding hybrid transmission networks, focusing on the interaction of HVDC and VSC technologies on AC Protection.

A. Hybrid system simulation and interactions:

- Dual operating mode for protections: This issue has been identified for the microgrids, as there is a difference in the magnitudes of short-circuit current in grid-connected and islanded modes [7]. This dual operation mode could be relevant for wider grid studies when there is black start and the system transitions from a weak power system to a strong one.
- Inertialess systems and stability of the AC Network: The AC system stability is governed by the synchronous machine capacity. However with the increase of inertialess system, the effect on the AC grid stability is unknown.

- Impact of controller gains on AC protections [8]. Challenges to the existing networks in different aspects including steady state, dynamic, and transient stability [40].
- Interactions between AC-DC networks: Numerous studies have been made on the interaction, but it is not fully known the extent of the interaction between the grids and the impact on power system protection of the connected countries (including the communication networks between relays and operators, or between relays).

B. Network modelling and Relay testing:

- Simplifications for studying AC-DC Grids: Generally for the analysis of AC or DC grids, there are simplifications made to the grid which is not the focus of the study. One of the points raised by [9] is to question the results obtained using simplifications, if there are any interactions which are being missed due to the simplifications made in studies.
- Testing relays in more realistic scenarios to verify relay parameters and real behaviour [10] - the authors have found some mis-match between the expected behaviour and the actual behaviour, which could lead to disturbances in the network.

4.2 AC Protection components

4.2.1 Basic components

The basic power system protections are generally composed by: Voltage and Current Transformers (VT and CT), Relays, Fuses, Circuit Breakers (CB), DC batteries (Table 4). It should be noted that some of the components used may vary depending on the network voltage.

4.2.2 Relay Protection Schemes

The aim of this section is to give a short overview of the main relay schemes and their application, as well as relevant guidelines for Transmission networks.

Based on literature review [11], [13], [15], there seem to be a variety of ways for classifying relay schemes, which are captured in the table below (Table 5).

Power System Protection – Basic Components
1. *Voltage transformers and current transformers*: To monitor and give accurate feedback about the healthiness of a system.
2. *Relays*: To convert the signals from the monitoring devices, and give instructions to open a circuit under faulty conditions or to give alarms when the equipment being protected, is approaching towards possible destruction.
3. *Fuses*: Self-destructing to save the downstream equipment being protected.
4. *Circuit breakers*: These are used to make circuits carrying enormous currents, and also to break the circuit carrying the fault currents for a few cycles based on feedback from the relays.
5. *DC batteries*: These give uninterrupted power source to the relays and breakers that is independent of the main power source being protected.

Table 4: Power system protection basic components [5].

Relay classification				
Transmission lines	Protected object	Principle	Function	Type
1) Non-pilot - Over-current - Directional over-current - Distance Protection 2) Pilot - Current differential - AC Pilot wire - Phase comparison - Directional comparison - Superimposed principle and directional traveling wave 3) Others	• Line • Feeder • Transformer • Generator • Busbar • Motor • etc	• Distance • Differential • Over-current • Residual current (Directional earth fault) • Over/under frequency • Over/under voltage • Directional	1) Protective 2) Regulating 3) Reclosing, synchronism check and synchronising 4) Monitoring 5) Auxiliary	• Electromechanical • Static • Digital • Numerical

Table 5: Relay classification simplified overview.

Some of the basic operating principles of relays are covered below:

- **Differential**
  The differential protection, as the name suggests is based on the difference between voltage or current between two circuits (using the same unit for comparison). Figure 20 illustrates an example of a pilot current differential protection, as the information is compared between the two relays (local and remote relay) via the communication link. When there is no fault, the difference is equal to zero or to the tapped loads on the line. In reality these measurements can contain errors due to CT errors, ration mismatch and line-charging currents.

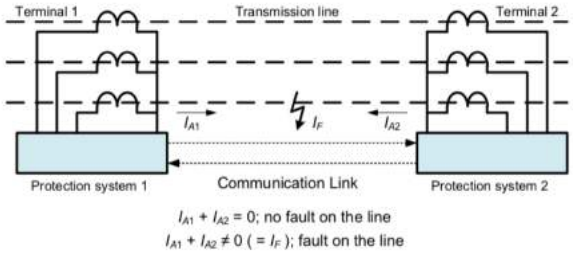

Figure 20: Pilot current differential protection of a transmission line [11].

The example below shows a non-pilot current differential protection scheme (Figure 21).

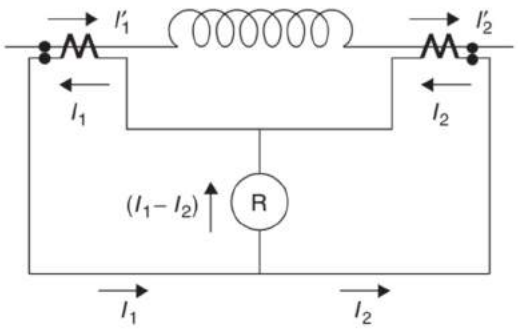

Figure 21: Non-pilot current differential protection of a transmission line [16].

- **Level Detector**
  Over-current detection can be achieved through a level detector relay and is considered the simplest form of protection. The relay trips the circuit breaker when the current is above a defined setting, known as the pickup value, based on the fact that the fault current is always greater than the operating current [13].

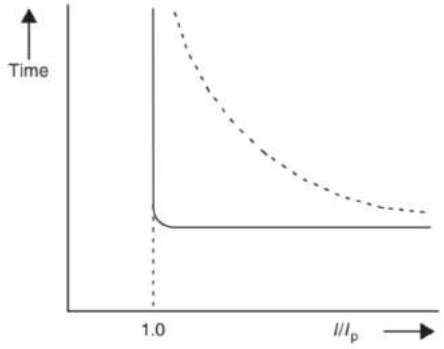

Figure 22: Level protection [13].

- **Distance**
  On transmission lines and feeders, the length, voltage, and configuration of the line may make this principle uneconomical. Instead of comparing the local line current with the far-end line current, the relay compares the local current with the local voltage. This, in effect, is a measurement of the impedance of the line as seen from the relay terminal. An impedance relay relies on the fact that the length of the line (i.e., its distance) for a given conductor diameter and spacing determines its impedance [13].

- **Magnitude**
  Under/over voltage and over-currents can be detected using the magnitude detection principle.

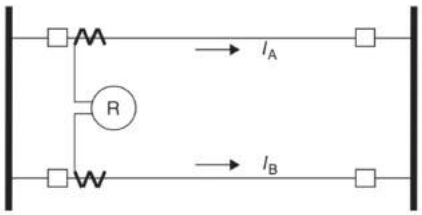

Figure 23: Magnitude comparison relaying for two parallel transmission lines [13].

The principle is based on the comparison between one or more quan-

tities with each other, including a defined tolerance. If the defined magnitude is excited then this will trip the relay. For example, comparing the current magnitude of two lines, IA and IB, if |IB|+ X (where X is a suitable tolerance) an the line B is not open, the relay would detect a fault on the line if this value was exceeded (|IB|+ X) [13].

- **Protection zones**
  The figure below shows the typical relay primary protection zones (Figure 24).

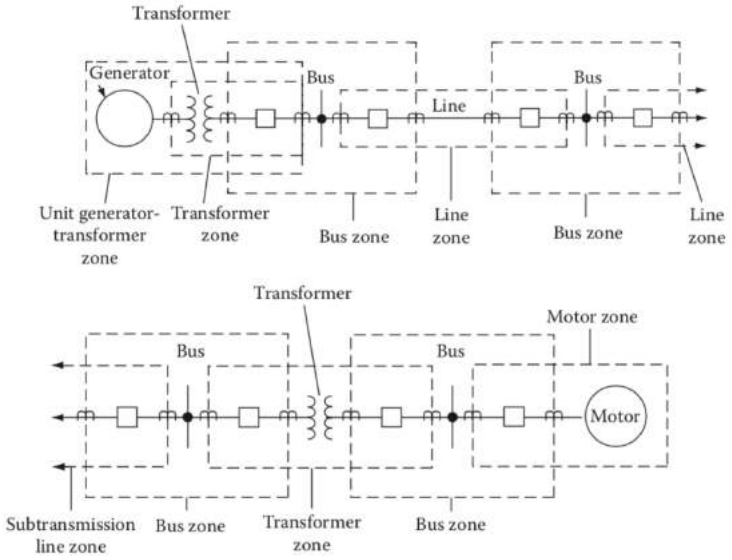

Figure 24: Typical relay primary protection zones [16].

For further details about applying relays to Transmission Networks, IEEE developed the "Guidelines for Protective Relay Applications to Transmission Lines" [11], which goes into further detail of the protection scheme variants and network variables considerations.

4.2.3 The Portuguese Transmission Network - Example

The section above listed the possible protection schemes available and the typical classifications made for protection relays. This section now aims at showing an example of the Portuguese transmission network, listing the specific protection schemes used in a real world context, based on [14].

- Differential protection;
- Distance protection;
- Pilot protection;
- Phase magnitude;
- Directional earth protection;
- MHO;
- Circuit breaker function;
- Switch-on-to-fault;
- Re-connection function;
- Synchrocheck (function checking the synchronism in the system).

4.3 AC Network fault time frame and fault clearing progress

This section intents to give a brief overview of fault propagation and fault clearing windows available in AC Transmission networks.

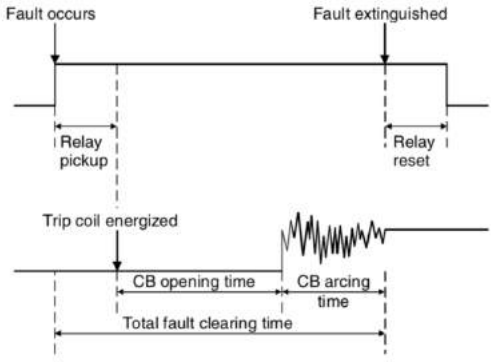

Figure 25: Typical fault clearing time frame [5].

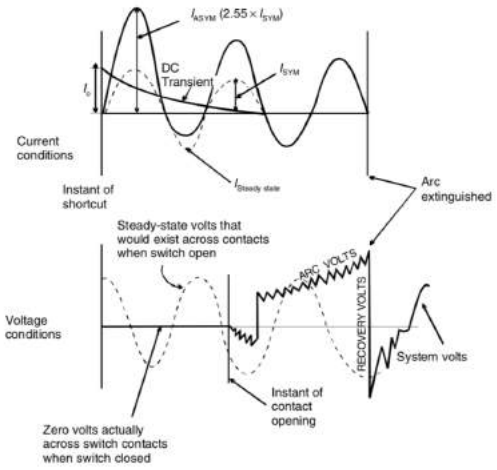

Figure 26: Behaviour under fault conditions [5].

In AC grids, the fault clearing time is limited by the synchronous generators ability to keep the synchronism. The critical clearing time is typically in the order of hundreds of milliseconds [6]. The total "fault clearing" is made up by the relay time (detect and trigger the CB) and the CB interrupting time. For HV (High Voltage) and EHV (Extra High Voltage) transmission systems, normal relay times range between 15-30ms and the circuit-breaker interrupting time range between 30-70ms [17].

4.4 Models for AC Protection focused studies

Based on the classification of the AC grid stability, Figures 10 and 11, and the relevant time frame for AC fault clearing (discussed in Section 4.3), it is possible to narrow down the sections relevant to power system protections, which are related to rotor angle stability, frequency stability, and AC voltage stability.

Protection units are modelled according to their application (what component they are protecting) and to ensure the network operational values discussed in Section 3.1 are respected. This section aims at listing some of the models, methods and softwares for AC power system protection studies.

4.4.1 Relay testing methodology overview

The methodology proposed in [18] is a high level overview for relay testing. The overall goal for testing relays is to use inputs that resemble the inputs that are seen by the component in a physical power system, to observe the actual behaviour of the device. Below are some of the applications of the approach or steps defined:

- Troubleshooting relay mis-operation (understand fault, adjust settings and lessons learnt);
- Equipment procurement (to test relay batches and compare behaviour for a specific network/application);
- Testing relay settings.

Below is a summary of the step by step description of [18].

Step 1. Deciding between relay model or physical relay To decide between using a physical or simulated relay model. Typically models are used for preliminary testing and/or evaluation of relays, whereas physical relays are used for testing afterwards to check the defined parameters.

Step 2. Interfacing requirements It is necessary to know what the interface(s) between the relay and power system will be, what other components are connected to the relay and how it gets the inputs from the grid. Thus ensuring that the received and transmitted signals match that of the desired test or real System.

1. *Define relay interfaces*: What components are connected to the relay, how it gets its system data.
   - Instrument transformer secondary (for voltage and current measurements)
   - Circuit Breaker or other control device (contact status)
   - Network Operator interface (communication or actuators)
2. *Interface between relay and power system:* How does the relay interface with the power system. The difference from the previous step is these are focused on how the relay interfaces with the system and other relays or control equipment.

- Instrument Transformers (like CT and VT): the signals received by the relays pass through, so they require the correct representation (most of the power system simulation packages will generate the analog waveforms that relate to the primary (network) level of voltage and current signals)
- Control equipment: correct contact modelling (accurate representation of the contact changes associated with operation of circuit breaker and communication channel during the fault clearing sequences)
- Communication channels (possible impacts of the faults on the channel behaviour needs to be considered)

3. *Representing dynamic interactions:* It is important to reflect dynamic interactions between the power system and the relays during both fault and normal operating conditions, as it is possible that normal operations may be misinterpreted as faults. The table below summarizes some relevant dynamic interactions.

Event	Dynamic Interaction
Autoreclosing	Automatic change of power system model
Power swing	Power oscilations between the equivalent sources
Switching transients	Circuit breaker switching sequences
Line energizing to a "Hot" bus	Synchronizing and synchro-check

Table 6: Summary of dynamic interaction requirements [18].

4. *Field vs. laboratory:* This will depend on the choice between physical or modelled relays firstly. In the case of modelled relays they will be connected to the simulation. Regarding physical relays, if they are tested in the laboratory, they can be physically placed next to each other and connected to the simulation. Whereas in the field, it must be possible to inject the test signals to physical relays.

Step 3. Interfacing options This part of the methodology is where model and the testing environment choices are made.

1. *Interfacing relay models*

2. *Interfacing physical relays:* To interface with physical relays it is necessary to have a D/A system, which allows to convert the transient signals simulated by the programs or recorded via digital fault recorder. The interface can be: open loop or real-time interface (requires a bi-directional link between the network models and the physical relay). The open-loop interface is used to replay fault condition (signals) into the relay, but the feedback is only captured for recording purposes.

4.4.2 Relay models and Interface between relay and power system models

As mentioned in Section 2.1, EMTP software is used in electromagnetic transient studies, including under fault conditions, which is in the interest for protection studies. Since the creation of the first EMT software, others have been developed, like the ATP (Alternate Transient Program) and PSCAD/EMTDC [34].

For power system protection studies, using relay models has various advantages, as it allows to design new relay prototypes, test relay parameters, personal training, as it allows to observe the processing of input and output signals in detail, during the relay's operation [34]. For these reasons there has been progress made towards integrating modelling software (e.g. MATLAB, FORTRAN) [34], used to define the relays, with EMTP and ATP software [34]. But also to test physical relays using power system models. Table 7 summarizes some of the relay modelling programs and the network EMTP type programs by [18].

There are also alternative programs which integrate the relay models and EMTP capabilities specifically for protection studies, which is the case for CAPE and ASPEN.

Table 7 summarizes some of these softwares, the integration of relay models and some proposed relay models. The first line indicates the references relevant for relay models or programs, while the second column contains references for the simulating programs. The lines across indicate the combination of the relay model and the network program.

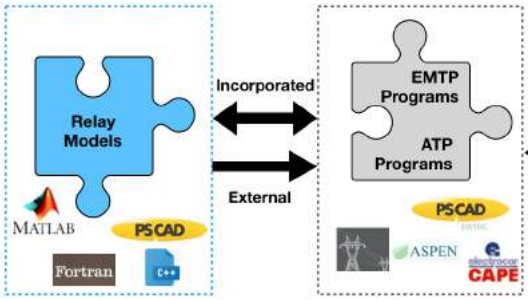

Figure 27: Interaction between models and simulation software.

The figure below illustrates an example of the various interactions between the user of the program (when there is a user interface), the relay model and the simulation program (ATP in this example).

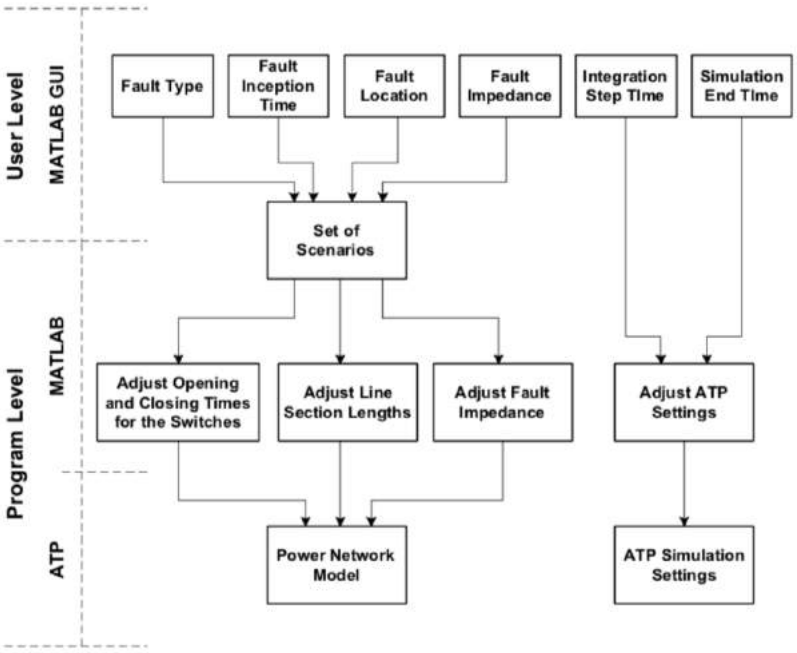

Figure 28: Hierarchy between user and program levels [18].

Some methodologies, like the one proposed by [34], propose a new approach in relay modelling, as the relays are modelled in the software PLSA

			Relay Models	TACS	MATLAB SIMULINK	C++	FORTRAN
			[19, 24] [19]	[20, 21] [22, 23] [24]	[39] [40]		
Network	EMTP	[25]		[20, 21] [22, 23] [24]	[25] [34]	[27] [28]	[36]
	ATP	[42]	[29, 30] [31, 32]		[37]		
	EMTDC	[41] [20]					
	PSCAD/ EMTDC				[38]		[34]
	PSSE/ EMTDC	[33]					
	CAPE	[44]					
	ASPEN	[45]					

Table 7: Interfacing relay models based on [18].

and embedded in the PSCAD/EMTDC code. PLSA was developed by the authors as a user-friendly software used to generate the relay models from parameters specified by the user. The code is then incorporated in the EMT software, this case PSCAD/EMTDC, so that the simulation includes both the modelled power system and the modelled relay. The advantage of using this methodology is to avoid compiling the component models and the EMTP separately, so all the signals are processed together.

Methodologies like the ones by [36, 35, 37, 38]. All of the above mentioned methodologies successfully incorporated models developed internal softwares with EMTP. The disadvantage, when compared to A, is that ex-

ternal programs must compiled separately or the subroutines of EMTP must be changed to accept external sub-routines [34].

4.4.3 Relay testing softwares

It is worth noting that there exist commercial softwares specifically developed for relay testing and which are used by different TSOs and DSOs around the world. PSS®E (PSS/E), Powertech TSA TTM, and PowerWorld Simulator, allow inclusion of some generic protection scheme elements, but this capability is not completely adequate or usually employed by utility planning engineers. So there are some specific software packages such as CAPE and ASPEN [40], employed for this purpose. These softwares have inbuilt relay models (or even databases) based on commercial relays, which can be added to real size grids for testing relay parameters or behaviour. The relays are defined based on the parameters and settings by the user.

4.4.4 Relay communication models

Relays nowadays are able to communicate between them, but can also be controlled by the network operator (pilot schemes). For this reason, the communication between relays and operator cannot be ignored when assessing the impact of HVDC grids or wind farms on relays, such as mentioned in [40]. This study refers to some of the existing models for relay communication.

4.4.5 VSC Modelling for grid studies

The guide [4] proposes various models for VSC, but only the type 5 and 6 are of interest, because they capture the variables required for electromagnetic transient studies that, as explained above are used for relay model testing.

- **Type 5: Average Value Models (AVM) based on switching functions** - The AC and DC system characteristics are modeled as controlled current and voltage sources, including the harmonic content resulting from the conversion process. The assumption in this module is that the capacitor voltages are balanced and it can only be implemented in EMT tools, which is the case of the study of AC-DC transients and design harmonic studies.

- **Type 6: Simplified Average Value Models**- The AC and DC characteristics are modeled as controlled current and voltage sources, similarly to type 5 (mentioned above). The difference is that they do not produce any switching harmonics. This type of model can be implemented in EMT and phasor-domain transient simulation tools. For EMT implementations, one of the advantages is that there is different detail in the upper and lower level controls (upper more detailed), which improves the simulation speed. Additionally this model may be suitable for large system AC/DC grid simulations.

4.4.6 Simulation Softwares and Tools

This section summarizes the softwares and/or tools mentioned in previous sections, and others which were not mentioned but have also been listed as available tools.

Software	Study types & Application
1. MATLAB SIMULINK	1.1. Used to develop models, particularly through SIMULINK 1.2. Used as an add-on for existing dynamic/EMTP software 1.3. User graphical interface
2. PSCAD	2.1. User graphical interface 2.2. Protection studies 2.3. EMT simulations
3. MATACDC	3.1. Uses sequential power flow approach. 3.2. Allows the study of the steady-state interactions between multiple non synchronized AC grids and DC systems based on VSC HVDC technology. 3.3. Open Source program with similar syntax to manpower
4. PLSA	4.1. Electromagnetic studies for protective relay models (integration of relay models and EMTP) 4.2. User graphical interface
5. PSS/E	5.1. Modelling protection for dynamic simulation 5.2. Dynamic power system simulation
6. CAPE	6.1. Modelling protection for dynamic simulation 6.2. Dynamic power system simulation
7. ASPEN	7.1. Specific for Power System Protection studies

Table 8: Some available power system protection Softwares and Tools.

4.5 Interaction between AC and DC Grids: focused on the impact on AC Protections

This section captures some of the findings or questions regarding the interaction between AC-DC networks, focused on imbalances caused to the AC grid and the impact on AC power system protections.

The figure below shows an example of a modern electrical grid, which demonstrates the shift in the network paradigm and operation philosophy: 1) Distributed generation - Offshore wind farms; 2) Greater interconnection between transmission grids. The distance of the connections have led to a preference of HVDC technology over AC, due to the fact that less lines are used for the same bulk power, which means a simpler implementation, but also due to the absence of reactive power. This is observed in HVDC connections in Europe and around the world [12]. One of the issues with using new technology is the impact on the existing infrastructures, particularly the AC grid and specifically AC Protection.

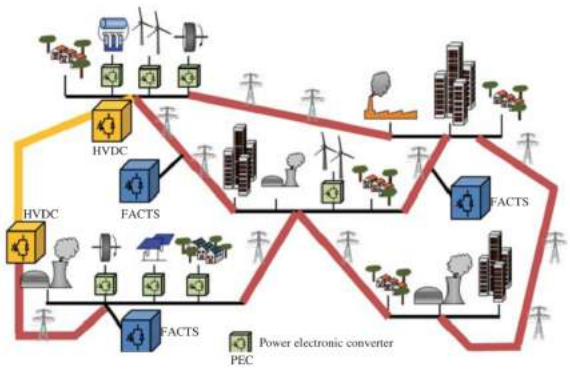

Figure 29: Modern scenario of the electrical grid [46].

Table 9 below provides an detailed overview of the AC-DC interactions and disturbances presented by [47]. These interactions and disturbances have been ranked in order of increasing time duration / decreasing frequency.

(Ranked in order of increasing time duration/decreasing frequency)

Interaction/Disturbing phenomena	Cause/Source/Effect of Phenomena	Time Duration/ Frequency Domain	Controls Influencing, Affecting or Controlling Phenomena
1. Steep front Surges/Overvoltages	Lightning, certain element switching	Generally <1ms	Controlled by equipment designs and arresters.
2.Commutation failures (start of)	Inverter side AC faults, AC voltage phase shifts or distortions, element switching	Commutation-by-commutation Cycle-by-cycle	Commutation margin angle (gamma) setting. Temporary gamma adjustments or "gamma kick" controls
3.Transient / switching surge overvoltage	Element switchings such as filter banks.	From few ms to few cycles	Controlled by equipment designs, arresters or operating switching restrictions.
4.Temporary overvoltage (TOV's)	Load rejections, transformer energizations, fault clearing.	From few cycles to usually <few hundreds ms. TOV's may be of fundamental frequency but may also involve low order (2^{nd} to 5^{th}) harmonic resonances or interactions.	DC fast firing angle control of reactive power. SVC or synchronous compensation control / actions. Fast filter / capacitor bank switching.
5. Recovery from AC faults.		Usually from about 100ms to 500ms. May involve TOV's, low order (2^{nd} to 5^{th}) harmonic distortion or interactions.	SVC or synchronous compensation control / actions. DC voltage-dependent-current limits (VDCL) applications. DC power (volt. /current) ramp-up. Fast filter / capacitor bank switching.
6. Recovery from DC fault		Usually from about 200ms to 700ms	Deionization set time (approx. 100ms minimum). VDCL applications. DC power (voltage/current) ramp up.
7. Transient AC undervoltages.	Remote AC faults (could be slow clearing), transformer energizations, sudden load increases, tripping of compensation elements.	From few cycles to usually <500ms. Involves fundamental frequency on AC and may involve power / voltage instability at zero frequency possibly leading to system voltage collapse. This instability may take seconds or even minutes.	DC fast firing angle control of active / reactive power. SVC or synchronous compensation control / actions. VDCL applications. DC current 'holding' / maximum DC current limiting. DC power reduction / amp-down. AC filters switching control. Tap changers.

Interaction/Disturbing phenomena	Cause/Source/Effect of Phenomena	Time Duration/ Frequency Domain	Controls Influencing, Affecting or Controlling Phenomena
8. Super-synchronous or "harmonic " instabilities	May grow from small perturbations and may involve control loops, transfer functions, harmonic resonances and transfers, non-theoretical harmonics, transformer saturation, Ferro resonance.	Frequency > fundamental	Instabilities generally cured by DC control design (such as phase-locked oscillator), by choice of control parameters, or by addition of special DC controls. Addition of special filters (2^{nd}, 3^{rd}, 5^{th}, etc.) SVC controls (2^{nd} harmonic)
9. Sub-synchronous instabilities	Control instability at frequency not necessarily related to AC system resonances; or may involve system sub-synchronous resonances and machine tensional mechanical oscillations	From about 5Hz to < fundamental frequency.	Prevented by proper DC control strategies, parameters or by addition of special DC controls. SVC controls.
10. Low-frequency (electromechanical) instabilities.	May involve system steady state or small disturbance stability for inter-machine or inter-area oscillations; may involve system transient stability for faults and major disturbances.	From about 0.1Hz to 3Hz.	Supplementary DC damping power control / modulation based on measured AC frequency, phase angle, voltage deviations, or power changes in parallel AC line. Basic DC responses such as recovery from faults, commutation failure, and compensation controls and actions may affect overall stability. Such things as machine damper windings (at higher frequencies) and power system stabilizer signals on machine voltage regulators (to damp oscillatory modes) in the AC system may not be directly influenced by the DC system or DC controls.
11. Steady state power frequency instability / excursions	May involve turbine governors, load-supply unbalance, certain AC line trips, load rejections, machine tripping, islanding; may involve steady state stability for governor oscillations (example –isolated generation feeding DC).	<0.3Hz.	Turbine governor control. Absolute frequency control by some power / frequency characteristic or droop control on DC. Discrete DC power changes for certain AC line or machine trips. Coordination of DC power control with machine control and characteristics.

Table 9: AC/DC interactions and disturbances [47].

This sections aims at capturing the high level interaction list, based on [4], [47], [48], which take into consideration the fact that VSC technology has become a preference over the LCC converter technology. Which are as follows:

- **DC Voltage droop settings:** This control action in the DC system

can be seen by the AC system as an abrupt power change, since the time frames for DC are much smaller than those for AC system stability problems. The AC protection units can trigger incorrectly as this could me misinterpreted as fault condition.

- **Time frame for hybrid network studies:** The study mentioned in [4] highlights the importance of developing an integrated detailed AC and DC system dynamic model, in order to capture possible interactions of the two systems, despite the general understanding that they operate in different time frames.

- **Frequency stability:** Changes in load demand cause a change to the AC system frequency, which is restored by altering the generation as a whole. This is a slow process, as it is accomplished by generator speed controllers. Through HVDC active power injection, which is done through VSC by drawing energy from the remote network, the frequency can be stabilised or controlled much faster than a normally controlled generator.

- **Short circuit level:** When AC networks expand, this will increase the short circuit level of the system, which means the switchgear need to be checked (possibly upgraded or replaced) and the relay parameters require revision. When adding HVDC link, due the component characteristics, it does not significantly increase short circuit current, when compared to conventional generation sources.

- **Reactive Power:** One of the VSC primary advantage compared to the LCC, is that they can independently control active and reactive power. But also, the reactive power can be controlled independently at each converter station. This allows VSC to support the AC system with reactive power. One of the issues is that connected to the AC systems is also the conventional Reactive Power Compensation equipment (e.g. shunt reactors). So the designers need to ensure the coordination between the converter station and the AC reactive power controls. If this is not achieved, one of the consequences is the "hunting" by AC system reactive power controls and excessive operation of AC breakers, which would compromise asset lifetime.

- **Harmonics:** The primary harmonic production from voltage source converters is in the form of voltage harmonics, which leads to dis-

tortion of the current waveform and consequently, current harmonics. Generally these harmonics are filtered by shunt filters, but this may not be possible for 100% of time, so occasionally or under specific circumstances, some of the harmonics will enter the AC system. It is important to note that the converter produces harmonics close to the effective frequency or multiples of the switching frequency. Which require further investigation to determine how to best introduce the filtering capabilities in protective relays. One of the mentioned scenarios is the ground loop current, which could lead to half-wave saturation of the iron core of the CT or VT, affecting the differential protection due to harmonics and current distortion.

- **AC Response to DC faults:** In the event of an internal VSC substation fault, the converter's valve is exposed to over voltage and overcurrent values greater than those experienced during an AC system fault. The type of fault, its location, transformer windings and grounding of the substation will determine the fault severity and characteristics. As the VSC is not able to block DC fault current, currently these will trip the AC CB.

The above mentioned interactions can be used for testing AC relays under specific conditions, and understanding some of the time frames behind these interactions is an important factor for correctly selecting models and simulation times.

5 Protection of DC Grids

Wei Liu (supervised by Jun Liang)

With the increasing demands of integrating renewable energy to grids, more and more attentions have focused on VSC-based HVDC systems. Modular multilevel converters (MMCs) are one of the most promising candidates that will be used to build DC grids. There is a trend that the existing HVDC links will be connected and make up an Multi-terminal DC (MTDC) system in future.

DC protection is one of the challenges when operating a VSC-based HVDC link or MTDC system. DC fault currents have no zero crossings and the propagation of DC faults is faster than AC faults due to the low impedance in DC grid. What is more, the semiconductor devices within DC grids, such as converters, DC circuit breakers cannot withstand overrating for a long time. The DC protection system should detect and clear the faults within several milliseconds (5-10ms). The protection system should include both primary protection and backup protection. Different protection methods are also needed in order to locate and isolate the DC faults.

Half-bridge MMCs (HB-MMCs) cannot interrupt DC fault currents due to the free wheeling diodes after being blocked as the two-level VSC. DC circuit breakers have been proposed and used in the DC grids to protect the DC faults. The time response of DCCBs is normally with few milliseconds. Mechanical DCCBs, solid state DCCBs, and hybrid DCCBs are the current technologies used to implement a DCCB. Considering the capital costs, power losses and operation speed of different kinds of DCCBs, hybrid DCCBs are mostly employed in HB-MMC HVDC systems.

Topologies with capability of DC fault handling is another solution in terms of DC side faults. Full-bridge sub-modules and other sub-modules are proposed to handle the DC faults. However, due to the extra power losses and costs caused by the new topologies, they are not widely adopted in current projects. With the increasing power demands, overhead line (OHL) will be used in MMC-based HVDC systems. Full bridge MMCs are more suitable in OHL systems than HB-MMCs due to the DC fault handling capability of FB-MMCs.

AC faults are also important aspects that need to be taken into consider-

ation in a hybrid AC/DC system. Grid-side AC faults and converter-side AC faults will cause different consequences. Grid-side AC faults can generate an balanced condition for the converter. Converters should have the low-voltage-ride-through (LVRT) capability according to the grid code. Converter-side AC faults cause a more severe condition. Protection system should block the converter and the main target is to avoid the damages caused by the faults.

DC protection is a key technology in systems with AC and DC networks. A DC protection system must clear a DC fault within several milliseconds. To ensure the stability and reliability of the whole system, both DC protection and AC protection must work coordinately.

5.1 Challenges for DC Protections

- DC fault current with no zero crossings: All mechanical circuit breakers (CBs) need natural zero crossing to interrupt the current arc. The absence of a natural zero crossing current make it difficult for the ACCB to be used in the DC grid directly. DCCBs should be developed and employed for DC protection. But they are more complex and costly [65].

- Low impedance in DC grids: In an AC system the impedances are made up of resistive and reactive parts, where reactive components ($2\pi fL$) may reach 10-20 times the resistive parts. However for DC grid, the series impedance is quite smaller than the AC grid because of the absence of transformers. And the steady magnitude of the DC component only takes into account the resistive parts. Therefore the rising time of the fault current is quite shorter compared to the AC system faults. The operating time for the DC protection should be within few milliseconds [65].

- Fault locating methods: Locating the faults in DC grids is more difficult because of the low impedances. Fault current limiters (FCLs) should be added to limit the di/dt and to help to locate the faults [65].

- Semiconductor-based devices in DC grid: Voltage-source converters, DCCBs and DC/DC converters in DC grids consist of semiconductor-based devices, which have small thermal constants and small capability of over-current and -voltage ratings. There is a strong requirement to clear the fault in a short time [65].

5.2 Modelling Technique on HVDC Converters

Based on the different objectives, there are different models for VSC-based converters. The summary of the most common methods are presented as follows:

- Full Physics Based models: Switches and diodes are represented by differential equations. It is not suitable for the grid models due to its complex character and time consumption problems [49].

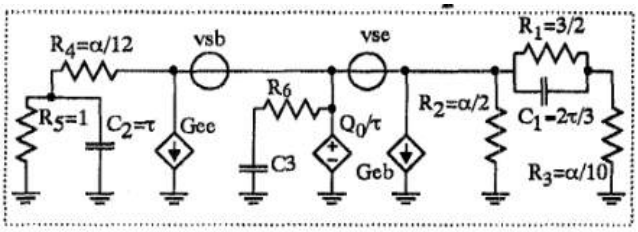

Figure 30: Full physics based model.

- Full Detail Models: The devices are modelled by the non-linear resistor and the conduction mode of the device is taken into consideration by this model. The IGBT switches are modelled using an ideal controlled switch and two non-ideal diodes illustrated in Figure 31. Full detailed models enable accurate analysis of the current distributions, but they can not accurately handle switching losses. The DC fault and submodule fault can be analyzed by the model.

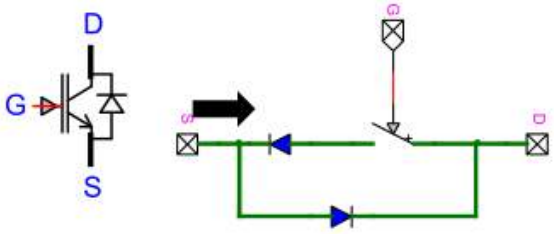

Figure 31: IGBT models.

- Models based on Simplified Switchable Resistances: The switching devices are represented by two-value resistors. The simplified model can

promote the speed of the simulation by simplifying the model of the power electronic switches. DC faults and internal faults of the MMC can be simulated using this kind of model.

- Detailed Equivalent Circuit Models: The model based on Thevenin/Norton equivalent method. Reduced electrical nodes can be acquired by the method and the influence of the capacitor in each module can be included [50]. The main idea is to reduce the number of electrical nodes in converter mode while maintaining simulation accuracy. Take HB submodules as an example, the equivalent model can be represented as shown in Figure 32. Finally all SMs in series can be replaced by an equivalent Thevenin circuit. This method can reduce the electrical nodes needed for the modelling and the nodes are independent with the SMs in the converter [51]. The model can be used to analyze the AC and DC performance, submodule level control and capacitor balancing algorithms.

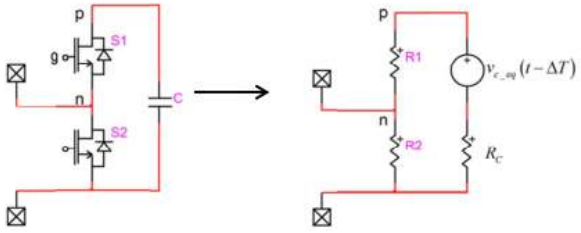

Figure 32: HB submodules models based on Detailed Equivalent Circuit.

- Average Value Models (AVM) based on switching functions: The controlled voltage and current sources are used to model the AC and DC side characteristics. The harmonics are also included and the model can be used to evaluate the DC grid system performance. The computational burden can be reduced by replicating the average response of switching device based on the controlled sources or the average functions.

- Simplified Average Value Models (AVM): The AC and DC side characteristics are modelled as controlled current and voltage sources. The controlled sources generated the waveform just as the control signal.

The switching harmonics and the internal characteristics are eliminated by the model. It can be used in large system AC/DC simulation.

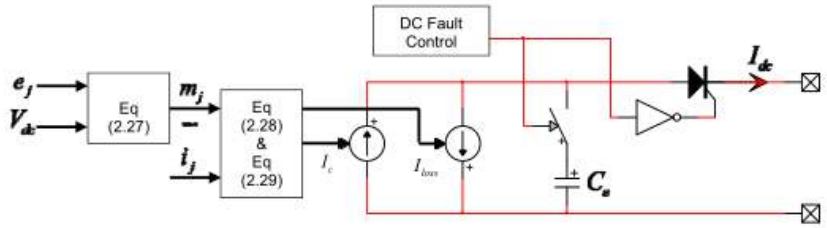

Figure 33: DC side representation of the MMC.

- RMS Load-Flow Models. This model takes the steady-state converter output into consideration but no transient modelling. This model is used mainly in hybrid AC/DC grids for power flow analysis purposes. And power losses can be added to the model [52]. And the model can be used to analyse the algorithm on the power flow [53], [54].

5.3 DC Grid Protection system

5.3.1 Time frame of DC protection Systems

A protection system is an essential part for the operation of the system. The basic protection requirements for the protection system of either AC or DC grids include [55]:

- Reliability: The protection system can operate during the fault and do not operate during other disturbances.
- Speed: Detection and isolation of the faults should be fast enough not to cause damage to the component of the system devices.
- Selectivity: The protection action should keep in the designed protection zone.

The advantage of an MTDC system is the low impedance in the transmission lines, which will generate lower power losses. However the low impedance DC grid will result in a huge inrush current during the DC fault in a very

short time scale. The protection system for the DC grid should isolate the fault within several milliseconds. And the maximum allowed current can be reached in 10ms [56]. The operation time of the different stages of the protection system must not exceed the acceptable protection time. And except of the primary protection, the secondary protection and back-up protection should be designed properly collaborated with the primary protection. In Figure 34, the protection system for the DC grid is shown.

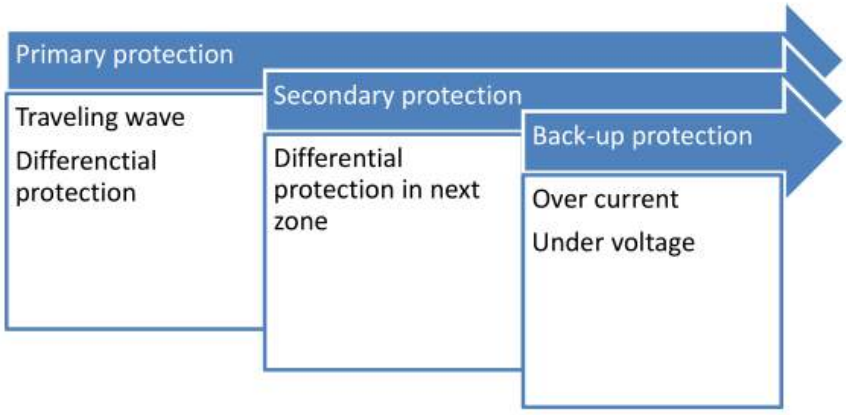

Figure 34: DC protection system [57].

The protection speed for the AC and DC system is quite different. A typical fault clearing time in AC systems is normally 4 cycles/80ms for the 50Hz system. The relay tripping needs 2 cycles and the operating time of the AC breaker consumes another 2 cycles. The time response for the AC protection is shown in Figure 35.

The primary protection for the AC system is around 80ms and the time delay for the backup protection is around 300ms. While for the DC protection, the time respond time for the relay is normally within 1ms as shown in Figure 36. The time response for the primary protection is around several milliseconds. The backup protection will be active within few milliseconds if the primary protection fail to clear the faults.

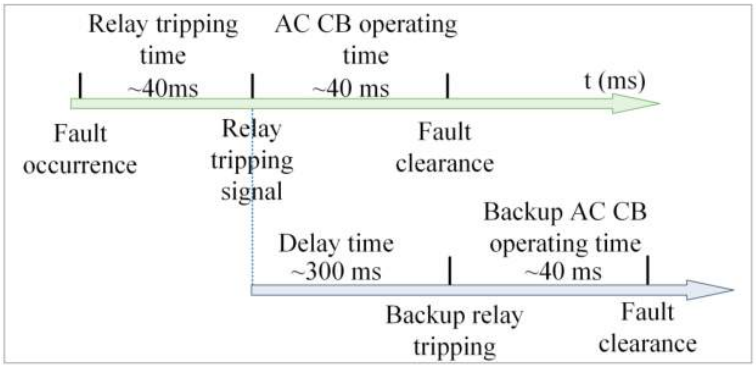

Figure 35: Time response for AC protection systems [58].

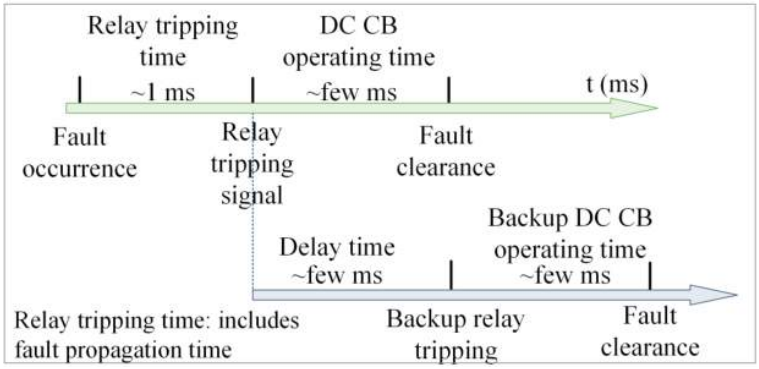

Figure 36: Time response for DC protection systems [58].

5.3.2 Bandwidth of DC measurement devices

In an AC power system, measurement devices for control or protection are normally the transformers. The bandwidth of the transformers is within few kHz. While for the HVDC protection systems, a higher bandwidth measurement device should be adopted. The bandwidth of the devices for the DC protection ranges from tens of kHz to a few MHz. And the sampling frequency used for DC protection is in the order of 100kHz [59]. Table 10 shows the bandwidth of the measuring devices in AC and DC systems.

Table 10: Bandwidth of the measuring devices in AC and DC systems [58], [60].

Type	Technology	Bandwidth	Application
CT	Electromagnetic (iron-core)	few kHz	AC
	Hybrid electro-optical (combined shunt and Rogowski coil)	few MHz	AC and DC
	Fibre optic current sensor (magneto-optic effect)	few MHz	AC and DC
	Zero-flux (Direct Current Current Transformer)	few hundred kHz	DC
	Zero-flux (Hall-effect current transformer)	few hundred kHz	DC
VT	Inductive voltage transformer	few kHz	AC
	Capacitor voltage transformer	few kHz	AC
	Compensated RC-divider	few MHz	AC and DC
	Fibre optic voltage sensor (magneto-optic effect)	few MHz	AC and DC

5.4 DC Protection Methods and Algorithms

DC fault clearing is very challenging as both the breaking operation and time requirements are more demanding than those for AC fault clearing. Therefore, detection and discrimination of the fault are important for DC fault clearance. Different kinds of protection methods have been proposed for DC faults.

- Current and Voltage Magnitude-Based Methods

  In HVDC system, voltage transducers equipped in the terminal of the MMC station measure the positive and negative pole-to-ground voltages for over- and under-voltage protection. After a DC fault, the voltages in the terminal change significantly, the detected voltage will be in accordance with predefined thresholds to generate the trip signals to protection the system [61]. The DC current will rapidly increase during the pole-to-pole DC fault. The magnitude, direction and duration criteria can be uesd to detect the DC faults. Due to the low accuracy and time delay of the Magitude-based Methods, these methods can not be used as a stand-alone strategy. The methods are normally used as the backup protection methods.

- Derivative-based Methods

  Current and voltage derivative methods, namely di/dt and dv/dt, are suitable not only for fault detection but also for DC fault discrimination. DC faults can be detected and located by the sign and magnitude of the DC voltage or current derivative. In case of a DC fault. the DC current and DC voltage change faster in the faulty link than in the non-faulty ones. A fault current limiter (FCL), which is normally a DC reactor as shown in Figure 37, should be employed at the DC link to smooth the waveforms and to limit the di/dt during the DC faults. Then the change rate of the DC reactor voltage provide another protection method. Based on this observation, [62] proposes the use of voltage across the DC terminal reactors for fast and accurate DC fault detection in a mesh HVDC grid.

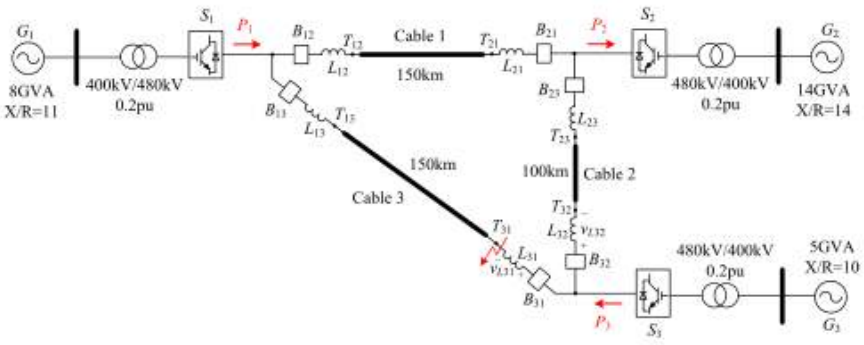

Figure 37: Meshed three-terminal HVDC transmission system with DC reactor at each end of the DC cables [62].

- Differential Protection Methods

  Differential protection with overcurrent backup protection is one of the most feasible method to protect the HVDC lines. The DC currents are measured at both ends of each cable and the current difference is used to detect and locate the faults. However, telecommunication is required and thus the detection speed and reliability are depended on the communication system. There the locally measured DC current is used as backup protection in case the failure of the communication.

- Travelling Wave-based Methods

Travelling wave-based methods are widely used in HVDC protection [63]. Fault current and voltages generate impulses, which travel from generating point to the line ends. This phenomenon is used in HVDC protection based on estimating first and second reflections at one terminal without the requirements of communication between the terminals.

5.5 DC Protection Devices

5.5.1 AC Circuit Breakers (ACCBs)

For point-to-point HVDC systems, ACCBs can be used to protect DC side faults. The VSC is blocked once the fault is detected and the DC side fault will be cleared by opening the grid side ACCBs. The AC side and DC side of the system will suffer from the short circuit current before the ACCB is switched off. The AC side circuit current during DC faults is shown in Figure 38. The sub-modules protect the semiconductors by employing the thyristors parallel with the diode to share DC fault currents. The HB sub-module with thyristor is shown in Fig.39. This methods suffer from a considerable outage time of the whole DC system due to the low speed of ACCBs and time to re-closure the healthy DC grid in the MTDC systems.

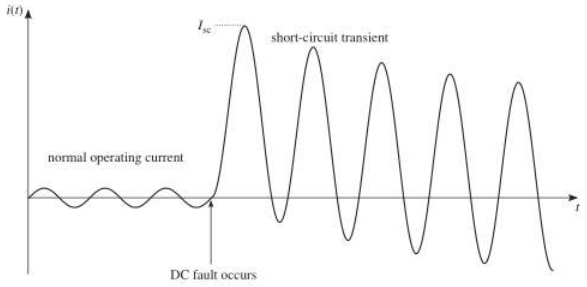

Figure 38: AC side current during the DC faults [64].

5.5.2 DC Circuit Breakers (DCCBs)

The current candidate technologies of DCCBs can be classified into three categories as: mechanical DCCBs, solid state DCCBs and hybrid DCCBs.

- Mechanical DCCBs

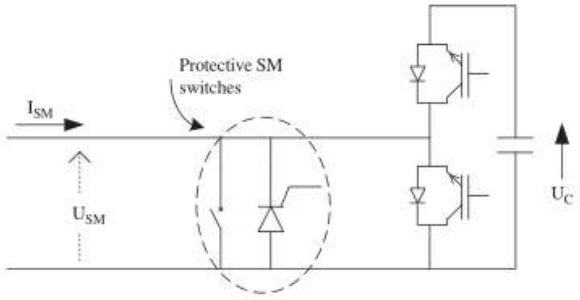

Figure 39: HB sub-module with thyristor [64].

The basic configuration of the mechanical DCCBs includes a normal current path, a LC resonant circuit and an energy dissipation current path. During the normal operation condition, the current flow through the mechanical switch. Once the fault is detected, the LC resonant circuit, as shown in Figure 40 and in Figure 41, can generate zero crossing point for the mechanical switch. Then the energy stored in the system will be consumed by the arrester in parallel. The interrupt time for the self-resonant mechanical DCCBs is normally 40-80ms. The interrupt time of the forced-current commutation resonant breaker can be several milliseconds. But it needs the pre-charge process for the resonant capacitors.

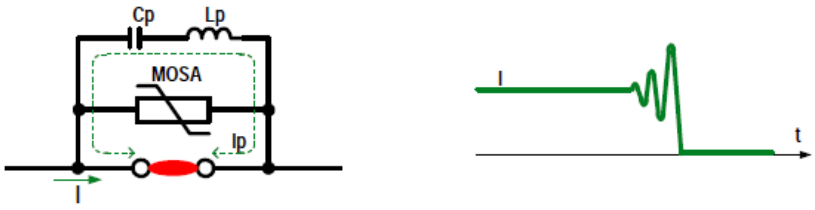

Figure 40: Self-current commutation resonant breaker.

- Solid State DCCBs

  The solid state DCCBs are implemented by semiconductor devices (e.g. IGBTs) in parallel with the energy absorbing branch. During the normal condition, the current flows through the semiconductor devices.

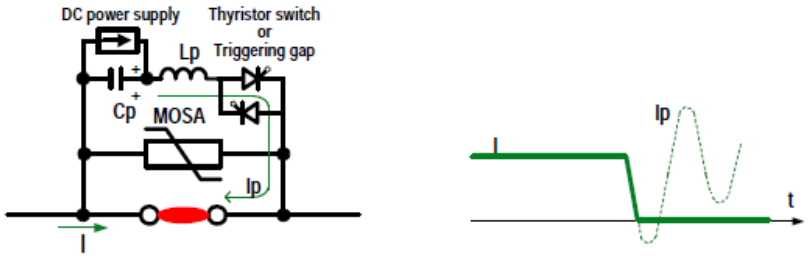

Figure 41: Forced-current commutation resonant breaker.

During the breaking operations, the semiconductor devices are turned off and the current transferred to the energy consumption branch. A topology of solid-state DCCBs is illustrated in Figure 42. And the response time of the solid state DCCB is given in Figure 43. The solid state DCCBs can interrupt the current in a very short time (few milliseconds) due to the fast response of the semiconductor (microseconds range). The main drawbacks of the solid state DCCBs are the power losses and the project costs. The conduction losses of the solid-state devices can be 30% the losses of a VSC. And the cost can be approximately 1/6 of the cost of a HVDC substation.

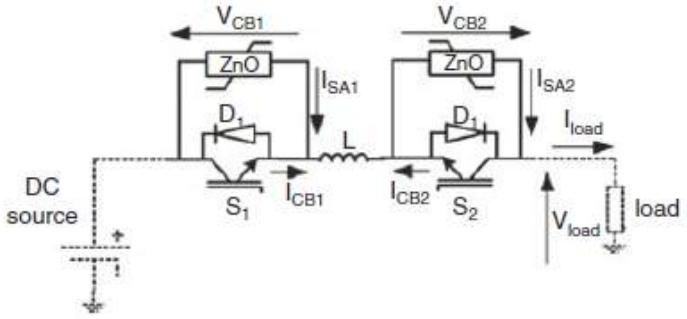

Figure 42: Solid state DCCB[65].

- Hybrid DCCBs

  The hybrid DCCBs combine the controllable semiconductor devices with fast mechanical breakers. The basic schematic of one possible

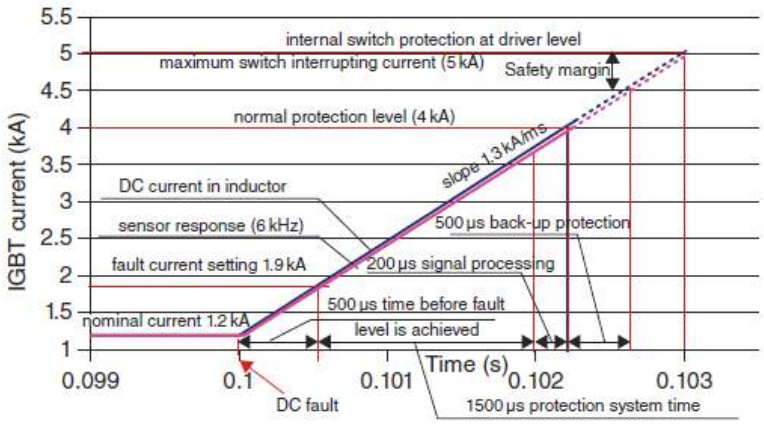

Figure 43: Time response of the solid state DCCB [65].

topology is shown in Figure 44. The mechanical CB is normally closed and rated for nominal current. The mechanical CB provide low loss conduction paths in normal conditions. The system current is transferred to the semiconductor paths once the DC faults are detected. The auxiliary semiconductor valve can generate a zero crossing point for the mechanical CB. The surge arresters will dissipate the fault energy and prevent over-voltages.

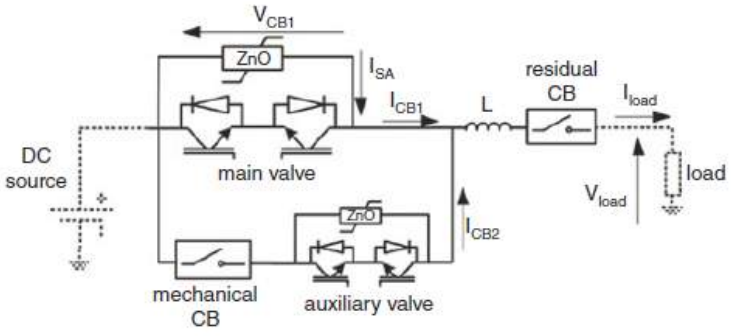

Figure 44: Topology of hybrid DCCB [65].

5.5.3 MMC Topologies with fault handling capability

The two-level and half-bridge based VSCs cannot interrupt the DC fault current due to the uncontrolled diode rectifier after the converters are blocked. In terms of the DC fault, various of SMs with the capability of DC fault handling have been proposed based on the MMC technology.

- Full-bridge SMs

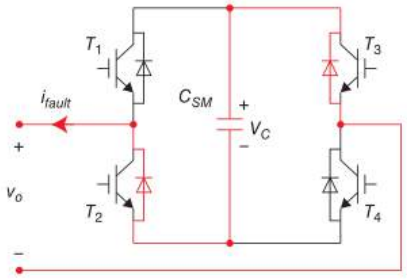

Figure 45: Full bridge sub-module [66].

In order to handle the DC fault, the MMC can also utilize the full bridge submodules. In Figure 45, it can be seen that four IGBTs are installed in one full-bridge submodule. It can generate three levels of voltages, namely, +Vc, 0, -Vc. Compared to the HB-submodules, the full bridge submodules will behave like a diode bridge, and the output voltage will be +Vc regardless of the current direction. The DC fault can be blocked and the DC fault current can be reduced by blocking the FB-MMC converter. Furthermore, the FB-MMC can even keep active due to its capability of the DC bus control.

- Clamp double SMs

The clamp double topology was first presented by Marquardt in 2010 [67] and the diagram of the topology is shown in Figure 46. The main objective of this topology is to reduce the power losses while keeping the DC fault handling capability. In case of DC-side faults, all active switches, including S5 should be switched off. After that, if the current is positive, one capacitor voltage will be seen by the output of the submodules. And if the current is negative, the two capacitors are in series to block the current. In any case, the DC fault current can be blocked

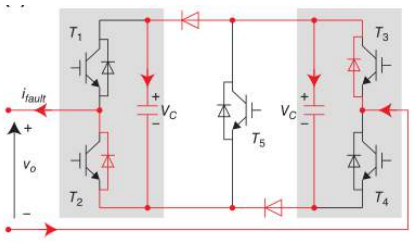

Figure 46: Clamp double sub-module [66].

by the clamp double submodules. But the physical implementation of the clamp double submodules is complex and needs more research when trying to use it in real projects.

- Cross connected SMs [68]

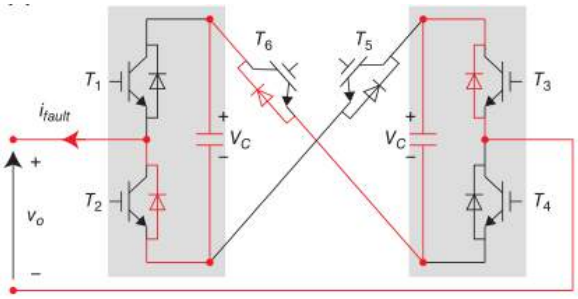

Figure 47: Cross connected sub-module [66].

The cross connected SMs use additional two clamp switches T_5 and T_6 to connect two HB SMs and can generate -2 V_c by switching OFF both T_5 and T_6 to block the DC fault, as shown in Figure 47. However, the two clamp switches T_5 and T_6 must be rated at twice the capacitor voltage thus the effective total number of switches required is the same as two FB SMs in addition to the need for series connection of two switches in the cross connected SMs.

- Hybrid SMs

The mixed SM is equivalent to the so-called hybrid MMC where the FB and HB SMs are mixed in each arm in the converter as shown in Figure 48 [69]. It can generate negative voltage $-V_c$, which allows the

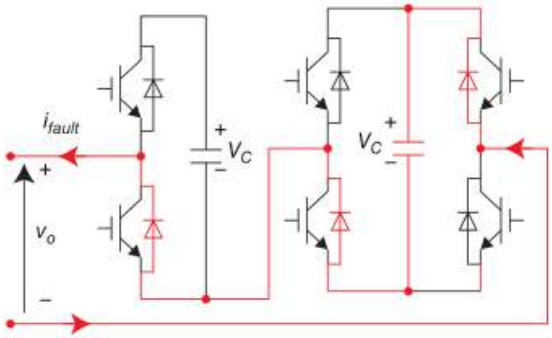

Figure 48: Mixed sub-module [66].

converter to block the DC fault and offers greater controllability than the HB SM.

5.6 Interaction between AC and DC systems: AC faults in hybrid AC/DC systems

5.6.1 Unbalanced ac faults

Three-phase voltages can become unbalanced due to AC faults or nonlinear load conditions. Normally a three-phase three-line system is used for the distributed generators. Then there are no zero-sequence components to be considered between AC grids and MMCs. However, during grid side AC fault condition, negative components and harmonics will be generated. And they will have influence on PLLs and control of MMCs. Figure 49 shows the voltage vector when grid voltages contain fundamental or fifth harmonic negative components.

The distortion in voltage vector will have an influence on the PLLs of MMCs. Figure 50 shows the basic structure of the SRF-PLL. Figure 51 shows that with the normal PLL, the phase angle of the voltage also has the distortion. The positive-sequence voltage vector cannot be properly obtained. A low bandwidth PLL should be used to obtain the proper phase angles. However it will have influence on the dynamic of MMCs. A decoupled double synchronous reference frame PLL (DDSRF-PLL) is proposed to get the positive fundamental phase angel under the unbalanced condition. The structure of the DDSRF-PLL is shown in Figure 52.

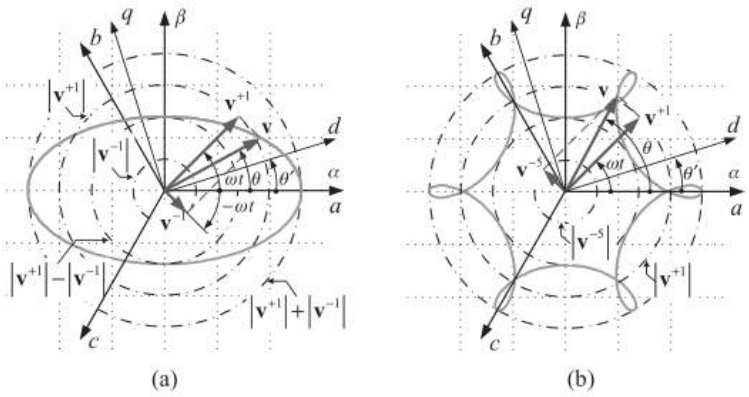

Figure 49: (a) Locus of an unbalance voltage vector (b) A distorted voltage vector [70]

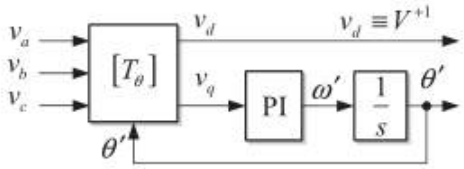

Figure 50: Basic diagram of the SRF-PLL [70].

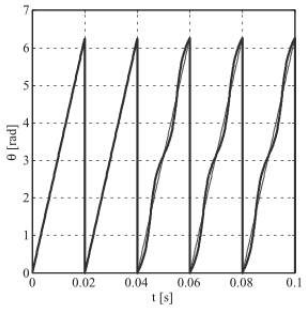

Figure 51: Voltage vector phase angle θ [70].

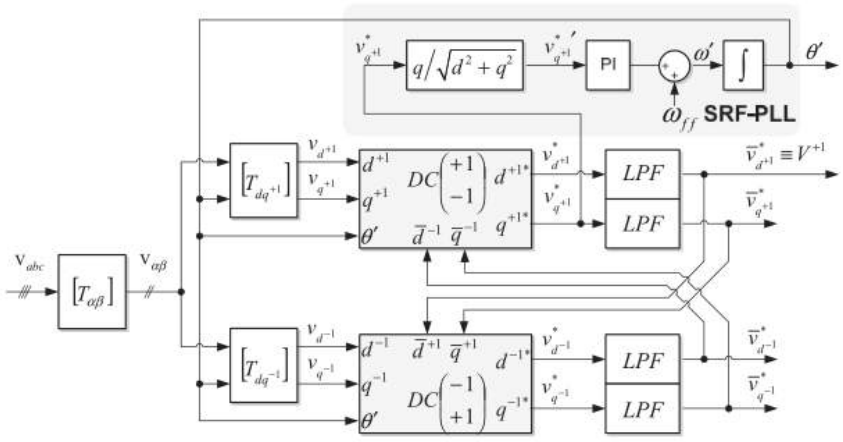

Figure 52: Structure of DDSRF-PLL [70].

5.6.2 Converter-side ac faults

Converter-side AC faults will have more severe influence on MMCs than grid side AC faults. A converter-side phase-to-ground fault can be caused by the failure of transformer isolation as shown in Figure 53.

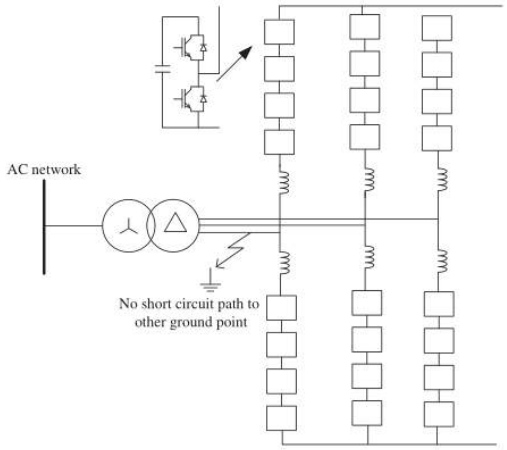

Figure 53: Converter-side AC fault [64].

For monopolar configurations, the converter-side AC fault will cause the oscillations in pole-to-ground DC voltages as shown in Figure 54. The os-

cillation happens in the pole-to-ground voltage. The whole DC bus voltage will not be influenced much. Blocking the converter and tripping ACCBs can clear this type of faults. However if the converter-side DC fault happens in a bipolar system, the fault current in grid side will have no zero-crossings even when the converter is blocked as shown in Figure 55. The ACCBs cannot act under this condition and a grounding method is proposed to solve the non-zero-crossing problem in [71].

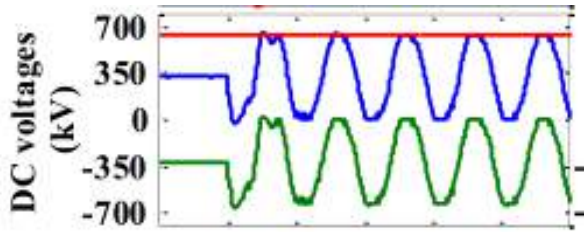

Figure 54: Pole-to-ground dc voltage oscillations [71].

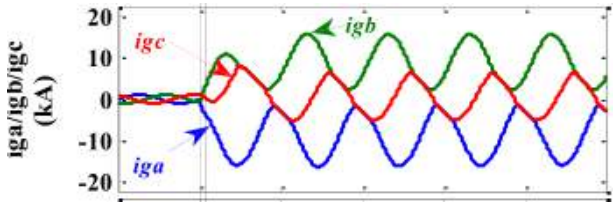

Figure 55: Grid side current during the fault for bipolar HB-MMCs [71].

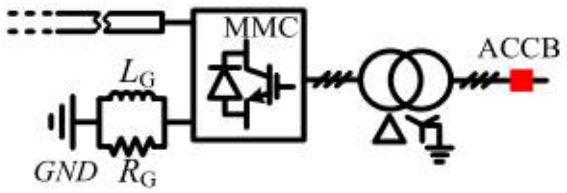

Figure 56: Grounding method to solve the non-zero-crossing problem [71].

AC side faults will have an influence on the MMCs. Grid-side fault results in an unbalance AC system or low voltage condition. The converter should be kept connected to the grid for a period of time according to the grid codes.

Therefore the control method must be proposed to keep the converter safe. Reactive power support is needed in some cases during the faults. However for the converter side AC fault, it can cause severe damages to MMCs if the protection system are not designed well. The objective of the protection of this type of fault is to keep the devices safe in the fault area. The converter should be blocked and grid side ACCBs should be tripped once the fault is detected.

References

[1] A. Aguado Cornago, et all, "The European Supergrid", Book, Clayes & Castleels Publications, 2015 University of Technology, 2007.

[2] European Union Regulation - Guideline on electricity transmission system operation, 2017, Available at: `Website,https://eur-lex.europa.eu/legal-content/EN/TXT/?uri=LEGISSUM:4309265`

[3] ENTSO-E - Guideline on electricity transmission system operation, 2017, Available at: `https://www.entsoe.eu/network$_codes/sys-ops/`.

[4] P. Beaumont; W. Brown; S. Chan; A. Deronja; N. Fischer; et all, "Impact of Voltage Source Converter (VSC) Based HVDC Transmission on AC System Protection", CIGRE Report, 2017.

[5] Leslie Hewitson; Mark Brown, "Practical Power System Protection (Practical Professional Books)", Book, ELSEVIER, 2004.

[6] Dirk Van Hertem; Oriol Gomis-Bellmunt; Jun Liang, "HVDC Technology and Technology for Offshore Grids" in HVDC Grids: For Offshore and Supergrid of the Future, IEEE, 2016, pp. doi: 10.1002/9781119115243.part2.

[7] S. Mirsaeidi; X. Dong; S. Shi and D. Tzelepis, "Challenges, advances and future directions in protection of hybrid AC/DC microgrids", IET Renewable Power Generation, vol. 11, no. 12, pp. 1495-1502, 18 10 2017, doi: 10.1049/iet-rpg.2017.0079.

[8] Beerten, J., "Modeling and Control of DC Grids", PhD Thesis, KU Leuven University, 2013.

[9] Shen, L.,"Model Integration and Control Interaction Analysis of AC/VSC HVDC Systems', PhD Thesis, University of Manchester, 2015.

[10] Büdenbender, C.; Mächtel, K.; Hensler, T., "How simulation-based protection testing can unveil potential problems in complex protection schemes", 2016.

[11] 'IEEE Guide for Protective Relay Applications to Transmission Lines', in IEEE Std C37.113-2015 (Revision of IEEE Std C37.113-1999) , 30 June 2016, doi: 10.1109/IEEESTD.2016.7502047.

[12] R. Heinrich, "Interaction of HVDC Grids and AC Power Systems: Operation and Control", KU Leuven University, 2017.

[13] Horowitz, Stanley H.; Phadke, Arun G.; Niemira, James K., "Power System Relaying", 4th Edition, John Wiley & Sons, 2014.

[14] Guerra, M., "Especificacao dos Requisitos de Um Sistema Automatico de Aquisicao e Tratamento de Oscilografia para Apoio a Manutencao dos Sistemas de Protecao da Rede Nacional de Transporte", Master Thesis, University of Porto, 2014.

[15] Freris, L.; Infield, D., "Renewable energy in power systems", Book, John Wiley & Sons, 2008.

[16] Sanders, M. P., Protective Relaying: Principles and Applications, IEEE Power and Energy Magazine, Vol. 13, 2015.

[17] Kundur, P., "Power System Stability and Control", Book, McGraw-Hill Inc, 1994.

[18] M. Kezunovic, S. Vasilic, D. Ristanovic, "Interfacing protective relays and relay models to power system modeling software and data files", Proceedings. International Conference on Power System Technology, Kunming, China, 2002.

[19] McLaren P. G.; Swift G. W.; Neufeld A.; Zhang Z.; Dirks E.; Haywood M., "Open System Relaying", IEEE Trans. on Power Delivery, July 1994.

[20] Domijan; M. V. Emami, "State Space Relay Modeling and Simulation Using the Electromagnetic Transient Program and Its Transient Analysis of Control System Capability", IEEE Trans. on Energy Conversion, vol. 5, no. 4, pp. 667-702, Dec. 1990.

[21] J. N. Peterson; R. W. Wall, "Interactive Relay Controlled Power System Modeling", IEEE Trans. on Power Delivery, vol. 6, no. 1, pp. 96-102, Jan. 1991.

[22] R. E. Willson; J. M. Nordstrom, "EMTP Transient Modeling of a Distance Relay and Comparison with EMTP Laboratory Testin", IEEE Trans. on Power Delivery, vol. 5, no. 3, pp. 984-990, Jul. 1993.

[23] A. K. S. Chaundhary; K. S. Tam; A. G. Phadke, "Protection System Representation in the Electromagnetic Transient Program", IEEE Trans. on Power Delivery, vol. 9, no. 2, pp. 700-711, Apr. 1994.

[24] R.W. Wall; B.K. Johnson, "Using TACS functions within EMTP to Teach Protective Relaying Fundamentals", IEEE Trans. on Power Systems, vol. 12, no. 1, pp. 3-8, Feb. 1997.

[25] H. W. Dommel, "Electromagnetic Transients Program Reference Manual (EMTP· Theory Book)", Book, Portland: Bonneville Power Administration, 1986.

[26] L. X. Bui; S. Casoria; G. Morin; J. Reeve, "EMTP TACS-FORTRAN Interface Development for Digital Controls Modeling", IEEE Trans. on Power Systems, vol. 7, no. I, pp. 314-319, Feb. 1992.

[27] A. Dysko; lR. McDonald; G.M. Burt; I. Goody; B. Gwyn,"Dynamic Modelling of Protection System Performance", Proc. of the 6th Inti. Con/. DPSP, Mar. 1997.

[28] A. Dysko; J.R. McDonald; G.M. Burt; J. Goody; B. Gwyn,"Integrated – Modelling Environment: A Platform for Dynamic Protection Modelling and Advanced Functionality", IEEE PES T&D Conf., Apr. 1999.

[29] J. A. Martinez-Velasco; Lj. Kojovic, "Modeling of electromechanical distance relays using the ATP", 32nd Universities Power Engineering Conf. UPEC '97 UMIST, 1997.

[30] Chul-Hwan-Kim; Woo-Gon-Jung; Il-Dong-Kim; Myang-Hee-Lee; Gi-Won-Lee,' An implementation of distance relaying algorithm based block pulse functions using EMTP-MODELS', IEEE '96 Proc. of the Inti. Conf. on Electrical Engineering, 1996.

[31] C.H. Kim; M.H. Lee; R.K. Aggarwal; A.T. Johns,"Educational use of EMTP MODELS for the study of a distance relaying algorithm

for protecting transmission lines", IEEE Trans. on Power Systems, vol. 15, 2000.

[32] T. Saengsuwan, "Modelling of distance relays in EMTP", Inti. Con. on Power Systems Transients, Budapest, Budapest, Hungary:Tech. Univ 1999.

[33] Samaan, N. A.; Dagle, J. E.; Makarov, Y. V.; Diao, R. R.; Vallem, M. R.; Nguyen, T. B.; Kang, S. W., Modeling of protection in dynamic simulation using generic relay models and settings. IEEE Power and Energy Society General Meeting, 2016–Novem. https://doi.org/10.1109/PESGM.2016.7741981.

[34] Perez, S. G. A.;Sachdev, M. S.; Sidhu, T. S.,"Modeling relays for use in power system protection studies", Canadian Conference on Electrical and Computer Engineering, May, 2005.

[35] Mahseredjian J.; Benmouyal G.; Lombard X.; Zouiti M.; Bressac B.; Gérin-Lajoie L.,"A link between EMTP and MATLAB for user-defined modeling", IEEE Transactions on Power Delivery, April 1998.

[36] Chaudhary; A.K.S.; Kwa-sur Tam; Phadke A. G., "Protection System Representation in the Electromagnetic Transient Program", IEEE Transactions on Power Delivery, April 1994.

[37] Mahseredjian J.; Benmouyal G.; Lombard X.; Zouiti M.; Bressac B.; Gerin-Lajoie L.,"A link between EMTP and MATLAB for user-defined modeling", IEEE Transactions on Power Delivery, Vol. 13, Issue 2, April 1998.

[38] Gole M; Daneshpooy A.,"Towards Open Systems: A PSCAD/EMTDC to MATLAB Interface", International Conference on Power Systems Transients (IPST97), Seattle, June22-26, 1997.

[39] Hualei Wang, "The Protection of Transmission Networks Containing AC and DC Circuits", PhD thesis, University of Bath, 2014.

[40] Khalifa, D.; Nour, M. (2016), "Assessment of transmission line protection with integrated offshore wind farm in UAE", 13th International Conference on Development in Power System Protection (DSPS), 2016.

[41] "PSCAD IEMTDC Manual", Winnipeg, Manitoba: Manitoba HVDC Research Center, 1988.

[42] "Alternative Transient Program (ATP) Rule Book", Portland: CanAm EMTP User Group, 1992.

[43] "Using MATLAB", Natick, MA: The MathWorks, Inc., Jan. 1999.

[44] CAPE, Available at: `https://www.electrocon.com/capeintro.php`.

[45] ASPEN, Available at: `http://www.aspeninc.com/web/`.

[46] H. Abu-Rub; M. Malinowski; K. Al-Haddad,"Power Electronics for Renewable Energy Systems, Transportation and Industrial Applications", Book, Wiley & Sons, 2014.

[47] Working Group JWG B5/B4.25, "Impact of HVDC Stations on Protection of AC Systems", CIGRE Report, December 2011.

[48] CIGRE, "Impact of HVDC Stations on Protection of AC Systems", CIGRE Technical Brochure, 2011, Available at: `https://e-cigre.org/publication/484-impact-of-hvdc-stations-on-protection-of-ac-systems`.

[49] A. G. M. Strollo. A new IGBT circuit model for spice simulation. In *Proc. PESC97. Record 28th Annual IEEE Power Electronics Specialists Conf.. Formerly Power Conditioning Specialists Conf. 1970-71. Power Processing and Electronic Specialists Conf. 1972*, volume 1, pages 133–138 vol.1, June 1997.

[50] U. N. Gnanarathna, A. M. Gole, and R. P. Jayasinghe. Efficient modeling of modular multilevel HVDC converters (MMC) on electromagnetic transient simulation programs. *IEEE Transactions on Power Delivery*, 26(1):316–324, January 2011.

[51] Hani Saad, Christian Dufour, Jean Mahseredjian, Sebastien Dennetiere, and Samuel Nguefeu. Real time simulation of mmcs using the state-space nodal approach. In *international Conference on Power Systems Transients, Vancouver, BC, Canada, July*, 2013.

[52] Li Gengyin, Zhou Ming, He Jie, Li Guangkai, and Liang Haifeng. Power flow calculation of power systems incorporating VSC-HVDC. In *Proc. PowerCon 2004. 2004 Int. Conf. Power System Technology*, volume 2, pages 1562–1566 Vol.2, November 2004.

[53] J. Beerten, S. Cole, and R. Belmans. A sequential AC/DC power flow algorithm for networks containing multi-terminal VSC HVDC systems. In *Proc. IEEE PES General Meeting*, pages 1–7, July 2010.

[54] M. Baradar and M. Ghandhari. A multi-option unified power flow approach for hybrid AC/DC grids incorporating multi-terminal vsc-HVDC. *IEEE Transactions on Power Systems*, 28(3):2376–2383, August 2013.

[55] Ilka Jahn, Niclas Johannesson, and Staffan Norrga. Survey of methods for selective DC fault detection in MTDC grids. 2017.

[56] Justine Descloux, P Rault, S Nguefeus, JB Curis, Xavier Guillaud, Frédéric Colas, and Bertrand Raison. HVDC meshed grid: Control and protection of a multi-terminal HVDC system. In *CIGRE 2012*, 2012.

[57] Cigré Working Group B4.57. Guide for the development of models for for HVDC converters in a HVDC grid. In *Cigré Technical Brochure*, 2014.

[58] M. Abedrabbo M. Wang. A review on AC and DC protection equipment and technologies: Towards multivendor solution. 2017.

[59] S. Pirooz Azad and D. Van Hertem. A fast local bus current-based primary relaying algorithm for HVDC grids. *IEEE Transactions on Power Delivery*, 32(1):193–202, Feb 2017.

[60] F. Jenau and G. Testin. Modern instrument transformer technologies for HHV AC and HVDC networks. In *Proc. Cigr´e India Symp., New Delhi, India*, 2009.

[61] C. D. Barker and R. S. Whitehouse. An alternative approach to HVDC grid protection. In *10th IET International Conference on AC and DC Power Transmission (ACDC 2012)*, pages 1–6, Dec 2012.

[62] R. Li, L. Xu, and L. Yao. DC fault detection and location in meshed multiterminal HVDC systems based on DC reactor voltage change rate. *IEEE Transactions on Power Delivery*, 32(3):1516–1526, June 2017.

[63] R. E. Torres-Olguin and H. K. H×idalen. Travelling waves-based fault detection method in multi-terminal HVDC grids connecting offshore wind farms. In *13th International Conference on Development in Power System Protection 2016 (DPSP)*, pages 1–7, March 2016.

[64] K. Sharifabadi, L. Harnefors, H.P. Nee, S. Norrga, and R. Teodorescu. *Design, Control and Application of Modular Multilevel Converters for HVDC Transmission Systems*. John Wiley & Sons, Incorporated, 2016.

[65] Dragan Jovcic and Khaled Ahmed. *High Voltage Direct Current Transmission: Converters, Systems and DC Grids*. Wiley-Blackwell, 10 2015.

[66] Lie Xu Rui Li. Review of DC fault protection for HVDC grids. *WIREs Energy Environ.2018;7:e278. https://doi.org/10.1002/wene.278*, 2017.

[67] R. Marquardt. Modular multilevel converter topologies with DC-short circuit current limitation. In *8th International Conference on Power Electronics - ECCE Asia*, pages 1425–1431, May 2011.

[68] A. Nami, L. Wang, F. Dijkhuizen, and A. Shukla. Five level cross connected cell for cascaded converters. In *2013 15th European Conference on Power Electronics and Applications (EPE)*, pages 1–9, Sept 2013.

[69] G. P. Adam, K. H. Ahmed, and B. W. Williams. Mixed cells modular multilevel converter. In *2014 IEEE 23rd International Symposium on Industrial Electronics (ISIE)*, pages 1390–1395, June 2014.

[70] Teodorescu, R. and Liserre, M. and Rodriguez, P. Grid Converters for Photovoltaic and Wind Power Systems.Wiley, 2011.

[71] G. Li, J. Liang, F. Ma, C. E. Ugalde-Loo and H. Liang, Analysis of Single-Phase-to-Ground Faults at the Valve-Side of HB-MMCs in HVDC Systems, in *IEEE Transactions on Industrial Electronics*.

Part IV
Control

Saman Dadjo Tavakoli (supervised by Eduardo Prieto and Oriol Gomis)

In this section, an overview on the control objectives of the conventional point-to-point HVDC link and multi-terminal dc (MTDC) grid is presented. The focus is on the control objectives and requirements of Voltage-Source-Converter (VSC)-based HVDC grids. First, the control objectives of HVDC grids are discussed. The HVDC links are categorized based on their applications; whether they are interconnected to main ac grids, off-shore wind farms, weak ac grids, and islanded passive grids. Then, the control requirements of MTDC grids are addressed, outlining the droop control requirements. Second, the control systems of conventional VSCs and Modular Multilevel Converters (MMC) are explained. It is also described how to achieve the control objectives using the outer and inner control loops of the converters. Finally, the modeling methods for the purpose of control system design are discussed.

6 Time frame for the purpose of control system design

The time frame for the control system design and the related modeling approach is chosen based on the control philosophy of VSCs. Since they adopt a cascaded control system (or multi-loop control system), there are various time constants associated to each control loops. The most inner control loop, which is normally output current control loop, has the fastest response and the shortest time constant which is generally in the order of milliseconds. In practical cases, it is chosen around 5 ms. The outer control loops, which are voltage and power control loops, are four to ten times slower than the inner control loop. Hence, we choose the time constant of the inner control loop as the time frame for the purpose of control system design and modeling method.

7 Overview of challenges associated with the control system design

The control system design for a grid-connected VSC has been extensively addressed in the current literatures. However, the control requirements in application of HVDC grid are still under investigation. There are several topics which need to be addressed:

- methodology for control system design while considering the dynamics of all VSCs, cables, dc-dc converters, and other major components of HVDC systems.
- the interactions between the control systems of VSCs located in the sending and receiving ends of HVDC system.
- the robustness of the control systems against severe disturbances.
- the dc voltage stability concerns in MMC-based MTDC grids.

8 Point-to-Point HVDC System Control

Up to 2017, there are 30 VSC-HVDC links in operation throughout the world and 36 more links are in planning stage [1]. Almost all of the links are point-to-point, except for two links in operation at Nan'ao island and Zhoushan in China, which are MTDC systems. The active and reactive power regulation take place at both ends of HVDC link. However, the selection of different control objectives depends on the application. For instance, in case of grid-forming application, the HVDC link should control frequency and ac voltage, whereas in the grid connected applications, the HVDC link needs only to regulate active and reactive power flow. Nonetheless, the dc voltage control is necessary for achieving active power balance in the HVDC link. Hence, one end of the HVDC link must regulate the dc voltage, while the other should control the active power or frequency. The reactive power regulation can be done independently at both ends of the HVDC link [2], [3], [4].

Point-to-point HVDC systems can be categorized based on the types of ac grids they are connected to as shown in Fig. 57. Each of the above-mentioned application requires certain control objective which are described in the following sections.

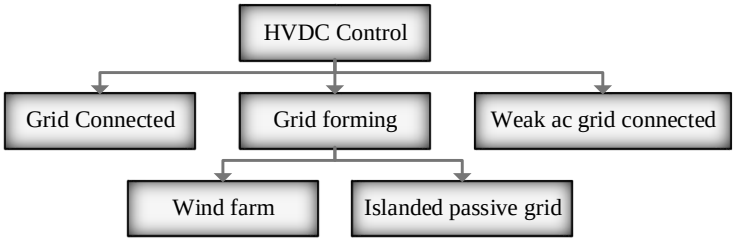

Figure 57: Classification of HVDC systems based on the types of ac grids.

Table 11: The control pairs at both ends of HVDC link connected between two main ac grids.

Sending End	**Receiving End**
P_{ac}, Q_{ac}	V_{dc}, Q_{ac}
P_{ac}, V_{ac}	V_{dc}, V_{ac}

8.1 Grid connected application

It is assumed that the main ac grid is strong (stiff) enough (with high short circuit ratio) to provide the HVDC grid with constant frequency and ac voltage at both ends. A typical HVDC link embedded between two main ac grids is shown in Fig. 58. The most common control objectives at the "sending" or "receiving" ends are as follows [5], [6], [7]:

- DC terminal voltage control (V_{dc})
- Active power control (P_{ac})
- Reactive power control (Q_{ac})
- AC voltage support (V_{ac})

The grid operator determines the control mode of a HVDC system for specific purposes. However, a HVDC station commonly chooses control of the control pairs that are indicated in Table 11 for the sending and receiving ends [6], [8].

Since active and reactive power control by HVDC link are of utmost importance, it is useful to have a look at the PQ diagram of HVDC link.

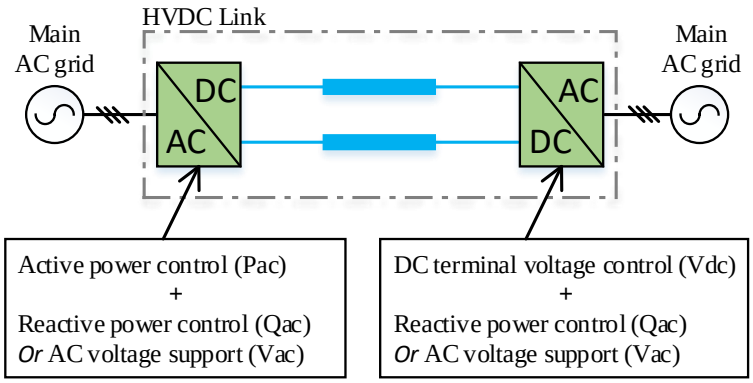

Figure 58: Conventional control functions in HVDC link between two ac grids

.

The PQ diagram of a typical HVDC system, as seen either from sending or receiving ends, is shown in Fig. 59 [9], [10]. The power control of an HVDC system is mainly limited by the VSC converter voltage and current limits and the requirements of the connected ac grid. As it can be seen from Fig. 59, inside the PQ diagram, the active and reactive power that the HVDC link is able to supply during normal conditions are defined by a rectangular area.

Recently, there have been some interests on power factor regulation by HVDC links [9]. In fact, the European Network of Transmission System Operators for Electricity (ENTSO-E) has revised the Network Code on High Voltage Direct Current (HVDC) connections to specify that the HVDC links shall be capable to operate at least in one of the following reactive control modes: ac voltage mode, reactive power mode, and power factor (PF) control mode [11].

8.2 Weak ac grid-connected application

As mentioned earlier, the characteristics of the ac grid have a major impact on the control system of an HVDC link. In case one end (or both ends) of the HVDC link is connected to a weak ac grid, some issues appear to the control system of HVDC system [12], [13], [14]. A weak ac grid can have two different characteristics [12]: high impedance ac grid, which can cause

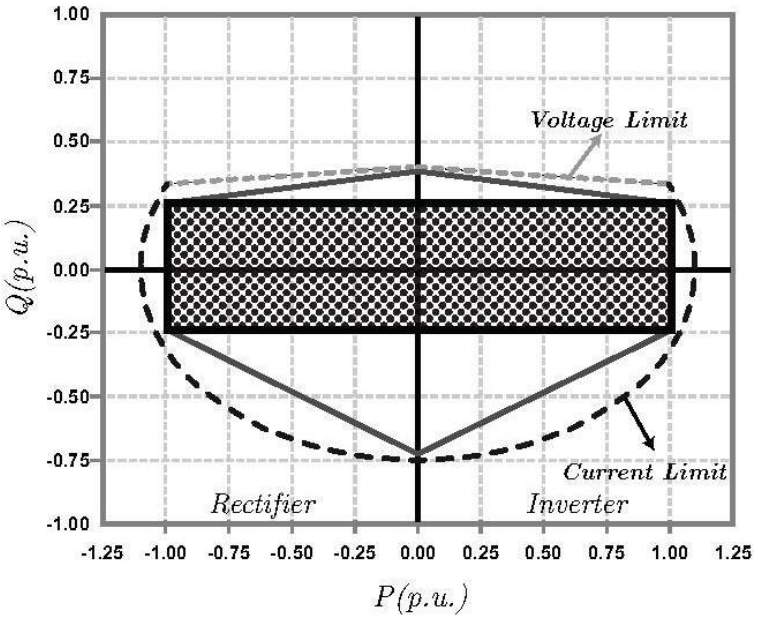

Figure 59: PQ diagram example of a HVDC link [10].

ac voltage instability and power transfer limitations; and low-inertia ac grid, which leads to major frequency deviations.

High impedance ac grid is normally characterized by its low short circuit ratio (SCR) [13]. Weak and very weak ac grids have the 2<SCR<3 and SCR<2, respectively. Although LCC HVDC systems are remarkably more vulnerable to high impedance ac grid, VSC HVDC systems also exhibit ac voltage instability if connected to very weak ac grid.

The influences of high impedance ac grid on the control system of a HVDC link are twofold [15]. First, as the ac grid becomes weaker, the power exchange capability with the HVDC grid reduces. With weak ac grid, there is only a narrow range of voltage enabling the full power export or import. Second, as the ac grid impedance increases, the voltage magnitude of the ac system becomes ever more sensitive to power variations of the HVDC system.

Typically, with low-inertia ac grids, the HVDC system is required to achieve frequency stabilization using frequency droop feedback. With high-impedance systems, the voltage stabilization may be required [12], [15], [16]. This is shown in Fig. 60.

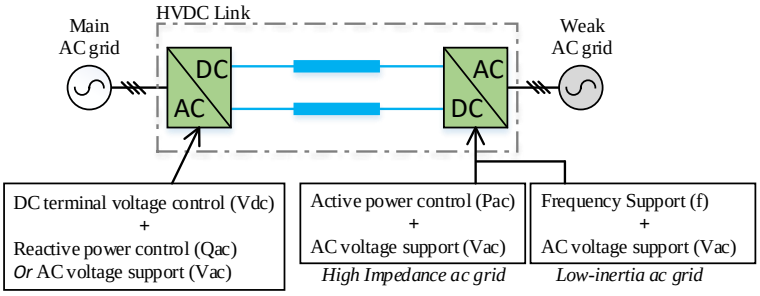

Figure 60: Control functions in HVDC link connected to a weak ac grid.

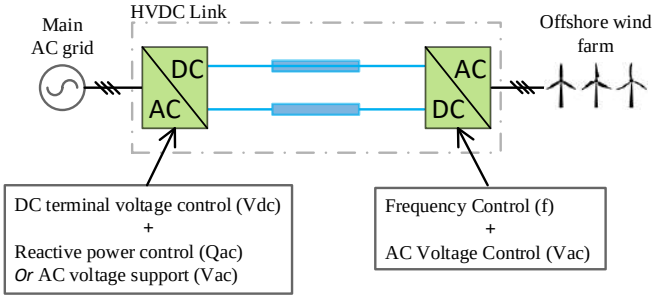

Figure 61: Control functions in HVDC link connected to an offshore wind farm.

8.3 Grid forming application

HVDC links connected to a wind farms or islanded oil/gas platform may be required to operate in grid-forming mode. In this mode of operation, HVDC link is responsible to perform the following control objectives:

- ac voltage regulation
- frequency control

(A) Wind farm application

In case the HVDC system is connected to an offshore wind farm, the most common control objectives are ac voltage and frequency control at the wind farm side of the HVDC link, while the ac grid side regulates the dc voltage and reactive power. [17], [18]. The overview of this system is shown in Fig. 61.

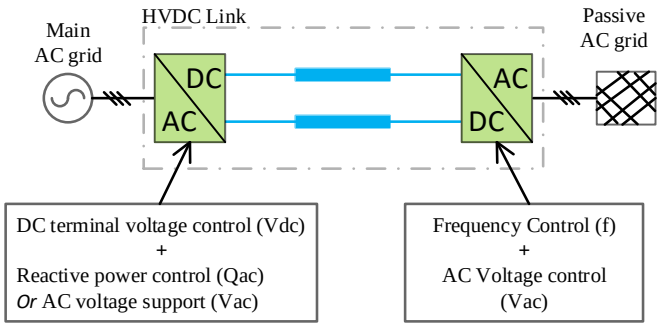

Figure 62: Control functions in HVDC link connected to a passive ac grid.

(B) Passive ac grid application

A passive ac grid is an ac network that has no inertia and no voltage controlling unit. An HVDC link can supply islanded/passive grids or gas/oil offshore platform [12]. Due to the limited number of power generating units in a typical islanded/passive ac grid, the HVDC link should provide ac voltage and frequency support for this network [19]. An overview of this control system is given in Fig. 62.

8.4 Additional functions performed by HVDC links

Due to the interactions between HVDC link and host ac network, and considering the control flexibility of VSC-based HVDC systems, further control objectives can be realized, such as power frequency damping and inertia emulation. The power oscillation damping (POD) is an electromechanical phenomenon that occurs between a large synchronous machine and a moderate-size ac grid [12]. The POD is typically realized through the power system stabilizer (PSS) of large generating units. However, the active/reactive power control loop of HVDC link can be modified to perform this control objective [20], [21].

9 Multiterminal DC Grid Control

Multiterminal DC (MTDC) grids pose several control challenges, among which the dc terminal voltage control is of utmost importance. As shown in Fig. 63 several converters are connected to the same dc terminal of a

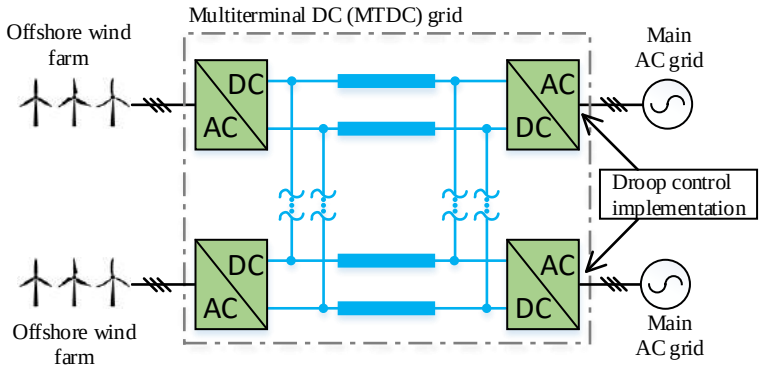

Figure 63: A generic topology of a MTDC grid.

MTDC grid. Then, different controllers can be implemented to maintain the stability of the network.

Referring to the current literature, there are several ways to classify the dc voltage control methods. The voltage control methods can be categorized based on centralized and distributed control systems as follows [22], [23]:

(A) Centralized dc voltage control:

- Master-slave: in this control strategy, a master station is responsible for regulating the dc voltage while other stations control power [24]. This control strategy has been practically implemented by Nan'ao MTDC grid [25]. The main drawback of this control strategy is its low reliability since the proper operation of the grid cannot be ensured if the master station fails [24], [26]. Moreover, the master station must be connected to a very strong ac grid to deliver high amount of power very fast to ensure dc voltage stability.

- Voltage margin control: the performance of master-slave control system can be further improved using voltage margin control. In case the master station reaches its maximum power or goes off-line, there are reserved stations to immediately take over the role of dc voltage control. However, the voltage margin control has the same instability issues of master-slave control which is due to only one station is regulating dc voltage at one time [27].

- Priority control: this dc voltage control approach, in fact, combines droop control with master-slave control. The station with high priority

operates in a constant voltage mode, and other stations in droop control mode. The main disadvantage of this approach is that when the MTDC grid becomes large, the coordination between stations to find high priority station is cumbersome [5].

(B) Distributed dc voltage control: Voltage droop control is a decentralized strategy in which dc voltage is controlled by multiple stations to maintain both voltage stability and power balance [24], [27]. A detailed discussion on the limitations and performance of droop controller is provided in [22]. In short, there are mainly three limitations associated with droop controller:

- DC voltage limit: the upper limit is determined by the specification of the switching devices and other dc components. The lower limit, however, depends on the converter control system. The upper and lower limits are shown in Fig. 64.
- Power limit: every converter station has a certain power rating and overload capability. The power limit appears as a hyperbolic curve in the I-V plane and as a vertical line in P-V plane, which is indicated in Fig. 64.
- DC current limit: the upper limit is based on the current ratings of the switching devices and other dc components.

Within the permissible region given in Fig. 64, the dc voltage droop controller is presented in Fig. 65. The droop controller in I-V plane and P-V plane would have different characteristics. In the I-V plane, the following equations describe the current-based and power-based droop equations:

$$droop\ in\ I-V\ plane: \begin{cases} \Delta I_{dc} = \frac{1}{k_I}\Delta U_{dc} \\ \Delta P_{dc} = (\frac{U_{dc0}}{k_I} + \frac{P_{dc0}}{U_{dc0}})\Delta U_{dc} + \frac{1}{k_I}\Delta U_{dc}^2 \end{cases} \tag{77}$$

$$droop\ in\ P-V\ plane: \begin{cases} \Delta P_{dc} = \frac{1}{k_P}\Delta U_{dc} \\ \Delta I_{dc} = (\frac{1}{k_P} - I_{dc0})\frac{\Delta U_{dc}}{\Delta U_{dc}+\Delta U_{dc0}} \end{cases} \tag{78}$$

The standard current and power-based droop characteristics are shown in Fig. 65; however, there are also other versions of droop controller such as deadband or undeadband droop controllers which are slightly different from the standard version. A detailed review on different droop controllers is provided in [22].

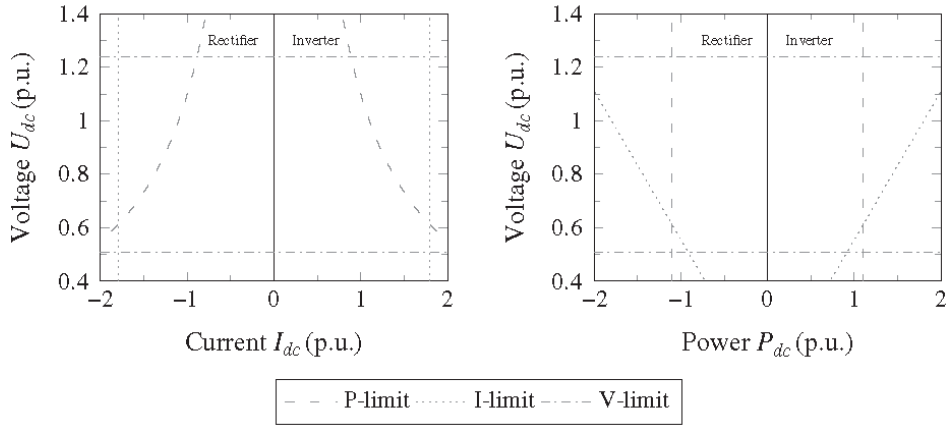

Figure 64: The limitations of dc voltage droop controller; the region inside the intersections of lines and curves is permissible for droop control operation [22].

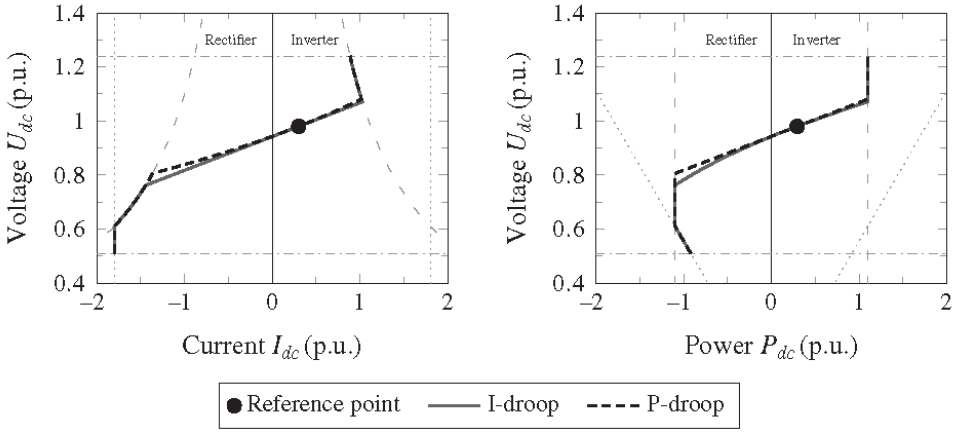

Figure 65: I-V curve and P-V curve for droop control [22].

10 Converter Control System

The control objectives discussed in the previous sections can be realized by the control systems of the VSC stations. The control systems of VSC and MMC have the same basics; however, MMC requires additional energy/current control systems. First, the control systems of the conventional

VSC are investigated and then the additional requirement of MMC are explained.

10.1 Control System of Conventional VSC

Various control systems have been proposed for VSC HVDC systems. Direct control using modulation index and phase angle has been widely implemented [5], [28], [29]. However, this type of controller is unable to independently regulate active and reactive power due to the high degree of coupling between control parameters. Another drawback of this control system is the lack of inner current control loops, which cannot limit the VSC output current.

The most popular control systems which are based on the inner current control loops are resonant controller and decoupled vector control. Since the decoupled vector control, known as "d-q control", provides better performance as compared with resonance control, this is the de facto control system for the VSC HVDC systems [5].

In d-q control approach, current and voltage variables are mapped to d-q axis and treated as dc waveforms under steady state conditions [30], [31]. This in turn, permits utilization of PI controller with simple structure and low dynamic orders. However, the d-q control requires a Phase-Locked Loop (PLL) to adjust the rotational speed of the dq-frame, θ, so that the q-component of grid voltage is forced to zero in steady state conditions.

In its most common structure, the d-q controller is based on the inner current loops which are decoupled so that the active and reactive power can be regulated independently. The references to the d-q current loops are provided by outer control loops which are usually the active and reactive power loops.

The d-q control system of a VSC is shown in Fig. 66. The control system can be divided into three parts: the internal control, inner control, and outer control. The internal control is commonly the modulation techniques used to drive the IGBT gate signals $g_1 \dots g_n$ based on the references provided by the inner control loops, m_{abc}. The inner current loops are essentially two PI regulators which make sure that the d-q current references are tracked with the desirable dynamics and zero steady state error. The outer control loops produce d-axis current reference from either active power reference (P_{ac}) or dc-link voltage reference (V_{dc}); and q-axis current reference from either reactive power reference (Q_{ac}) or ac terminal voltage reference (V_{ac}).

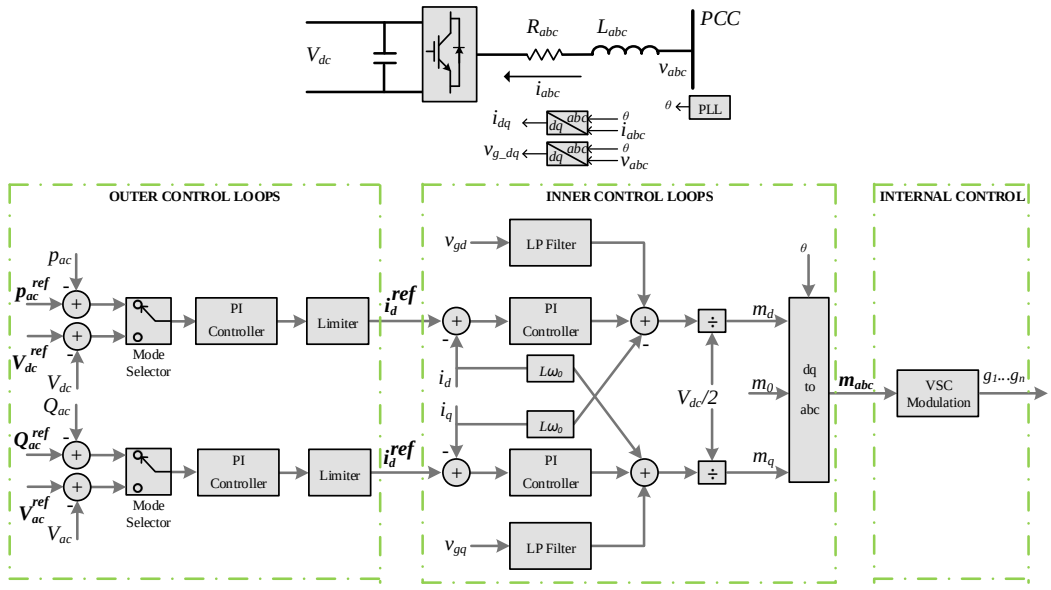

Figure 66: dq control of VSC HVDC system.

The common practice is that the outer control loops (power and voltage loops) operate with lower bandwidth compared with the relatively high bandwidth of the inner control loops (current loops). Ideally, for any cascaded control system with fully decoupled operation, the outer control loops should be at least four to ten times slower than the inner control loops [5], [32], [33]. A detailed discussion on how to design and tune this control system is provided in [30].

10.2 Control System of MMC

The structure of a MMC is presented in Fig. 67. Each leg of the MMC contains two arms (upper and lower), and each arm is made up of hundreds of submodules (SMs). Various topologies for submodules have been introduced in literature; however, for the purpose of control system design we only consider half bridge topology for submodule.

In order to control the MMC shown in Fig. 67, various approaches have been proposed in literature. However, the following classification can be made [34], [35]:

- Non-energy control approach (uncompensated modulation): This ap-

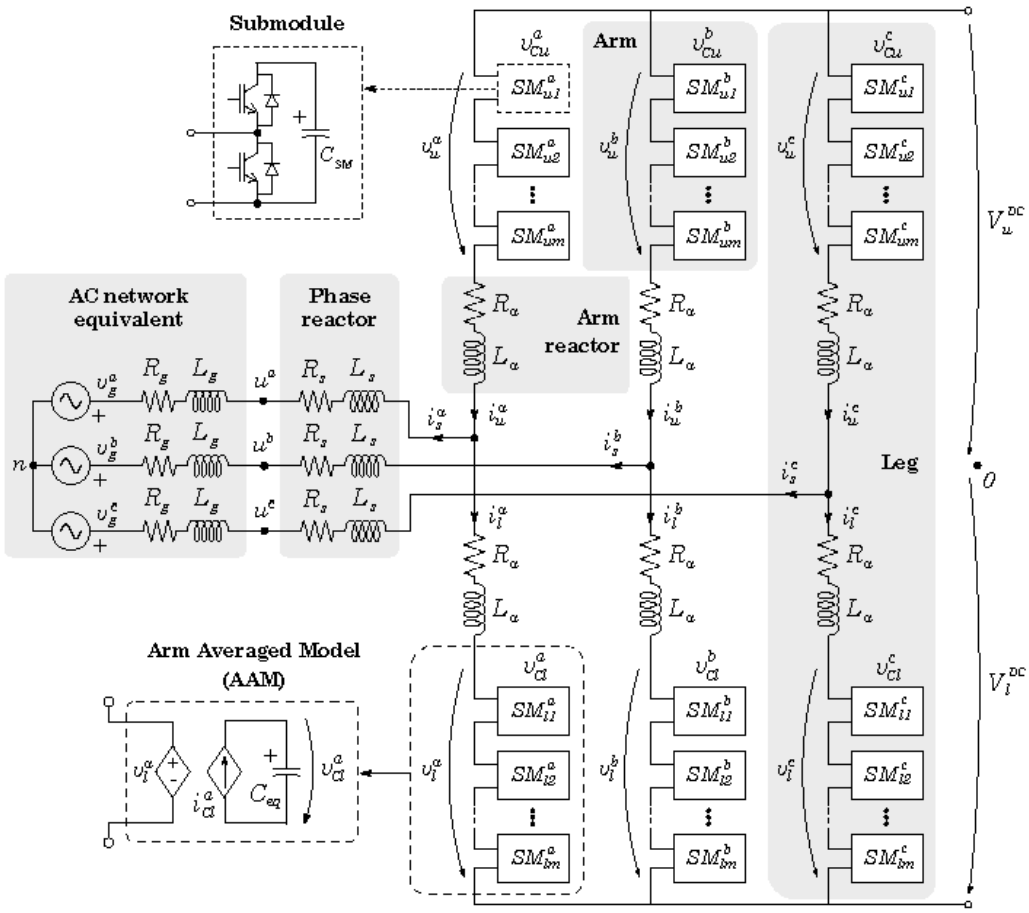

Figure 67: Typical structure of MMC [34].

proach includes direct voltage modulation [36] or open-loop modulation [37], which are known to be asymptotically stable but their transients depend on the converter impedances rather than being imposed by a controller, leading to slow time constant and undesirable dynamics [38]. Moreover, a Circulating Current Suppressing Control (CCSC) is required to eliminate circulating current inside the MMC [39].

- Energy-controlled approach (compensated modulation): This approach is also called closed-loop control approach [40], in which no parasitic voltage components appear, but it requires arm energy controllers to

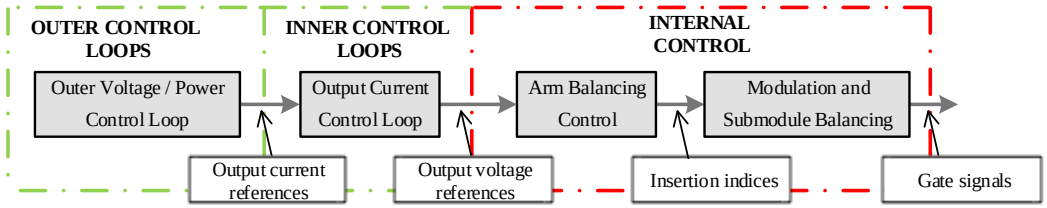

Figure 68: Typical control system of MMC.

ensure an asymptotically stable system [41].

General Scheme for MMC Control System

The general control structure of MMC is shown in Fig. 68. The control loop for the output current has the highest bandwidth (fast response) of all nested control loops and it can be regarded as the heart of the control system. The output of the current control loop is voltage references which can be forwarded directly to the modulation control in case of conventional VSC. However, due to the complexity of MMC, the voltage references are used to control the circulating current and capacitor voltage balancing. Then, the result references, known as insertion indices, are fed into another control stage including modulation and submodule balancing control. Finally, gate signals are produced and applied to the relevant submodule [41].

Referring to Fig. 68, the inner current loop and outer power/voltage loop are similar to the control system of conventional VSC (see Fig. 66). But, the internal control of MMC is more complicated than conventional VSC. Two specific control functions are performed by Arm Balancing Control: circulating current control, which in fact, controls the charging and discharging of the submodule capacitors; and the sum capacitor voltage control (arm voltage control), which makes sure the sum capacitor voltages converge to dc-link voltage [41].

The main control approaches for sum capacitor voltage control are as follows: direct voltage control [42], closed loop voltage control [43], and open loop voltage control [43]. A detailed discussion on the advantages and disadvantages of each control approach is given in [41].

Energy-based Control System of MMC

The energy-based control system is shown in Fig. 69(a). A very detailed

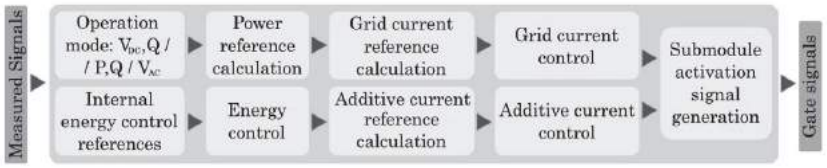

(a)

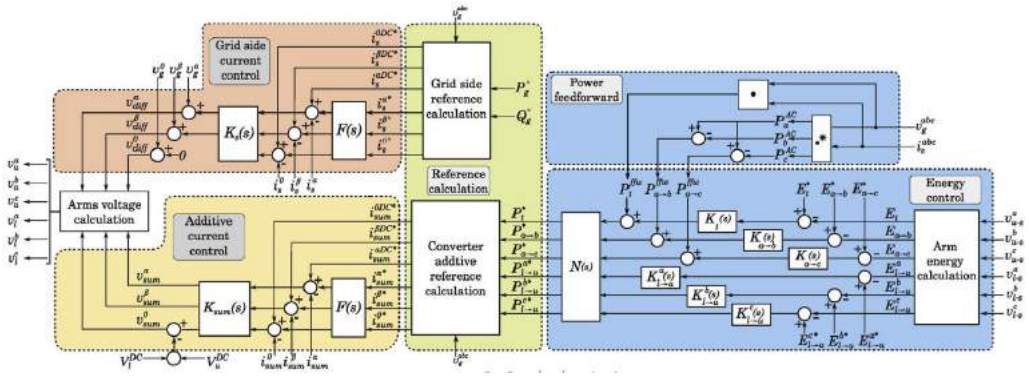

(b)

Figure 69: Energy-based control system of MMC; (a) block diagram, (b) detailed control system [45].

discussion on this control system is provided in [34] and [45]. In this approach, two control systems are operating together to produce the voltage references for the modulation and submodule balancing systems of a MMC. One control system is responsible for controlling the output current (power) of MMC, while another takes the role of controlling the internal energy of the MMC. As indicated in Fig. 69(b), the control system has the following sections:

- Grid side (output) current control: this controller is common with conventional VSC control systems. It is identical to Fig. 66 in dq frame; however, it is also possible to design the controller in $\alpha\beta$ frame to regulate the grid current, i_s, at the fundamental frequency.

- Additive current control: this control system is responsible for regulating the currents flowing through arms and circulating inside the MMC, i_{sum}. This control system is somewhat independent from the grid side current control, meaning that both current controllers can be treated

as two decoupled systems. The control system of i_{sum} operates to make sure the internal energy of the MMC is balanced based on the references received from outer control loops.

- Reference calculation: this part of the control system mainly produces references based on mathematical equations. There is no control loop inside and only references for grid current and additive current, respectively, i_s and i_{sum}, are generated.
- Power feedforward: the exchanged power inside MMC is calculated here and feedforward signals for energy loops are provided. This is done only to improve the dynamics of the energy control loops and it has no impact on the steady state performance.
- Energy control: energy control is the outer controller which calculates the exchanged energy between three legs and dc link, and between upper and lower arms of each leg. Using PI controllers, the outputs of energy control loops are references of exchanged power between legs and arms.

11 System Modeling for Control System Design

In this section, the dynamic modeling of grid-connected conventional VSC, MMC, and HVDC cable is carried out.

11.1 Modeling of grid-connected conventional VSC

The conventional VSC can be modeled in three phase abc frame, $\alpha\beta$ frame, and d-q frame. However, the most common approach is to use d-q frame and implement conventional PI controllers since all variables would be dc quantities. Referring to the VSC shown in Fig. 66, the three-phase ac grid voltage can be written as

$$V_{ga}(t) = \hat{V}_g \; cos(\omega_0 \; t + \theta_0) \tag{79}$$

$$V_{ga}(t) = \hat{V}_g \; cos(\omega_0 \; t + \theta_0 - \frac{2 \; \pi}{3}) \tag{80}$$

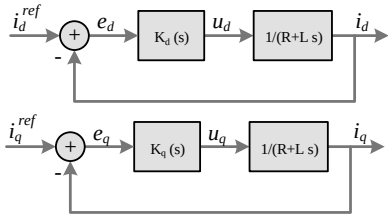

Figure 70: Simplified inner current control loops of VSC.

$$V_{ga}(t) = \hat{V}_g \; cos(\omega_0 \; t + \theta_0 - \frac{4 \; \pi}{3}) \tag{81}$$

where $\hat{V}_g$ is the peak value of the line-to-neutral voltage, ω_0 is the AC system (source) frequency, and θ_0 is the source initial phase angle. The space-phasor equivalent of the grid three-phase voltages can be written as [30],

$$\overrightarrow{V}_g = \hat{V}_s \; e^{j(\omega_0 t + \theta_0)} \tag{82}$$

The dynamics of the ac side of the VSC are described by the following space-phasor equation:

$$L \; \frac{d \; \overrightarrow{i}}{dt} = -R \; \overrightarrow{i} + (\overrightarrow{V}_t - \overrightarrow{V}_s) \tag{83}$$

where, R and L are the output filter resistance and inductance, respectively; and V_t is the converter ac terminal voltage. Assuming that the PLL adjusts the rotational speed of d-q frame, applying the d-q transformation would result in the following dynamic equations:

$$L \; \frac{di_d}{dt} = L\omega_0 i_q - Ri_d + V_{td} - V_s \tag{84}$$

$$L \; \frac{di_q}{dt} = -L\omega_0 i_d - Ri_q + V_{tq} \tag{85}$$

The plant transfer functions of the VSC can be simply obtained from (84) and (85). The design and tuning of the inner current control loops are based on the above-mentioned equations. It is worth mentioning that the terms $(L\omega_0 i_q)$ and $(-L\omega_0 i_d)$ appear in the equations due to the d-q transformation.

The complete model of a grid-connected VSC, including controllers, is shown in Fig. 66; however, the inner current control loops can be further simplified with two independent control loops as presented in Fig. 70.

The PI controllers, $K_d(s)$ and $K_q(s)$, have similar proportional and integral coefficients,

$$K_d(s) = K_q(s) = \frac{k_p\ s + k_i}{s} \tag{86}$$

A common practice is to select the coefficients as follows:

$$k_p = \frac{L}{\tau_i} \quad and \quad k_i = \frac{R}{\tau_i}$$

where τ_i is the time constant of the resultant close loop system. This time constant is a design choice: it should be small for fast current control response, but large enough such that $1/\tau_i$, which is the bandwidth of the closed loop system, is smaller (10 times) than the switching frequency of VSC. Depending on the requirement and application, τ_i is chosen in the range of 0.5 to 5 ms [30].

The current references, indicated in Fig. 70, can be supplied by the outer power/voltage control loops as shown in Fig. 66. As discussed earlier, the dq-axis reference can be calculated by ac power, which is,

$$i_d^{ref} = \frac{2}{3V_{sd}}\ P_s^{ref} \tag{87}$$

$$i_q^{ref} = -\frac{2}{3V_{sd}}\ Q_s^{ref} \tag{88}$$

This method is known as feedforward control which has robustness issues [5]. An alternative way is to regulate power using a PI controller as indicated in Fig. 66. Moreover, it is also possible to use dc-link voltage and ac voltage, Vdc and Vac, to generate, respectively, the d and q-axis current references. However, the inner current control loops of Fig. 70 are at the heart of all available control schemes.

11.2 Modeling of MMC

Dynamics and control of MMC is fully described in [41]. Since the typical MMCs in HVDC application may have very high number of sub-modules (400 level MMC), very detailed models of MMC may include thousands of semiconductor switches and normally must use small numerical integration time-steps to accurately represent high-frequency events [46]. The computational burden introduced by detailed models may not be necessary for the

purpose of control system design. It is possible to estimate the similar behavior and dynamic response by implementation of simplified MMC models. These simplified models also known as average models replicate the average response of switching devices [47], [48], [49].

The detailed switching models which include all ac and dc components of variables can be obtained systematically. Generalized voltage-based state-space modeling including control loops is proposed in [50]. Another detailed model suitable for energy-based control system is addressed in [51]. For a power system dynamic simulation and control design approaches, the comprehensive switching level models have no key dynamic contribution to the dynamics of the integrated system [52], [53], [54]. Moreover, in [46], it is shown that the proposed average model accurately replicates the dynamic performance of the detailed switching model. Hence, for the purpose of MMC modeling, the average model will be adopted.

The following modeling approach of MCC is adopted mainly from [34], [36], [45]. Referring to Fig. 67, the dynamic equations of the MCC per phase are ($j = a, b, c$)

$$V_u^{DC} - v_u^j - v_g^j - v_n = R_a i_u^j + La\frac{di_u^j}{dt} + (R_s + R_g)i_s^j + (L_s + L_g)\frac{di_s^j}{dt} \tag{89}$$

$$V_l^{DC} - v_l^j - v_g^j - v_n = -R_a i_l^j - La\frac{di_l^j}{dt} + (R_s + R_g)i_s^j + (L_s + L_g)\frac{di_s^j}{dt} \tag{90}$$

where,
R_a, L_a: arm resistance and inductance.
R_s, L_s: as filter resistance and inductance.
V_u^{DC}, V_l^{DC}: upper and lower voltages of the HVDC link.
v_g^j : thevenin ac grid voltage.
v_u^j, v_l^j: voltages applied by the upper and lower arms.
i_u^j, i_l^j: current flowing through the upper and lower arms.
i_s^j: ac grid current.

It is a common practice to define the following variables for convenience:

$$\begin{cases} v^j_{diff} = 1/2(-v^j_u + v^j_l) \\ v^j_{sum} = v^j_u + v^j_l \\ i^j_{sum} = 1/2(i^j_u + i^j_l) \\ R = R_s + R_g + R_a/2 \\ L = L_s + L_g + L_a/2 \end{cases} \quad and \quad \begin{cases} v^j_u = -v^j_{diff} + 1/2 v^j_{sum} \\ v^j_l = v^j_{diff} + 1/2 v^j_{sum} \\ i^j_u = 1/2 i^j_s + i^j_{sum} \\ i^j_l = -1/2 i^j_s + i^j_{sum} \end{cases}$$

In the above-mentioned definitions, v^j_{diff} is called differential voltage which is approximately equal to the ac grid voltage; v^j_{sum} is the additive voltage approximately equal to the sum of the dc poles voltages. i^j_{sum} is the circulating current flowing through the arms of phase j and has no impact on the grid ac current.

Adding and subtracting (89) and (90) and replacing the variables defined above, we have

$$\frac{1}{2}(V^{DC}_u - V^{DC}_l) + v^j_{diff} - v^j_g - v_n = R\, i^j_s + L\, \frac{di^j_s}{dt} \tag{91}$$

$$v^j_{sum} - (V^{DC}_u + V^{DC}_l) = -2R_a\, i^j_{sum} - 2L_a\, \frac{di^j_{sum}}{dt} \tag{92}$$

Equations (91) and (92) describe the dynamics of MMC and are therefore suitable for small-signal analysis and control system design. However, it is not easy to transform them into d-q frame and make them dc quantities. It is well-known that i^j_{sum} contains both dc and ac components [50], [51]:

- A dc component associated with the total internal energy of converter,
- A fundamental frequency component that can be associated with the energy exchange between the upper and lower arms,
- A second harmonic component associated with the double frequency characteristics of the single phase power flow in each phase.

Hence, the modeling of MMC becomes complicated as variables with mixed ac and dc components cannot be transferred into the d-q frame easily. Various approaches are introduced to overcome this problem. The detailed modelings in [50] and [51], in fact, consider all components of variables and introduce

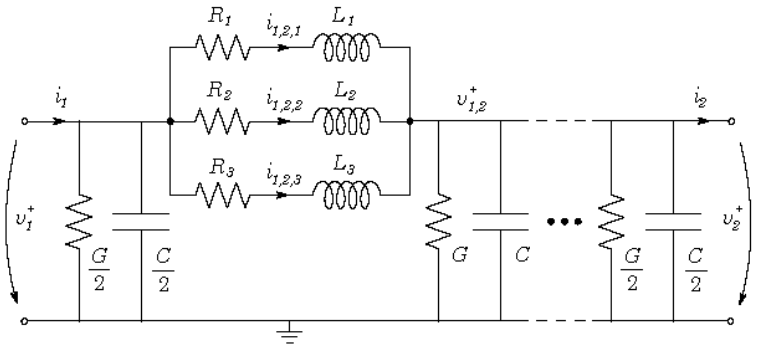

Figure 71: Cable model with parallel series branches [34].

several transformation frames; however, for the purpose of control system design, the models are unnecessarily complicated. More simplified approaches are delivered in [34] and [45]. However, the basic dynamic equations (91) and (92) are similar in all approaches.

11.3 Modeling of HVDC Cable

The dynamic behavior of HVDC cable has a major impact on the stability of the system. There are two main methods to model cables: lumped and distributed parameters models. Regarding the former, cascaded pi-sections are used; while in the later method, the wideband known as Universal Line Model is usually the preferred alternative for accurate Electromagnetic Transient simulations [34], [55]. However, these models cannot be adopted in state-space modeling. This issue is addressed in [56], deriving a lumped parameters vector fitting based model with parallel branches that accurately reproduce the detailed wideband models [57].

This model is presented in Fig. 71, where v^+ refers to the positive monopole corresponding to $1/2V_{DC}$ in steady state conditions. The more cascaded sections are considered for this model, the more accurate response can be obtained. Some studies considered only one section [56], [58]. However, higher number of sections are required for long cables (five sections or more). For n sections, $(1 + 4n)$ differential equations are obtained [34]:

$$\frac{dv_1}{dt} = \frac{4}{C}(i_1 - \sum_{k=1}^{3} i_{1,2,k} - \frac{G}{4}v_1) \tag{93}$$

$$\frac{di_{i,i+1,k}}{dt} = \frac{1}{2L_k}v_1 - \frac{1}{2L_k}v_{i,i+1} - \frac{R_k}{L_k}i_{i,i+1,k} \quad i = 1, ..., n \quad and \quad k = 1, 2, 3 \tag{94}$$

$$\frac{dv_2}{dt} = \frac{4}{C}(\sum_{k=1}^{3} i_{n,n+1,k} - i_2 - \frac{G}{4}v_2) \tag{95}$$

$$\frac{dv_{i,i+1}}{dt} = \frac{2}{C}(\sum_{k=1}^{3} i_{i,i+1,k} - \sum_{k=1}^{3} i_{i+1,i+2,k} - \frac{G}{2}v_{i,i+1}) \quad i = 1, ..., n, \ n \geq 2 \tag{96}$$

where,
i_1, i_2: input and output currents of the cable.
v_1, v_2: total voltages at each cable terminal.
$v_{i,i+1}$: total voltage after section $i, i+1$.
$i_{i,i+1,k}$: current flowing through section $i, i+1$, branch k.
R_k, L_k: equivalent pole resistance/inductance of branch k.
C, G: equivalent pole capacitance/admittance.

References

[1] VSC-HVDC Newsletter, 5, (3), February 2017.

[2] A. Korompili, Q. Wu, H. Zhao,: 'Review of VSC HVDC connection for offshore wind power integration', Renewable and Sustainable Energy Reviews, June 2016, 59, pp. 1405-1414.

[3] C. Du, 'VSC-HVDC for industrial power systems', dissertation, Göteborg: Chalmers University of Technology, 2007.

[4] J. Pan, R. Nuqui, L. Tang, P. Holmberg,: 'VSC-HVDC control and application in meshed AC networks', ABB 2009, Available from `http://www.abb.com/hvdc`.

[5] R. Shah, J. C. Sanchez, R. Preece, M. Barnes: 'Stability and control of mixed AC–DC systems with VSC-HVDC: a review', IET Generation, Transmission and Distribution, May 2018, 12, pp. 2207-2219.

[6] S. Mariéthoz, A. Fuchs, M. Morari,: 'A VSC-HVDC decentralized model predictive control scheme for fast power tracking', IEEE Trans. Power Deliv., 2014, 29, pp. 462–471.

[7] W. Wang, A. Beddard, M. Barnes, et al.: 'Analysis of active power control for VSC-HVDC', IEEE Trans. Power Deliv., 2014, 29, (4), pp. 1978–1988.

[8] N. Chaudhuri, B. Chaudhuri, R. Majumder, A. Yazdani,: 'Multi-terminal direct-current grids modeling, analysis, and control', Wiley-IEEE Press, 2014.

[9] A. Perilla, J.L. Rueda Torres, M.A.M.M. van der Meijden, et al.: 'Analysis of a power factor regulation strategy for an embedded point-to-point MMC-HVDC system', in Proc. IEEE International Energy Conference (ENERGYCON), Limassol, Cyprus, June 2018.

[10] M. Davies, M. Dommaschk, J. Dorn, J. Lang, D. Retzmann, D. Soerangr, HVDC PLUS Basics and Principle of Operation, Siemens Energy Sector. Available: https://www.energy.siemens.com/br/pool/br/transmissaode-energia/transformadores/hvdc-plus-basics-and-principle ofoperation.pdf.

[11] European-Commission, "ENTSO-E Network Code on Requirements for Grid Connection of High Voltage Direct Current Systems and Direct Current-Connected Power Park Modules." Official Journal of the European Union, August 2016.

[12] A. Khaled, J. Dragan,: 'High voltage direct current transmission: converters, systems and DC grids', Wiley Press, 2015.

[13] C. Guo, W. Liu, C. Zhao, R. Iravani,: 'A frequency-based synchronization approach for the VSC-HVDC station connected to a Weak AC grid', IEEE Trans. Power Deliv., June 2017, 32, pp. 1460–1470.

[14] M. F. M. Arani, Y. Abdel-Rady I. Mohamed,: 'Analysis and performance enhancement of vector-controlled VSC in HVDC links connected to very weak grids', IEEE Trans. Power sys., January 2017, 32, pp. 684–693.

[15] L. Zhang, L. Harnefors, H. Nee,: 'Interconnection of two very weak AC systems by VSC-HVDC links using power-synchronization control', IEEE Trans. Power sys., FEBRUARY 2011, 26, pp. 344–355.

[16] J. Z. Zhou, H. Ding, S. Fan, Y. Zhang, A. M. Gole,: 'Impact of short-circuit ratio and phase-locked-loop parameters on the small-signal behavior of a VSC-HVDC converter', IEEE Trans. Power Deliv., OCTOBER 2014, 29, pp. 2287–2296.

[17] L. Shen, M. Barnes, J.V. Milanovic, et al.: 'Potential interaction between VSC-HVDC and STATCOM'. 18th Power System Computation Conf. (PSCC), August 2014.

[18] M. Amin, M. Molinas,: 'Understanding the Origin of oscillatory phenomena observed between wind farms and HVdc systems', IEEE Journal of Emerging and Selected Topics in Power Electronics, March 2017, 5, pp. 378–392.

[19] L. Zhang, L. Harnefors, H. Nee,: 'Modeling and control of VSC-HVDC links connected to island systems', IEEE Trans. Power sys., May 2011, 26, pp. 783–792.

[20] L. Zeni, R. Eriksson, S. Goumalatsos, M. Altin, et al.: 'Power oscillation damping from VSC–HVDC connected offshore wind power plants', IEEE Trans. Power Deliv., April 2016, 31, pp. 829–838.

[21] J. L. Domínguez-García, C. E. Ugalde-Loo, F. Bianchi, O. Gomis-Bellmunt,: 'Input–output signal selection for damping of power system oscillations using wind power plants', Electrical Power and Energy Systems, 2014, 58, pp. 75–84.

[22] D. Van Hertem, O. Gomis-Bellmunt, J. Liang,: "Hvdc grids for offshore and supergrid of the future", Wiley Press, 2014.

[23] L. Zhang, Y. Zou, J. Yu, V. Vittal, G. G. Karady, D. Shi, Z. Wang,: "Modeling, control, and protection of modular multilevel converter-based multi-terminal HVDC systems: a review," CSEE JOURNAL OF POWER AND ENERGY SYSTEMS, 3, pp. 340–352, Dec. 2017.

[24] K. Rouzbehi, A. Miranian, J. I. Candela, A. Luna, and P. Rodriguez,: "A generalized voltage droop strategy for control of multiterminal DC grids," IEEE Transactions on Industry Applications, 51, pp. 607–618, Feb. 2015.

[25] H. Rao,: "Architecture of Nan'ao multi-terminal VSC-HVDC system and its multi-functional control," CSEE Journal of Power and Energy Systems, 1, pp. 9–18, Mar. 2015.

[26] X. Chen, L. Wang, H. S. Sun, and Y. Chen,: "Fuzzy logic based adaptive droop control in multiterminal HVDC for wind power integration", IEEE Transactions on Energy Conversion, 32, pp. 1200– 1208, Sep. 2017.

[27] Z. D. Wang, K. J. Li, J. G. Ren, L. J. Sun, J. G. Zhao, Y. L. Liang, W. J. Lee, Z. H. Ding, and Y. Sun,: "A coordination control strategy of voltage-source-converter-based MTDC for offshore wind farms," IEEE Transactions on Industry Applications, 51, pp. 2743–2752, Aug. 2015.

[28] D. Jovcic, L.A. Lamont, L. Xu,: 'VSC transmission model for analytical studies'. IEEE Power and Energy Society General Meeting, 2003.

[29] A.J. Beddard: 'Factors affecting the reliability of VSC-HVDC for connecting offshore wind farms'. PhD dissertation, School of Electrical and Electronic Engineering, The University of Manchester, 2014.

[30] A. Yazdani, R. Iravani,: "Voltage-Sourced Converters in Power Systems", IEEE-WILEY Press, 2010.

[31] C. Schauder, H. Mehta,: 'Vector analysis and control of advanced static VAr compensators', IEE Proc. C, Gener. Transm. Distrib., 1993, 140, pp. 299– 306.

[32] C. Barker,: 'HVDC plenary session-grid', IEEE EPEC, Winnipeg, MB, Canada, October 2011.

[33] S. Skogestad, I. Postlethwaite,: 'Multivariable feedback control: analysis and design', Wiley Press, Chichester, UK, 2001.

[34] E. Sánchez-Sánchez, E. Prieto-Araujo, A. Junyent-Ferré, O. Gomis-Bellmunt,: "Analysis of MMC energy-based control structures for VSC-HVDC links," IEEE JOURNAL OF EMERGING AND SELECTED TOPICS IN POWER ELECTRONICS, DOI: 10.1109/JESTPE.2018.28031361, Feb. 2018.

[35] G. Bergna, J. A. Suul, S. D'Arco,: "State-space modelling of modular multilevel converters for constant variables in steady-state," IEEE 17th Workshop on Control and Modeling for Power Electronics, COMPEL, 2016.

[36] L. Harnefors, A. Antonopoulos, S. Norrga, L. Angquist, H. P. Nee,: "Dynamic analysis of modular multilevel converters," IEEE Trans. Ind. Electron., 60, pp. 2526–2537, 2013.

[37] L. Angquist, A. Antonopoulos, D. Siemaszko, K. Ilves, M. Vasiladiotis, and H.-P. Nee,: "Open-loop control of modular ultilevel converters using estimation of stored energy," IEEE Trans. Ind. Appl., 47, pp. 2516–2524, 2011.

[38] E. Prieto-Araujo, A. Junyent-Ferr´e, C. Collados-Rodr´ıguez, G. Clariana- Colet, O. Gomis-Bellmunt,: "Control design of Modular Multilevel Converters in normal and AC fault conditions for HVDC grids," Electr. Power Syst. Res., 152, pp. 424–437, 2017.

[39] Q. Tu, Z. Xu, and L. Xu, "Reduced Switching-frequency modulation and circulating current suppression for modular multilevel converters," IEEE Trans. Power Del., 26, pp. 2009–2017, 2011.

[40] A. Antonopoulos, L. Angquist, and H.-P. Nee,: "On dynamics and voltage control of the Modular Multilevel Converter," 13th European Conf. on Power Electronics and Applications, EPE-ECCE, 2009.

[41] K. Sharifabadi, L. Harnefors, H. P. Nee, S. Norrga, and R. Teodorescu,: "Design, control and application of modular multilevel converters for HVDC transmission systems", Wiley Press, 2016.

[42] L. Harnefors, A. Antonopoulos, S. Norrga, L. Ängquist, H.-P. Nee,: "Dynamic analysis ofmodular multilevel converters," IEEE Transactions on Industrial Electronics, 60, pp. 2526–2537, Jul. 2013.

[43] A. Antonopoulos, L. Ängquist, and H.-P. Nee,: "On dynamics and voltage control of the modular multilevel converter," Proceedings of the 13th European Conference on Power Electronics and Applications, pp. 1–10, Sep. 2009.

[44] L. Ängquist, A. Antonopoulos, D. Siemaszko, K. Ilves, M. Vasiladiotis, H.-P. Nee,: "Open-loop control of modular multilevel converters using estimation of stored energy," IEEE Transactions on Industry Applications, 47, pp. 2516–2524, Dec. 2011.

[45] E. Prieto-Araujoa, A. Junyent-Ferréb, C. Collados-Rodrígueza, G. Clariana-Coleta, O. Gomis-Bellmunt,: "Control design of Modular multilevel converters in normal and AC fault conditions for HVDC grids," Electric Power Systems Research, 152, pp. 424–437, 2017.

[46] J. Peralta, H. Saad, IEEE, Sébastien Dennetière, Member, IEEE, J. Mahseredjian, S. Nguefeu,: "Detailed and averaged models for a 401-Level MMC–HVDC system," IEEE Trans. Power Del., 27, pp. 1501–1508, July 2012.

[47] H. Saad, J. Peralta, S. Dennetière, J. Mahseredjian, J. Jatskevich, J. A. Martinez, A. Davoudi, et al.:"Dynamic averaged and simplified models for MMC-Based HVDC transmission systems," IEEE Trans. Power Del., 28, pp. 1723–1729, July 2013.

[48] S. R. Sanders, J. M. Noworolski, X. Z. Liu, and G. C. Verghese,: "Generalized averaging method for power conversion circuits," IEEE Trans. Power Electron., 6, pp. 251–259, Apr. 1991.

[49] S. Chiniforoosh, J. Jatskevich, A. Yazdani, V. Sood, V. Dinavahi, J. A. Martinez, and A. Ramirez, "Definitions and applications of dynamic average models for analysis of power systems," IEEE Trans. Power Del., 25, pp. 2655–2669, Oct. 2010.

[50] G. Bergna-Diaz , J. Freytes , X. Guillaud, J. A. Suul,: "Generalized voltage-based state-space modeling of modular multilevel converters with constant equilibrium in steady state", IEEE Trans. Power Elect., 6, pp. 707–725, June 2018.

[51] G. Bergna-Diaz, J. A. Suul, S. D'Arco,: "Energy-based state-space representation of modular multilevel converters with a constant equilibrium point in steady-state operation", IEEE Trans. Power Elect., 33, pp. 4832–4851, June 2018.

[52] SL. hen, M. Barnes, J.V. Milanovic, et al.: 'Potential interaction between VSC-HVDC and STATCOM'. 18th Power System Computation Conf. (PSCC), August 2014.

[53] N. Ahmed, L. Ängquist, S. Norrga, et al.: 'A computationally efficient continuous model for the modular multilevel converter', IEEE J. Emerg. Sel. Top. Power Electron., 2014, 2, pp. 1139–1148.

[54] S. Cole, J. Beerten, R. Belmans,: 'Generalized dynamic VSC MTDC model for power system stability studies', IEEE Trans. Power Syst., 2010, 25, pp. 1655–1662.

[55] A. Morched, B. Gustavsen, M. Tartibi,: "A universal model for accurate calculation of electromagnetic transients on overhead lines and underground cables," IEEE Trans. Power Del., 14, pp. 1032–1038, 1999.

[56] S. Akkari, E. Prieto-Araujo, J. Dai, O. Gomis-Bellmunt, X. Guillaud,: "Impact of the DC cable models on the SVD analysis of a Multi-Terminal HVDC system," 19th Power Syst. Computation Conf., PSCC, 2016.

[57] J. Beerten, S. D'Arco, J. A. Suul,: "Frequency-dependent cable modelling for small-signal stability analysis of VSC-HVDC systems,"IET Gener. Transm. Distrib., 10, pp. 1370–1381, 2016.

[58] J. Freytes, S. Akkari, J. Dai, F. Gruson, P. Rault, X. Guillaud,: "Small-signal state-space modeling of an HVDC link with modular multilevel

converters," IEEE 17th Workshop on Control and Modeling for Power Electronics, COMPEL, 2016.

Part V
Conclusions

This deliverable is the outcome of the research performed within Work Package 3 of the InnoDC project. It is the result of an effort to study different aspects of AC and DC grid operation in the following domains: reliability, stability, protection and control. The aim of the report has been to highlight the challenges associated with AC/DC grids; provide an overview of the state-of-the-art regarding the operation of these grids; and discuss the time frames and modelling complexity relevant to each of the domains of power system operation.

Below is a summary of the topics that were covered, main takeaways and ideas for the continuation of the project:

Reliability As the current method of reliability assessment, the N-1 reliability criterion, does not consider the likelihood of occurrence of a contingency and may lead to situations of either higher costs of measures taken or of higher operational risk. Moreover, there is an escalation in system uncertainties due to a multitude of factors such as the increased renewable generation, intra-day markets and development of smart grids. Thus, there is a need to switch to risk-based or probabilistic reliability criteria for optimal grid operation. Owing to the large-scale development of HVDC grids and their property of robust control, it is envisaged to consider the controllability of HVDC grid elements into the existing reliability assessment process and to mitigate system uncertainty. In view of the above, an implementation of the security constrained optimal power flow with added flexibility from HVDC elements is envisaged for ensuring reliable grid operation. As the AC/DC SCOPF problem exhibits huge computational size and difficulty in dealing with the discrete variables, the possibility to utilize convex relaxations for the same are discussed. Finally, the development of a multi-stage AC/DC SCOPF is proposed so as to provide flexible options to a system operator for reliable grid management in an environment of uncertainty.

Stability The increase in the number of power electronic-interfaced devices in the grid has improved the overall grid controllability but, in turn, gave rise to dynamic issues that could eventually take the system to an unstable state.

As the same time, there is an uncertainty regarding the limits and accuracy of traditional transient stability programs to study this new phenomena and to what extent the models used today are accurate. In view of that, the principles behind the traditional phasor-based modelling were reviewed and a summary of the most commonly used phasor-based models for the main AC/DC power grid components was provided. Future work will focus on the development of reduced-order models for different AC system studies.

AC Protection With the integration of VSC based HVDC link, the AC power system network faces new challenges, different from all the experience gathered to date. Despite the continued study and simulations of the interactions between the AC and DC grids, the interactions and the challenges which the AC system, more precisely, the AC transmission protections face, are still not fully understood. The focus will be to complete the list of potential challenges of HVDC and VSC technology on AC transmission protection systems. Including gathering experience from current super grid connections or HVDC technology users on AC systems from all over the world; Some of the methods or generic approach for relay parameters setting and testing were described, which support Protection Engineers. The next step will be to understand how test cases are designed, which will support the work going forward. Modelling and testing relays can be done by combining external models (using MATLAB, C++) with EMTP software, or by utilising software package which has inbuilt simulation options and commercial relay models. The second is the most common approach for TSO Protection Engineers and will be the focus of the efforts going forward. The goal is to continue to assess current software packages and better in-depth understanding of the relay models and simulation definitions available within these tools. This will allow a more realistic testing or simulation, because the models can resemble real systems. To support this testing it is necessary to understand what VSC-based HVDC networks models are more appropriate for the type of testing, including simplifications and main time frame applications.

DC Protection DC protection is an essential part for the stability and reliability of a hybrid AC/DC system. DC grid protection and the interaction between AC and DC networks were discussed in Section 5. The challenges for DC protection has been given firstly. Then the DC protection system and time frame of DC protection were analyzed. Different DC protection

devices (such as ACCBs, DCCBs, FB-MMCs) were discussed in terms of their different characteristics. Finally, the interaction of the AC and DC network was analyzed based on ac faults and possible solutions were given. Future work will cover the analysis of DC protection in both point-to-point links and MTDC systems. Cables and overhead lines will also be included to analyze the transient characteristics of DC faults.

Control This chapter of the report considers various aspects of the control systems in HVDC application. First, the control objectives and requirements are described based on the types of ac grids the HVDC system is connected to. HVDC systems are divided into three main categories, including grid connected, grid forming, and weak ac grid connected. Each of them requires certain control objectives which slightly alters the control system of converter. Second, the concept of multiterminal dc grid is introduced, which is followed by a brief discussion on the various dc voltage control alternatives with focus on the droop controller. Since the control objectives of an HVDC system are realized only through power electronic converters, the control systems of conventional voltage source converters and modular multilevel converters are explained. Only the cascaded (multiloop) control system in dq-frame is considered. Finally, the modeling of various components of HVDC systems are addressed. The dynamic equations and transfer functions of grid-connected converters are derived in dq-frame, and HVDC cable is modeled adopting a lumped parameters vector fitting based approach.